

**A STUDY OF NEUTRINO PROPAGATION AND OSCILLATIONS
BOTH IN VACUUM AND IN DENSE MEDIA**

By

Kenneth Albert Kiers

B. Sc. (Physics) McMaster University, 1991

A THESIS SUBMITTED IN PARTIAL FULFILLMENT OF
THE REQUIREMENTS FOR THE DEGREE OF
DOCTOR OF PHILOSOPHY

in

THE FACULTY OF GRADUATE STUDIES
DEPARTMENT OF PHYSICS

We accept this thesis as conforming
to the required standard

THE UNIVERSITY OF BRITISH COLUMBIA

September 1996

© Kenneth Albert Kiers, 1996

In presenting this thesis in partial fulfilment of the requirements for an advanced degree at the University of British Columbia, I agree that the Library shall make it freely available for reference and study. I further agree that permission for extensive copying of this thesis for scholarly purposes may be granted by the head of my department or by his or her representatives. It is understood that copying or publication of this thesis for financial gain shall not be allowed without my written permission.

Department of Physics and Astronomy

The University of British Columbia
Vancouver, Canada

Date September 19, 1996

Abstract

The phenomenon of neutrino oscillations has been studied for many years and is quite well understood. There remain, however, several issues related to the localization of neutrinos in space and time which have not been entirely resolved. In this thesis we present a detailed study of several of these issues and we present some novel approaches which are useful in their resolution.

We begin by examining the effects of coherent and incoherent broadening on the oscillations of relativistic neutrinos. Such effects are due to distinct physical processes which could in principle be controlled at the source. We show under very general assumptions that these two types of broadening cannot be distinguished at the detector. The consequences of these issues for the oscillations of solar neutrinos is also discussed.

We then present a novel approach to account for the localization in space and time of neutrinos in a typical neutrino oscillation experiment. This is accomplished by modelling the source and detector as spatially and temporally localized oscillators. This simple model allows us to study the effects due to the mass of the exchanged neutrinos and due to the time resolution of the detector.

We then study the propagation of neutrinos in dense media. It is shown that the asymmetry of the dispersion relation as a function of the neutrino's momentum leads to several interesting and amusing effects. The dispersion relation has a minimum at a non-zero value of the momentum $p \sim \rho G_F$, where ρ is the number density of particles in the medium. We show that as a result of this minimum a Dirac (but not Majorana) neutrino may be "trapped" by the medium provided its momentum is less than a critical value which is of order ρG_F .

Table of Contents

Abstract	ii
Table of Contents	iii
List of Figures	vi
Preface	vii
Acknowledgements	viii
Dedication	ix
1 Introduction	1
1.1 Neutrino Masses and Mixings	4
1.2 Neutrino Oscillations	8
1.2.1 Neutrino Oscillations in Vacuum	9
1.2.2 Matter Enhanced Oscillations and the MSW Effect	11
1.3 A Closer Look	17
1.3.1 Neutrino Oscillations and the Uncertainty Principle	18
1.3.2 An Apparent Ambiguity in the $B-\bar{B}$ System	20
1.4 Outline of the Remainder of the Thesis	23
2 Coherence Effects in Neutrino Oscillations	26
2.1 Introduction	26
2.2 Coherent versus Incoherent Broadening	31

2.2.1	An Example	32
2.2.2	Measuring Observables which Commute with Momentum	34
2.2.3	Unrealistic Measurements which CAN Identify Wave Packets	38
2.2.4	General Theorem	40
2.2.5	Consequences	46
2.3	Summary and Conclusions	49
3	Neutrino Oscillations in a Model with a Source and Detector	51
3.1	A Wave Packet Approach	57
3.2	An Approach Using a Current	62
3.3	A Toy Model for a Neutrino Source and Detector	65
3.3.1	A Single Species of Neutrino	68
3.3.2	Several Neutrinos	83
3.3.3	The Non-relativistic Case	92
3.4	Towards a More Realistic Calculation	94
3.5	Summary and Conclusions	101
4	Coherent Neutrino Interactions in a Dense Medium	105
4.1	Introduction	105
4.2	A Simple Model with One Neutrino Flavour	107
4.2.1	Solution to the Dirac Equation	111
4.2.2	Neutrino Trapping	114
4.2.3	The Majorana Case	123
4.3	Dispersion Relations for Two Neutrino Flavours	124
4.3.1	Dirac Case	124
4.3.2	Majorana Case	131
4.3.3	The Vector Model	133

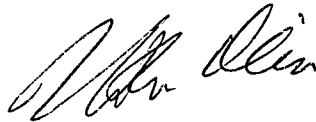
4.3.4	Neutrino Oscillations	134
4.4	Discussion and Conclusions	135
5	Conclusions	137
	Bibliography	141
	Appendices	
A	Majorana Neutrinos	146
A.1	The Majorana Condition	146
A.2	A Majorana Neutrino in Matter	149
B	Derivation of a Position-dependent Probability Using a Current	151
C	Derivation of the $t_2 \rightarrow \infty$ Limit of $\mathcal{A}_{\text{step}}$	156

List of Figures

1.1	Neutrino interactions in a medium	13
1.2	Neutrino effective masses in matter	15
2.1	Plane wave and wave packet	41
3.1	Detection efficiency for the step function detector	76
3.2	Detection probability for the gaussian detector	79
3.3	Mass dependence of the gaussian detector	81
3.4	Oscillation probabilities as a function of distance	87
3.5	Separation of wave packets for different time resolutions	89
3.6	Constant flavour-conserving probability as a function of m_2	93
3.7	Schematic illustration of the source/detector system	95
3.8	Plot of the matrix element squared as a function of m	100
4.1	Feynman diagram corresponding to the electron density	108
4.2	One-loop diagrams contributing to the neutrino self-energy in a simple model	110
4.3	Dispersion relations for a neutrino in an electron “gas”	113
4.4	Dispersion relations and reflection coefficient in a medium	120
4.5	One-loop diagrams contributing to the neutrino self-energy in a realistic model	126
4.6	Dispersion relations for two neutrinos	130
4.7	Dispersion relations in the two-neutrino vector model	134

Preface

The second chapter of this thesis is taken with only minor changes from a recently published paper of which I am a co-author. (Abstracted with permission from K. Kiers, S. Nussinov and N. Weiss, "Coherence effects in neutrino oscillations," Phys. Rev. **D** 53 (1996) pp. 537-547. Copyright 1996 The American Physical Society.) The ideas in this paper grew out of joint discussions between all of the authors based on some earlier work of Prof. Nussinov. The calculations in this paper were done independently by the three authors.

A handwritten signature in black ink, appearing to read "John Klein", is centered on the page.

Preface

The second chapter of this thesis is taken with only minor changes from a recently published paper of which I am a co-author. (Abstracted with permission from K. Kiers, S. Nussinov and N. Weiss, “Coherence effects in neutrino oscillations,” *Phys. Rev. D* **53** (1996) pp. 537-547. Copyright 1996 The American Physical Society.) The ideas in this paper grew out of joint discussions between all of the authors based on some earlier work of Prof. Nussinov. The calculations in this paper were done independently by the three authors.

To Greta, Joshua and Joel

Chapter 1

Introduction

The neutrino has long been an object of fascination for physicists. The neutrino interacts so weakly with matter that one might suppose *a priori* that it is a rather uninteresting particle. History, however, has shown this not to be the case. Indeed, the neutrino was first postulated by Pauli in 1930 as the resolution to a long-standing puzzle in nuclear physics [1]. Prior to Pauli's idea, it had seemed that energy was not conserved in nuclear beta decay. Since the decay was thought to be a two-body decay, the outgoing "beta" particle (an electron or positron) should have been mono-energetic. What was observed, however, was that the beta energy spectrum was continuous [2]. This behaviour was a mystery until Pauli suggested that maybe an additional weakly-interacting particle was also being emitted and was actually carrying off part of the energy. The discovery of the neutrino by Reines and Cowan [3] in 1956 finally confirmed Pauli's idea.

In the decades since the neutrino's discovery, it has also become clear that it is a major player in several other physical processes. For example, it is estimated that neutrinos carry off up to 90% of the energy emitted in a supernova explosion [4]. The idea that a huge pulse of neutrinos accompanies a supernova burst was verified in 1987 with the observation – both visually and via its large neutrino pulse – of Supernova 1987A [5].

Arguably the most intriguing role of the neutrino is that which it plays in the understanding of our own sun. As Bahcall has pointed out [6], the photons which we observe coming from the sun originate from near its surface, and thus they only give direct information about the outer 5-10% of the sun's shell. By way of contrast, the neutrinos which

we detect from the sun originate from nuclear fusion reactions deep within its core. Since the neutrinos interact so weakly, they come streaming out nearly freely and thus provide a sensitive probe of the sun's inner workings. A small industry has developed over the past 35 years whose aim it is to compute very accurately the fluxes of neutrinos expected at the earth due to all of the different nuclear reactions which are assumed to take place in the sun [7, 8]. Despite the continued refinements of the "standard solar model," however, the four "pioneering" experiments which measure neutrino fluxes [9] have consistently measured values which are *too small* by a factor of two or three. This mismatch between the predicted and measured values of the solar neutrino fluxes constitutes the famous "solar neutrino problem."

The solar neutrino problem has steadfastly refused solutions which are based on reworking the standard solar model; indeed, the standard solar model has been found to be extremely robust concerning its predictions of neutrino fluxes [8]. While there are several alternative ways in which one might hope to solve the problem (see, for example, the discussion in Ref. [14]), a very natural solution is a particle physics solution based on the work of Wolfenstein [15] and Mikheyev and Smirnov [16]: the so-called "MSW effect." In the MSW resolution of the solar neutrino problem, the neutrinos produced in the core of the sun, which are "electron" neutrinos, are resonantly converted into "muon" (or "tau") neutrinos as they exit the sun. The observed shortage of neutrinos on earth is then explained by the fact that the current experiments are only sensitive to electron neutrinos. This hypothesis will be put to the test in the near future when the Sudbury Neutrino Observatory (SNO) experiment [17] gets underway, since SNO will have a "flavour-blind" mode which will be sensitive to *all* neutrino types. The SNO detector will contain about one kiloton of heavy water and will be able to detect neutrinos through the reaction

$$\nu + d \rightarrow \nu + p + n, \quad (1.1)$$

which has the same cross-section for all neutrino flavours.

The MSW resolution of the solar neutrino problem requires physics beyond the “Standard Model” [18] of particle physics. In particular, it requires that neutrinos be massive and that they be “mixed.” Neutrinos which are massive and mixed can in general undergo “oscillations,” that is, a neutrino produced as a certain “flavour” (electron, muon, tau, . . .) can at some point later in time be detected as a neutrino of a *different* flavour. This rather remarkable possibility was first pointed out by Pontecorvo [19]. The MSW effect is an extension of Pontecorvo’s “vacuum” oscillations to the case in which the oscillations occur in matter.

Another puzzle in neutrino physics is the “atmospheric neutrino anomaly.” Electron and muon neutrinos are produced copiously in the earth’s upper atmosphere due to the decays of charged pions and kaons. The primary decay chains of the pions and kaons are $\pi^+, K^+ \rightarrow \mu^+ \nu_\mu \rightarrow e^+ \nu_e \bar{\nu}_\mu \nu_\mu$ and $\pi^-, K^- \rightarrow \mu^- \bar{\nu}_\mu \rightarrow e^- \bar{\nu}_e \nu_\mu \bar{\nu}_\mu$ so that, to a first approximation, one expects about twice as many muon-type neutrinos compared to electron-type neutrinos. Extensive Monte Carlo simulations have been performed and the ν_μ/ν_e flux ratio may be calculated with an estimated uncertainty of about 5%. Several collaborations have measured this ratio and the results have been somewhat confusing. Two of the groups consistently measure a value of the ν_μ/ν_e flux ratio which is consistent with the Monte Carlo simulations and the rest of the groups consistently measure a value which is about half the expected value [20]. It may be possible to use neutrino oscillations to explain concurrently the solar neutrino problem and the atmospheric neutrino anomaly [20, 21].

In this thesis we shall examine some of the issues associated with the production, propagation and detection of neutrinos, both in vacuum and in matter. In order to motivate this study, we begin in Sec. 1.1 with a brief overview of neutrino masses and mixings. This is followed in Sec. 1.2 by a discussion of neutrino oscillations and the

MSW effect. We also mention briefly the range of parameters which may be used to solve the solar neutrino problem and the atmospheric neutrino anomaly. In Sec. 1.3 we take a closer look at the idea of “particle oscillations,” first by examining the relation between neutrino oscillations and the uncertainty principle (Sec. 1.3.1) and subsequently by considering an apparent ambiguity which arises in the “conventional” treatment of oscillations in the “ $B - \bar{B}$ ” system (Sec. 1.3.2). The oscillations in this system are analogous to those which may occur in the neutrino system. The ambiguity which arises in the $B - \bar{B}$ system is actually rather dramatic (it involves a relative factor of “2” in the value inferred from $B - \bar{B}$ oscillations for the $B_H - B_L$ mass difference.) The ambiguity also has a perfect analogy in the neutrino system, which serves as a signal that the “conventional” derivation of neutrino oscillations must be treated with some care. We conclude the chapter in Sec. 1.4 with a brief outline of the remainder of the thesis.

1.1 Neutrino Masses and Mixings

Part of the mystery associated with the neutrino is due to the fact that some of its fundamental properties are simply unknown. What *is* known is that the neutrino interacts only very weakly, that it is spin-1/2 and that it is neutral. But there is at least one important question which has so far gone unanswered: Is the neutrino strictly massless or does it have a finite (possibly very small) mass? As we shall see below, the differences between these two scenarios are quite profound, even if the neutrino mass is quite small. If the neutrino has a mass, there are further unknowns. For example, since the neutrino is electrically neutral, it could be either a Dirac or a Majorana fermion, in contradistinction with all of the known elementary fermions, which are Dirac fermions. Furthermore, there could be mixing between the different neutrino “flavours” in analogy with the known Cabibbo-Kobayashi-Maskawa (CKM) mixing in the quark sector of the Standard

Model [18].

In this thesis we shall usually work within the context of a minimal extension to the electroweak sector of the Standard Model (SM) of particle physics. The “minimal extension” which we have in mind is simply that the neutrinos will be allowed to be massive, which is not the case in the regular SM. The electroweak sector of the SM is based on the gauge group $SU(2)_L \times U(1)$ which is spontaneously broken via the Higgs mechanism down to $U(1)$. The leptons are arranged into left-handed doublets and right-handed singlets under the original $SU(2)_L$ symmetry as follows

$$\begin{pmatrix} \nu_{\alpha L} \\ \ell_{\alpha L} \end{pmatrix}, \quad \ell_{\alpha R}, \quad \alpha = e, \mu, \tau, \quad (1.2)$$

where the subscripts L and R refer to the left- and right-chiral projections of the fields, respectively. The simplest way to extend the SM and give masses to the neutrinos is to add right-handed singlet fields $\nu_{\alpha R}$. The corresponding (Dirac) mass terms in the Lagrangian (after spontaneous symmetry breaking) are then of the form

$$\mathcal{L}_{\text{mass}}^D = -m (\bar{\nu}_L \nu_R + \bar{\nu}_R \nu_L). \quad (1.3)$$

This procedure has the advantage of being simple and of being in perfect analogy with the way masses are given to the other elementary fermions. If the neutrino is nearly massless, however, the Yukawa couplings in the neutrino sector need to be several orders of magnitude smaller than those in the charged lepton sector of the theory, and it is difficult to understand why this should be. In all fairness, however, the existing hierarchy of masses among the other fermions – which varies over five orders of magnitude – is also not well-understood, so in some sense this procedure is no more troublesome than what is already done for the other fermions.

Another possibility – which arises because neutrinos are electrically neutral – is that the neutrino is a Majorana particle, by which we mean that it is its own anti-particle.

This condition is expressed in terms of the neutrino field operators as

$$\nu = \nu^C \equiv \mathbf{C}\nu\mathbf{C}^{-1}, \quad (1.4)$$

where \mathbf{C} is the charge conjugation operator [22, pp. 17-30]. In the Majorana case it is possible to construct a mass term using only a left-handed field and its charge-conjugate:

$$\mathcal{L}_{\text{mass}}^M = -m \left(\overline{\nu_L^C} \nu_L + \bar{\nu}_L \nu_L^C \right), \quad (1.5)$$

where $\nu_L^C \equiv (\nu_L)^C$. For more details regarding Majorana neutrinos the reader is referred to Appendix A.

It is generally thought that the SM is most likely to be a low-energy approximation to some more fundamental theory whose structure is as yet unknown. Although the SM has, for the most part, stood up extremely well under intense experimental investigation [23], there are several reasons for thinking that it may not yet be “fundamental” itself [24]. It is possible in many such extensions of the SM to generate small neutrino masses in a natural way via the so-called “see-saw” mechanism by including mass terms of both the Majorana and Dirac types [25]. Consider the simplest case in which we have a single left-handed “doublet” field and another right-handed “singlet” field with the following mass matrix

$$\mathcal{M} = \begin{pmatrix} 0 & m_D \\ m_D & m_M \end{pmatrix}, \quad (1.6)$$

where m_D is the Dirac mass term and m_M is the Majorana mass term for the singlet field. It is easy to verify that if we set m_M to be some very large mass (a “normal” mass at the energy scale of the new physics) and m_D to be a mass on the scale of the charged leptons, then diagonalizing the mass matrix yields one very heavy neutrino (with mass $\sim m_M$) and one very light neutrino (with mass $\sim m_D^2/m_M$). If the heavy neutrino is sufficiently massive, it effectively decouples from the theory and all that is observed at

low energies is the very light neutrino. This is the see-saw mechanism in its simplest form.

At present there is no direct experimental evidence for a non-vanishing neutrino mass. The experimental upper bounds on the neutrino masses are given by [26]

$$m_{\nu_e} < 15 \text{ eV, tritium } \beta \text{ decay} \quad (1.7)$$

$$m_{\nu_\mu} < .17 \text{ MeV, } \pi \rightarrow \mu \nu_\mu \quad (1.8)$$

$$m_{\nu_\tau} < 24 \text{ MeV, } \tau \rightarrow \nu_\tau + n\pi, \quad (1.9)$$

in which the limit on the electron neutrino mass is understood to be only approximate¹. The recent results of the Liquid Scintillator Neutrino Detector (LSND) experiment [28], which has reported evidence for $\bar{\nu}_\mu \rightarrow \bar{\nu}_e$ oscillations, may be regarded as indirect evidence for a massive neutrino. The results of this experiment will be summarized briefly in Sec. 1.2.2.

As we have indicated above, if the neutrinos are not all massless, then it is quite natural to suppose that there is mixing between the neutrino flavours. By this we mean that the neutrino “mass eigenstates” (the states with definite masses and well-defined dispersion relations) are not the same as the “flavour eigenstates” (the states which are produced in weak interactions in association with the same-flavour charged leptons.) The relation between the mass basis and the weak basis is expressed as a relation among the neutrino fields as follows

$$\nu_\alpha(x) = \sum_{i=1}^3 \mathcal{U}_{\alpha i} \nu_i(x), \quad \alpha = e, \mu, \tau, \quad (1.10)$$

where \mathcal{U} is a unitary matrix. In general, some of the phases in \mathcal{U} are removable. One finds that in the general case of n neutrino flavours there are $\frac{1}{2}(n-1)(n-2)$ non-removable

¹The Particle Data Group has recently removed its former limit of $m_{\nu_e} < 5.1 \text{ eV}$ [27], since the tritium β decay experiments which were used to set the limit have consistently arrived at a value of $m_{\nu_e}^2$ which is *negative*. In the current version of the *Review of Particle Physics*, the limit is stated as only being approximate.

(CP -violating) phases for pure Dirac neutrinos and $\frac{1}{2}n(n-1)$ non-removable phases for pure Majorana neutrinos [29]. Furthermore, for exactly massless neutrinos, any mixing can be “rotated away” by a suitable redefinition of the fields.

We point out that while the mixing expression, Eq. (1.10), is an *exact* relation among the neutrino fields, there exists in general no such relation among the neutrino *states*; in fact, a Fock space of flavour neutrino states does not exist [30]. The states which we are referring to here are defined in the mathematical sense of the “single particle states” which are obtained by letting canonical creation operators act on the vacuum. No such states exist because one cannot define appropriate canonical creation and annihilation operators. Thus one ought not to speak of, for example, an “electron neutrino” as being produced in a certain experiment. Rather, a ν_1 is produced with a given amplitude, a ν_2 is produced with a given amplitude, et cetera. The ν_i are the “physical” particles which are produced and which propagate with well-defined dispersion relations. For relativistic neutrinos these considerations may be overlooked, since in that case it is possible to construct “approximate” flavour eigenstates [30]. In the conventional treatment of neutrino oscillations for relativistic neutrinos, for example, this point may be (and is) ignored completely.

In the remainder of this thesis we shall always assume, unless otherwise stated, that neutrinos are both massive and mixed. These assumptions lead quite naturally to the phenomenon of “neutrino oscillations.”

1.2 Neutrino Oscillations

Oscillation phenomena are well-known in physics and typically occur because the initial and final states in a given experiment are not eigenstates of the Hamiltonian. Since such states are not “stationary,” the overlap of the initial state with the time-evolved state

is in general not unity, but oscillates in time. Thus, for example, a spin placed in a magnetic field precesses if it is not initially aligned with the direction of the magnetic field. The same reasoning may be applied in the case of particle oscillations. In the kaon system, for example, the initial state produced in an experiment is either the K^0 or the \bar{K}^0 , but the eigenstates of the free Hamiltonian are the K_L and the K_S , which are linear combinations of the K^0 and \bar{K}^0 and which are nearly (but not quite) degenerate in mass. If one calculates the probability of detecting a K^0 as a function of time, one finds that this probability does in fact oscillate. This fact has also been confirmed experimentally [31].

1.2.1 Neutrino Oscillations in Vacuum

In the following we outline the “conventional” derivation of the formula describing neutrino oscillations in vacuum, considering the case in which there are two neutrino flavours whose mixing is parametrized by an angle θ . The more general case with extra neutrino flavours follows in complete analogy. Taking the mixing relation (1.10) to be a relation among *states*, we have

$$\begin{aligned} |\nu_e\rangle &= \cos\theta|\nu_1\rangle + \sin\theta|\nu_2\rangle, \\ |\nu_\mu\rangle &= -\sin\theta|\nu_1\rangle + \cos\theta|\nu_2\rangle, \end{aligned}$$

where $|\nu_{1,2}\rangle$ represent the states with definite masses $m_{1,2}$. Suppose we produce an electron neutrino at time $t=0$ and we wish to know the probability to detect an electron neutrino at some later time. Since the mass eigenstates are eigenstates of the Hamiltonian, their time development is well-defined and we obtain

$$P_{\nu_e \rightarrow \nu_e}(t) = |\langle \nu_e | \nu_e(t) \rangle|^2 = 1 - \sin^2(2\theta) \sin^2\left(\frac{\Delta E t}{2}\right), \quad (1.11)$$

where $\Delta E = \sqrt{p_2^2 + m_2^2} - \sqrt{p_1^2 + m_1^2}$. The probability of observing a muon neutrino at time t is similarly given by

$$P_{\nu_e \rightarrow \nu_\mu}(t) = |\langle \nu_\mu | \nu_e(t) \rangle|^2 = \sin^2(2\theta) \sin^2\left(\frac{\Delta E t}{2}\right), \quad (1.12)$$

so that the sum of the probabilities is unity, as it ought to be. Assuming that the neutrinos are produced with equal momentum p and that they are relativistic, we find

$$\Delta E \simeq \frac{\Delta m^2}{2p}, \quad (1.13)$$

where we have set $\Delta m^2 \equiv m_2^2 - m_1^2$. Noting that experimentally one would observe spatial, not temporal, oscillations we set $t \approx x$ (the neutrinos are relativistic) and obtain the well-known vacuum oscillation formula

$$P_{\nu_e \rightarrow \nu_e}^{\text{vac}}(x) = 1 - \sin^2(2\theta) \sin^2(\pi x / L_{\text{osc}}^{\text{vac}}), \quad (1.14)$$

where $L_{\text{osc}}^{\text{vac}}$ is the “vacuum oscillation length”,

$$L_{\text{osc}}^{\text{vac}} = \frac{4\pi p}{\Delta m^2} \simeq 2.48 \left(\frac{p}{1 \text{ MeV}} \right) \left(\frac{1 \text{ eV}^2}{\Delta m^2} \right) \text{ m}. \quad (1.15)$$

Typical energies for solar neutrinos are in the MeV range. Since the mass-squared splitting is simply unknown, the oscillation length could easily vary from meters ($\Delta m^2 \sim 1 \text{ eV}^2$) to hundreds of thousands of kilometers ($\Delta m^2 \sim 10^{-8} \text{ eV}^2$.)

In order for the vacuum oscillations of neutrinos to solve the solar neutrino problem, the mixing angle θ needs to be rather large. Suppose that the mass-squared splitting is moderate, so that the oscillation length is small compared to the earth-sun distance. Since neutrinos are expected with a range of energies, and since they are produced at different initial positions within the sun, the oscillations would tend to be smeared out so that all that would be observed on earth would be the average flavour-conserving probability

$$\langle P_{\nu_e \rightarrow \nu_e}^{\text{vac}} \rangle = 1 - \frac{1}{2} \sin^2(2\theta). \quad (1.16)$$

At best, this could reduce the initial flux by a factor of one half (although one could do better by incorporating another neutrino flavour.) Alternatively, if the mass-squared splitting were extremely tiny, then the oscillation length could be on the order of the earth-sun distance. In that case one would observe a large loss of flux if the earth-sun distance were close to one of the minima of Eq. (1.14). Furthermore, for a sufficiently mono-energetic neutrino beam, one could conceivably observe the actual oscillations of the electron neutrino flux due to the 3% annual variation of the earth-sun distance. We will examine this possibility, as well as some of the interesting physics questions associated with it, in Chap. 2.

If the mixing angle θ is small, then it would appear that neutrino oscillations could not account for the large deficit of neutrinos from the sun. Following a clever observation by Wolfenstein [15], however, Mikheyev and Smirnov [16] showed that it is possible to have nearly complete conversion of electron- to muon-type neutrinos *inside* the sun due to a resonant effect, *no matter how small the mixing angle*, provided the mixing angle and mass-squared difference are non-zero. This effect is now known as “the MSW effect.”

1.2.2 Matter Enhanced Oscillations and the MSW Effect

Neutrinos propagating in some medium interact with it only via the weak interactions. The magnitude of the incoherent interaction with the medium is incredibly tiny, since the cross-section for scattering is proportional to G_F^2 , where G_F is the Fermi coupling constant. As a result, a neutrino could typically pass through several *million* suns before being scattered even once! One might suppose, then, that the matter in the sun could have very little effect on the propagation of a neutrino as it exits the sun’s core. As it happens, however, there is an effect due to the *coherent* interactions with the medium which can be rather sizeable, since it is proportional to G_F , not G_F^2 . These coherent interactions with the medium are not scattering events *per se*, since by definition coherent

interactions must leave the medium in the same state. The net effect of the coherent interactions with the background is to give the neutrino an “index of refraction” as it passes through the medium.

The original observation of Wolfenstein [15] was that the indices of refraction corresponding to different neutrino flavours in a given medium would in general not be equal. The resulting mismatch in the phases of the waves corresponding to different neutrino flavours can then lead to a *resonant enhancement* of the neutrino oscillation formula. Thus, even for a small (vacuum) mixing angle, the presence of the medium can lead to large-amplitude oscillations. This is rather remarkable!

For relativistic neutrinos in matter one can derive the formula for the neutrino index of refraction in perfect analogy with the derivation of the index of refraction of light in a medium [32] to obtain

$$n_\nu = 1 + \frac{2\pi\rho f(0)}{p^2}, \quad (1.17)$$

where ρ is the number density of the scatterers in the medium, p is the neutrino’s momentum and $f(0)$ is the forward scattering amplitude for the neutrino incident on the scatterer ².

In general there are two types of interactions which contribute to n_ν , those due to Z^0 (“neutral-current”) exchange and those due to W^\pm (“charged-current”) exchange. Fig. 1.1 shows the Feynman diagrams for these two cases. In the case which is typically of interest the background contains electrons, but no muons, so that only the electron neutrino gets a contribution due to the charged current process. This is what leads to the mismatch between the indices of refraction for the electron and muon neutrinos. For future reference we note that a simple calculation of the charged current diagram in

²For non-relativistic neutrinos or for ultra-high densities (like those in a neutron star, for example) the “index of refraction” concept is not as helpful. Chap. 4 is devoted to a general analysis which examines the propagation of neutrinos under such conditions.

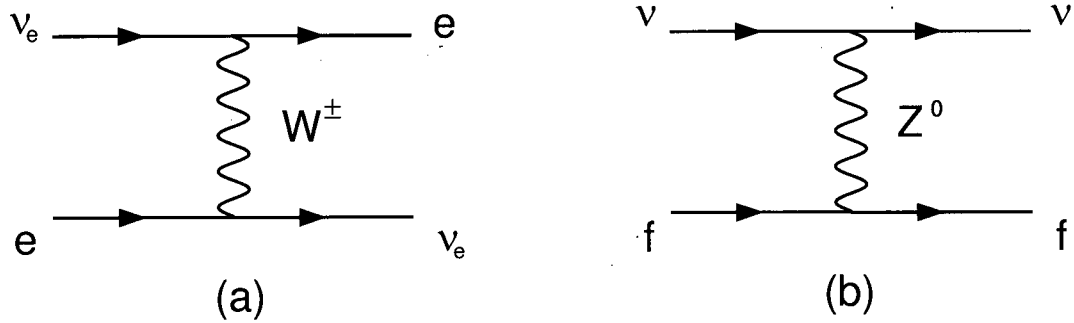


Figure 1.1: Neutrino weak interactions in a medium through (a) charged-current and (b) neutral-current exchange. In (b), “f” stands for all fermions in the medium.

Fig. 1.1(a) yields

$$f_{c.c.}(0) = \frac{G_F p}{\sqrt{2}\pi}. \quad (1.18)$$

For a constant-density background medium, the neutrino oscillation formula may be found by first inserting the neutrino indices of refraction into a Schrödinger-like equation as follows [33]

$$i \frac{d}{dt} \begin{pmatrix} |\nu_e\rangle \\ |\nu_\mu\rangle \end{pmatrix} = \left[\frac{1}{2p} \mathcal{U} \begin{pmatrix} m_1^2 & 0 \\ 0 & m_2^2 \end{pmatrix} \mathcal{U}^\dagger + \begin{pmatrix} p n_{\nu_e} & 0 \\ 0 & p n_{\nu_\mu} \end{pmatrix} \right] \begin{pmatrix} |\nu_e\rangle \\ |\nu_\mu\rangle \end{pmatrix}, \quad (1.19)$$

where the mixing matrix \mathcal{U} is given by

$$\mathcal{U} = \begin{pmatrix} \cos \theta & \sin \theta \\ -\sin \theta & \cos \theta \end{pmatrix}. \quad (1.20)$$

Eq. (1.19) may be diagonalized by setting

$$\begin{aligned} |\nu_e\rangle &= \cos \theta_m |\nu_1^m\rangle + \sin \theta_m |\nu_2^{rmm}\rangle, \\ |\nu_\mu\rangle &= -\sin \theta_m |\nu_1^m\rangle + \cos \theta_m |\nu_2^m\rangle, \end{aligned}$$

where θ_m is the neutrino mixing angle in matter, defined by

$$\sin^2(2\theta_m) = \frac{(\Delta m^2 \sin(2\theta))^2}{(A - \Delta m^2 \cos(2\theta))^2 + (\Delta m^2 \sin(2\theta))^2}, \quad (1.21)$$

with

$$A \equiv 2p^2(n_{\nu_e} - n_{\nu_\mu}) = 2\sqrt{2}pG_F\rho_e, \quad (1.22)$$

in which ρ_e is the number density of electrons in the medium. The key point to note is that only the *difference* between the indices of refraction is important. Since the neutral-current contributions are equal for the two neutrino flavours, they cancel, leaving only the charged-current piece. This is why the expression (1.22) depends only on the density of electrons. Proceeding as we did in the case of vacuum oscillations, we find that the electron neutrino survival probability in matter has a form similar to Eq. (1.14),

$$P_{\nu_e \rightarrow \nu_e}^{\text{mat}}(x) = 1 - \sin^2(2\theta_m) \sin^2\left(\pi x/L_{\text{osc}}^{\text{mat}}\right), \quad (1.23)$$

where the oscillation length in matter is defined to be

$$L_{\text{osc}}^{\text{mat}} = \frac{\Delta m^2 L_{\text{osc}}^{\text{vac}}}{\left[(A - \Delta m^2 \cos(2\theta))^2 + (\Delta m^2 \sin(2\theta))^2\right]^{1/2}}. \quad (1.24)$$

Eqs. (1.21) and (1.22) show that $\sin^2(2\theta_m)$ varies as a function of the background density and is equal to unity when

$$A = A^{\text{res}} \equiv \Delta m^2 \cos(2\theta), \quad (1.25)$$

that is, when

$$\rho_e = \rho_e^{\text{res}} \equiv \frac{\Delta m^2 \cos(2\theta)}{2\sqrt{2}pG_F}. \quad (1.26)$$

When this condition is satisfied, the electron neutrino survival probability varies between zero and one, and hence we say that the oscillations have been “resonantly enhanced,” with Eq. (1.26) defining the resonance condition.

Mikheyev and Smirnov [16] extended the analysis of Wolfenstein, allowing the density of the background medium to vary with position. In particular, they showed that if an electron neutrino is emitted in a region of high electron density ($\rho_e \gg \rho_e^{\text{res}}$) and if it

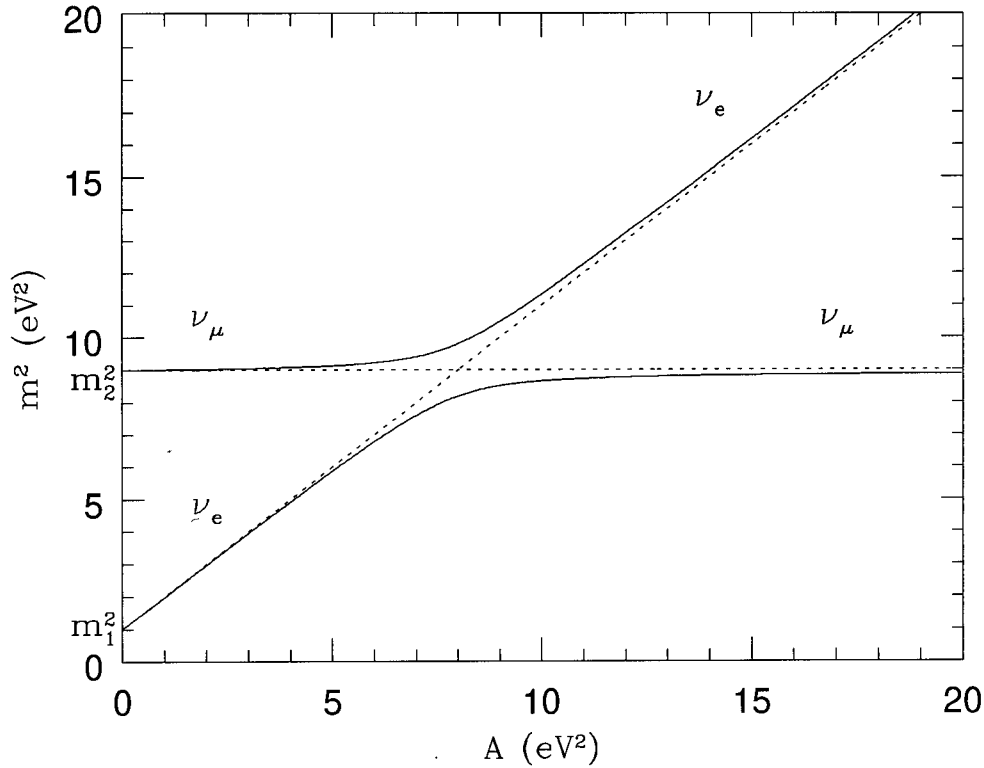


Figure 1.2: Plot of the effective mass squared for the two “matter eigenstates” as a function of $A \propto \rho_e$, with $m_1=1$ eV and $m_2=3$ eV. The solid line corresponds to $\theta=0.1$ and the dotted line to $\theta=0$.

propagates across the resonance to a region of low electron density, then it may be almost completely converted into a muon neutrino. The efficiency of the conversion depends in part on how quickly the density varies in the vicinity of the resonance. Mikheyev and Smirnov’s main observation follows from a straightforward application of the “adiabatic theorem” [34]. The adiabatic theorem says that if a state is prepared in an eigenstate of the Hamiltonian at some initial time and if some parameter of the theory is varied sufficiently slowly, then the state will “follow” the evolution of the eigenstate. In our case this means that if an electron neutrino is emitted at some very high density (so that $\nu_e \approx \nu_2^m$) and if its propagation across the resonance can be considered “adiabatic,”

then when it gets to a region of very low density, it will be in the state $\nu_2 \approx \nu_\mu$ (for small θ .) This phenomenon is demonstrated by the plot in Fig. 1.2, which shows the effective mass squared of the neutrino matter eigenstates plotted as a function of A , which is proportional to the electron density. A neutrino which undergoes adiabatic conversion stays on one of the solid curves as it moves through the resonance from higher to lower density. The resonant conversion of electron- to muon-type neutrinos is known as the MSW effect.

It is well-known in general how to calculate corrections to the adiabatic approximation [35]. In the neutrino case, the corrections lead to the following expression for the average flavour-conserving probability for a neutrino which is emitted in a region of high density and which propagates out to the vacuum [33]

$$\langle P_{\nu_e \rightarrow \nu_e}^{\text{adiab}} \rangle = \frac{1}{2} + \left(\frac{1}{2} - P_c \right) \cos(2\theta) \cos(2\theta_m), \quad (1.27)$$

where P_c is the “jump probability” [36], which gives the probability to have a *nonadiabatic* transition. This probability is calculable and depends on the rate of change of the density at resonance.

Very extensive numerical studies have been performed which examine the MSW effect using realistic density profiles for the sun. All of the current solar neutrino data can be accommodated in a two-neutrino model with just two parameters, Δm^2 and $\sin^2(2\theta)$. There are two favoured regions of the parameter space (the so-called “small-angle” and “large-angle” solutions), given approximately by [14]

$$\Delta m^2 \sim 6 \times 10^{-6} \text{eV}^2, \quad \sin^2(2\theta) \sim 7 \times 10^{-3} \quad (\text{solar}) \quad (1.28)$$

$$\Delta m^2 \sim 2 \times 10^{-5} \text{eV}^2, \quad \sin^2(2\theta) \sim .8 \quad (\text{solar}). \quad (1.29)$$

Independent fits to the atmospheric neutrino data typically require [37, 20, 21]

$$\Delta m^2 \sim (.5 - 5) \times 10^{-2} \text{eV}^2, \quad \sin^2(2\theta) \sim (.5 - 1) \quad (\text{atmospheric}), \quad (1.30)$$

so that in order to reconcile the two ranges it is necessary to go to a three-neutrino model. That this is possible has been shown in Refs. [20, 21].

In addition to the above indirect “hints” that neutrinos could be massive and mixed, there has also been a recent report of evidence for $\bar{\nu}_\mu \rightarrow \bar{\nu}_e$ oscillations at the Liquid Scintillator Neutrino Detector (LSND) experiment at the Los Alamos Meson Physics Facility (LAMPF) [28]. In this experiment muon anti-neutrinos are produced by the decays of anti-muons at rest. The detector, placed about 30 m from the source, searches for electron anti-neutrinos via the reaction $\bar{\nu}_e p \rightarrow e^+ n$. The LSND collaboration reports the observation of 22 such events with a total estimated background of 4.6 ± 0.6 events. The main region of the two-neutrino parameter space which is consistent with their data is bounded by $5 \times 10^{-2} \text{ eV}^2 < \Delta m^2 < 3 \text{ eV}^2$ and $2 \times 10^{-3} < \sin^2(2\theta) < 1$, which is marginally consistent with the region of parameter space typically used to resolve the atmospheric neutrino anomaly (see (1.30).)

1.3 A Closer Look

In the preceding sections we have given a fairly brief overview of neutrino physics, having focused in particular on the phenomenon of neutrino oscillations. We have so far shown that neutrino oscillations are of interest because, at the very least, they might provide the resolutions to two current outstanding problems in physics, namely the solar neutrino problem and the atmospheric neutrino anomaly. We would argue, however, that the oscillation phenomenon is a fascinating subject in its own right because it involves many subtle questions of quantum mechanics and quantum field theory. The more or less “standard” derivations presented up to this point gloss over most of these subtleties, but now we shall examine some of them in greater detail.

1.3.1 Neutrino Oscillations and the Uncertainty Principle

The first issue which we will examine has to do with the coherence between the mass eigenstates. In our above derivation of neutrino oscillations we assumed that the amplitudes for the various mass eigenstates to propagate from the production to the detection points should be added *coherently*. Indeed, if the neutrinos are viewed as “exchange” particles in the over-all interaction this would appear to be quite natural. But suppose a very precise measurement of the momenta of all of the other particles involved in either the production or detection process could be made. This would in principle allow for a determination of the mass of the exchanged neutrino and would thus destroy the coherence between the various mass eigenstates. If such a measurement could be made, the oscillations would somehow have to be wiped out. But what is the mechanism whereby this would occur?

The question of how an accurate measurement of the neutrino’s mass destroys the oscillations of neutrinos was first considered in a famous paper by Kayser [38]. The solution to the problem follows from a straightforward application of the uncertainty principle. Suppose that we wish to observe neutrino oscillations as a function of the distance between the production and detection points in a given experiment. In order that the oscillations not be immediately washed out, we must require that the uncertainties in the positions of both the production and detection points be much less than the oscillation length,

$$\Delta x \ll L_{osc}^{vac}. \quad (1.31)$$

This in turn requires that the uncertainty in the neutrino’s momentum satisfy

$$\Delta p \gg \frac{1}{L_{osc}^{vac}} = \frac{m_2^2 - m_1^2}{4\pi p}. \quad (1.32)$$

But now suppose that a very accurate measurement of the energies and momenta of the

other particles involved in the production or detection is made, allowing for a determination of the neutrino's mass squared

$$m_\nu^2 = E_\nu^2 - p_\nu^2. \quad (1.33)$$

If the errors in the momentum and energy are uncorrelated, then the error in the squared mass is

$$\delta m_\nu^2 = 2E_\nu \Delta E_\nu + 2p_\nu \Delta p_\nu. \quad (1.34)$$

In order to be able to differentiate experimentally between the two masses, we require that $\delta m_\nu^2 \leq m_2^2 - m_1^2$, which, together with (1.34), yields

$$2p_\nu \Delta p_\nu \leq \delta m_\nu^2 \leq m_2^2 - m_1^2, \quad (1.35)$$

so that

$$\Delta p_\nu \leq \frac{m_2^2 - m_1^2}{2p}, \quad (1.36)$$

which violates the relation (1.32) (neglecting a factor of 2π .) Thus, as soon as a sufficiently precise determination of the neutrino's mass can be made, the uncertainty principle requires the uncertainty in the neutrino's position to be of the same order as the oscillation length and the oscillations are completely washed out.

The above discussion highlights the fact that any realistic discussion concerning neutrino oscillations necessarily assumes that the neutrinos involved have some finite width in momentum and energy, that is, they may be described by wave packets. This observation follows from our above comments, but is clear also from an extreme example: if the neutrinos are taken to have, for example, perfectly well-defined momenta, then they may be described by (infinite) plane waves and so it is non-sensical to talk about oscillations as a function of distance. In the following subsection, we start to examine the importance of adopting a clear and self-consistent approach to particle oscillations by considering an example in the $B-\bar{B}$ system.

1.3.2 An Apparent Ambiguity in the $B-\bar{B}$ System

Given our discussion in the previous section concerning neutrino oscillations and the uncertainty principle, it is clear that any treatment of neutrino oscillations which employs only plane waves must be treated with some care. An amusing example of what can go wrong has recently been discussed by Lipkin [39]. Lipkin considers the “conventional” treatment of $B-\bar{B}$ oscillations and shows that there is some ambiguity in how one ought to convert the oscillation probability which is calculated – which is a function of time – into one which is a function of position. The latter probability is one which corresponds to something which can be measured in an experiment while the former describes a “non-experiment.”

The conventional calculation of $B-\bar{B}$ oscillations proceeds in the same way as that for neutrinos. We shall for simplicity neglect the effects due to CP violation and to the finite lifetimes of the two mass eigenstates, B_L and B_H . We define

$$\begin{aligned} |B^0\rangle &= (1/\sqrt{2})(|B_L\rangle + |B_H\rangle), \\ |\bar{B}^0\rangle &= (1/\sqrt{2})(|B_L\rangle - |B_H\rangle), \end{aligned}$$

and suppose that a B^0 is produced at $t=0$. In the usual approach, the probability to detect a \bar{B}^0 as a function of time is then given by³

$$P_1(t) \equiv |\langle \bar{B}^0 | B^0(t) \rangle|^2 = \frac{1}{4} |e^{-iE_L t} - e^{-iE_H t}|^2 = \sin^2 \left(\frac{(m_H^2 - m_L^2)t}{2(E_L + E_H)} \right), \quad (1.37)$$

with $E_{L,H} = \sqrt{p^2 + m_{L,H}^2}$. In order to convert this to a function of x , we may take

$$x = vt = \frac{p t}{\frac{1}{2}(E_L + E_H)}, \quad (1.38)$$

³Lipkin actually calculates the ratio of the probabilities to detect a \bar{B}^0 or a B^0 , but the essence of the argument is unchanged in the case which we examine.

where v is the average velocity of the two eigenstates, so that the oscillation probability in space is then given by

$$P_1(x) = \sin^2 \left(\frac{(m_H^2 - m_L^2)x}{4p} \right). \quad (1.39)$$

This is the result which is usually obtained. One could alternatively argue that the two mass eigenstates will travel at different speeds and so will arrive at a given position at *different* times, with

$$x = \frac{p}{E_L} t_L = \frac{p}{E_H} t_H. \quad (1.40)$$

Thus we could define

$$P_2(t_L, t_H) = \frac{1}{4} \left| e^{-iE_L t_L} - e^{-iE_H t_H} \right|^2, \quad (1.41)$$

so that

$$P_2(x) = \sin^2 \left(\frac{E_H t_H - E_L t_L}{2} \right) = \sin^2 \left(\frac{(m_H^2 - m_L^2)x}{2p} \right). \quad (1.42)$$

The oscillation length in the above expression differs from that in (1.39) by a factor of two! This analysis goes through nearly unchanged for the case of neutrinos and again gives an ambiguous factor of two in the oscillation length. Furthermore, similar factors of two have come up recently in calculations dealing with oscillations in the kaon system [40]; in these latter cases, the extra factor of two is argued (incorrectly) to be a real effect. Note that in the case of the oscillations of neutral mesons, the presence or absence of the factor of two affects the value which is inferred from experiments for the mass-squared difference between the mass eigenstates.

Lipkin's main point in his calculation is to emphasize that the ambiguity in question simply does not come up if the calculation is performed directly as a function of distance instead of as a function of time. He argues on kinematical grounds that in general the energies of the two mass eigenstates should be taken to be the same and that their momenta should be taken to be different. When the resulting phase difference between

the two mass eigenstates is calculated, it is automatically then a function of distance. The oscillation probability resulting from such considerations is found to agree with Eq. (1.39), which is the “usual” result with no factor of two.

The method proposed by Lipkin – in which the energies of the mass eigenstates are taken to be equal so that oscillations are calculated directly in space – yields the correct result. It does not, however, really provide any insight into what goes wrong with the former calculation. Lowe, *et al.* [42] have recently argued that the ambiguous factor of two which appears may be resolved by looking at the wave functions which are interfering in order to give rise to the oscillations. In the first approach (see Eq. (1.37)), the terms which are interfering correspond to the same space-time point and the resulting expression leads to the correct formula for the oscillation probability. In the second case (see Eq. (1.41)), the interference terms are due to wave functions corresponding to *different* space-time points. They argue that this is simply incorrect and thus yields the wrong answer. Wave functions corresponding to different space-time points cannot interfere ⁴.

But the question remains: How does one correctly model the fact that the two mass eigenstates may in general arrive at the detector at different times? The answer is that this simply can't be done using plane waves; wave packets are required ⁵. In general the two mass eigenstates *will* arrive at different times, given by $t_i = x/v_i$. The oscillating piece in the oscillation probability does not come from either of the “peaks” of the wave packets, however. It comes from the interference term between the two wave packets and

⁴The situation would appear to be a bit more subtle than this, since *amplitudes* corresponding to different space-time points are routinely allowed to interfere in particle physics. A generic calculation of the amplitude for some scattering event involves an integral over all of space-time so that the square of this amplitude effectively allows pieces corresponding to different space-time points to interfere. Nonetheless, the ad hoc prescription which leads to Eq. (1.42) is incorrect.

⁵Lipkin's point of view is that in order for oscillations to be observed, there needs to be nearly a 100 % overlap between the mass eigenstate wavepackets [43]. In this case the wave packets may be assumed to arrive at the same time. In general, however, the peaks of the wave packets could be separated.

thus gets its main contribution from some time intermediate between t_1 and t_2 . A consistent approach to calculating the oscillation probability as a function of distance needs somehow to give a correct prescription for how one ought to sum up the contributions corresponding to different times.

1.4 Outline of the Remainder of the Thesis

In this chapter we have given a brief introduction to the physics of neutrinos. We have noted that if neutrinos are indeed massive, then it is quite natural to suppose that they are also “mixed”, that is, that the neutrino fields involved in the weak interactions are linear combinations of the “mass eigenstate” fields. We have shown that such mixing leads quite generally to “neutrino oscillations”: if a neutrino of a given flavour is produced, there is a non-zero probability that it may be detected as having a different flavour at some later time. Furthermore, this probability oscillates with the distance between the source and detector. We then considered the generalization of the neutrino oscillation formula to the case in which the neutrino propagates in matter. It was shown that the coherent scattering off the background could give rise to an enhancement of the neutrino oscillations (the MSW effect.) We then discussed how neutrino oscillations could be used to resolve the so-called “solar neutrino problem” and “atmospheric neutrino anomaly.”

In Sec. 1.3 we returned to a discussion of neutrino oscillations and examined the relation between neutrino oscillations and the uncertainty principle. It was argued that any realistic discussion of particle oscillations must assume that the particles themselves are localized to some extent, that is, that they should be described by wave packets, not plane waves. An example of what can go wrong in a plane wave approach was then examined. It was found that attempting to model the effects due to the localization of the particles using only plane waves can lead to errors. In the specific case which we

studied, of oscillations in the $B - \bar{B}$ system, it was found that confused reasoning could in fact lead to a relative factor of “two” in the oscillation length.

The plan of the remainder of the thesis is as follows. We begin in Chap. 2 by considering whether it is possible to observe the oscillations between the sun and the earth of the mono-energetic neutrinos produced by Beryllium decay in the sun. In order to observe such oscillations it is necessary that the energy spread of the initial “beam” not be too wide. We summarize the various sources of energy broadening for these neutrinos and then consider in general whether it is possible to distinguish experimentally between the two basic types of broadening – “coherent” and “incoherent” – at the detector. It is shown that while such effects are due to distinct physical processes which could in principle be controlled at the source, they are in general indistinguishable at the detector.

In Chap. 3 we construct a simple model of a neutrino source/detector system which allows us to rigorously define the oscillation probability in terms of the distance between the source and detector. In order to motivate our study, we first examine two other approaches to the problem which do not explicitly include the source and detector. In both cases we find that there are difficulties which arise and which do not seem to have a straightforward solution. We find that the approach which directly employs a source and detector has several advantages, the main one of which is that the objects which are calculated have very clear physical meanings. Furthermore our approach gives several insights into the effects of the time resolution of the detector.

Chap. 4 contains a study of the propagation of neutrinos in very dense media. We find that in general the dispersion relations of such neutrinos have minima at non-zero values of the momentum; this feature leads to several amusing results. Furthermore, we observe that for Dirac neutrinos the minimum of the dispersion relation is generically below the vacuum mass of the neutrino so that neutrinos with small enough energy will be trapped by the medium. It is found that Majorana neutrinos are in general not trapped by the

medium.

Chap. 5 contains a brief summary of our main results and some concluding remarks.

Chapter 2

Coherence Effects in Neutrino Oscillations

2.1 Introduction

Approximately twenty-five years ago an interesting suggestion was made for probing very small values of Δm^2 using the 3% annual variation of the earth–sun distance [19, 45]. In this case, rather than simply observing a net average decrease in the electron neutrino intensity by an amount $\sin^2(2\theta)/2$ one could observe the actual oscillations of the electron neutrino flux. The idea is to use the ν_e 's from e^- capture on Be



which results in a neutrino energy $E_\nu \sim .86$ MeV with a small energy spread. Thus if the neutrino oscillation length

$$L_{\text{osc}} = \frac{4\pi E_\nu}{\Delta m^2} \quad (2.2)$$

is within one or two orders of magnitude of the variation $\Delta R \sim 5 \times 10^{11}$ cm of the earth–sun distance then, depending on the value of $\sin^2(2\theta)$, it may be possible to see the neutrino oscillations provided Δm^2 is in the range $10^{-9} - 10^{-11} \text{eV}^2$.

In order for the above scenario to work, it is essential that the spread in energy ΔE of the neutrino “beam” is not too wide. This is especially true in this case since $R/\Delta R \gg 1$. If ΔE is too large then by the time the neutrinos arrive at the earth the oscillation patterns for neutrinos of different energies get sufficiently out of phase to wipe out any potentially observable oscillations. This results simply in a decrease of the total ν_e intensity by an amount $\sin^2(2\theta)/2$. A coherence length L_{max} is usually defined as

the distance at which a neutrino of energy E has undergone one oscillation more than a neutrino of energy $E + \Delta E$. This coherence length is given by

$$L_{\max} = \frac{4\pi E^2}{(\Delta m^2) \Delta E} = L_{\text{osc}} \left(\frac{E}{\Delta E} \right) \quad (2.3)$$

and the total number of complete oscillations will be

$$N_{\max} = \frac{L_{\max}}{L_{\text{osc}}}. \quad (2.4)$$

Thus when $\Delta E/E$ is larger than about $1/30$ we can no longer observe the oscillations and a narrow energy range ΔE is therefore required.

The above argument assumed that the energy spread of the neutrino beam is incoherent in origin in the sense that it is due to slightly different energies of various neutrinos. The main origin of this energy spread ΔE is that the continuum electrons which are captured by the Be have an energy spread $\Delta E_e \sim kT$ which translates into a similar spread $\Delta E_\nu \sim kT$ of the emerging neutrino energies. Another slightly smaller contribution to $\Delta E_\nu \equiv \Delta E$ originates from the different Doppler shifts due to thermal nuclear velocities (relative to the line of sight). This phenomenon is an analog of the well-known Doppler broadening in atomic spectroscopy[46].

It is also possible for “coherent broadening”—by which we mean the quantum mechanical spread δE of a **single** neutrino – to lead to the loss of the oscillation pattern[47]. The well known natural line width in atomic spectroscopy:

$$\delta E \sim \Gamma \sim (\tau_{\text{decay}})^{-1} \quad (2.5)$$

is an example of coherent broadening. The finite lifetime τ_{decay} of the level interrupts the classical emission of the wave-train and limits the size of the wave packet δx to

$$\delta x = c\tau_{\text{decay}}. \quad (2.6)$$

Another example of coherent broadening is the collisional broadening (also known as the “pressure broadening”) of the neutrino line. It stems from the interruption of coherent emission by collisions of the emitting atoms. The corresponding wave packet size is given by an analog of Eq. (2.6) but with τ_{decay} replaced by $t_{\text{collision}}$ – the effective time interval between “relevant collisions”. This (nuclear) collisional broadening effect has been extensively studied as the major contributor to the loss of coherence in neutrino oscillations. There have been various estimates of the strength of the effect leading to estimates of the size of $\delta x = ct_{\text{collision}}$ [47, 48, 46, 49].

A third contribution to the coherent broadening which seems likely to contribute even more to the energy spread δE of the neutrino wave packet is the small size of the wave packets of the captured electrons. Since the K electron ionization energy in beryllium $E_{\text{ion}} = Z^2 R_y = 16 R_y \sim 250 \text{ eV}$ is small in comparison with the thermal $kT \sim \text{keV}$ energy, the capture in reaction (2.1) is primarily that of continuum electrons. An electron wave packet of size δ_e will traverse the (point like) nucleus in a time

$$\delta t = \frac{\delta_e}{v_e} \quad (2.7)$$

where v_e is the velocity of the electron. Because the weak interaction underlying the capture process (2.1) is local, the time available for the ν_e emission is δt and the size of the outgoing ν_e wave packet will be

$$\delta_\nu = \delta t \times c = \frac{\delta_e}{v_e}. \quad (2.8)$$

The thermal kinetic energy of a typical electron is $\frac{1}{2}m_e v_e^2 \sim \frac{3}{2}kT$. Thus

$$v_e = \sqrt{\frac{3kT}{m_e}} \sim .08 \quad (2.9)$$

In order to estimate the appropriate wave packet size δ_e to be used in Eq. (2.7), we note that the electrons suffer many random collisions in the hot core which tend to localize

the wave function and reduce the wave packet size. If the only information available is that the electrons are in thermal equilibrium then δ_e is expected to be of the order of the thermal wave length, given by

$$\delta_e \sim \frac{2\pi}{m_e v_e} \sim \frac{2\pi}{\sqrt{3m_e kT}} \quad (2.10)$$

which then leads to a neutrino wave packet size

$$\delta_\nu = \frac{2\pi}{\delta E_\nu} \sim 6 \times 10^{-8} \text{cm}. \quad (2.11)$$

This δ_ν is **smaller** (and the corresponding coherent broadening is **larger**) than all previous estimates ¹.

The three mechanisms described above all lead to the conclusion that neutrinos are emitted in the sun as wave packets with a rather small size δ_ν corresponding to “coherent broadening” of the neutrino line by an amount $\delta E \sim 2\pi/\delta_\nu$. This coherent broadening also leads to the loss of the oscillation pattern[47] after a coherence length L_{coh} which is precisely equal to the coherence length L_{max} derived in Eq. (2.3). This result can be derived technically by decomposing the wave packet into plane waves of energy E with a probability distribution

$$P(E) = |\Psi(E)|^2 \quad (2.12)$$

and repeating the discussion leading to Eqs. (2.3) and (2.4). This leads to identical conclusions but with ΔE replaced by the energy spread δE of the distribution.

There is, however, a simple intuitive explanation for how the oscillations are lost in terms of the wave packet of the neutrino in configuration space. This derivation is originally due to Nussinov [47]. Suppose an electron neutrino wave packet is emitted at

¹Since, as we shall show, coherent broadening also leads to the loss of the oscillation pattern, it is important to note that $\delta E_\nu/E_\nu \sim .002 \ll 1/30$, which is the limit above which oscillations could not be observed.

$t = 0$ from the solar core. At $t = 0$ the ν_e can be written as a superposition of two wave packets with identical shape ² corresponding to the mass eigenstates $|\nu_1\rangle$ and $|\nu_2\rangle$.

$$|\nu_e(t = 0)\rangle = \cos(\theta)|\nu_1\rangle + \sin(\theta)|\nu_2\rangle \quad (2.13)$$

This initial wave packet will quickly spread in the directions (x, y) perpendicular to the direction of motion but the spreading in the direction of motion (z) is negligible due to Lorentz contraction effects. Due to the different mass of the ν_1 and ν_2 their wave packets travel with a different (group) velocity

$$\Delta v = v_2 - v_1 = \frac{\Delta m^2}{2E^2} \quad (2.14)$$

Thus after a time t has elapsed and the neutrino has traveled a distance $r \sim t$ from the source the two wave packets move with respect to each other by an amount

$$\Delta r = \Delta v t \sim \frac{\Delta m^2}{2E^2} r \quad (2.15)$$

Neutrino oscillations are simply the “beating” of the two wave packets as they slide relative to each other by $\Delta r = \lambda$ with

$$\lambda = \frac{2\pi}{E} \quad (2.16)$$

the wavelength of the neutrino. The oscillation length of Eq. (2.2) is then recovered as:

$$L_{\text{osc}} = \{\text{value of } r \text{ for which } \Delta r = \lambda\} = \frac{\lambda}{\Delta v} = \frac{4\pi E}{\Delta m^2} \quad (2.17)$$

The total number of possible neutrino oscillations is simply the total number of wavelengths within the wave packet, $N_{\text{max}} = \delta\nu/\lambda = E/\delta E$. After this number of oscillations the two wave packets do not overlap at all and all oscillations are lost. Thus the coherence distance L_{coh} which is the maximum distance over which we see oscillations is given by

$$L_{\text{coh}} = N_{\text{max}} L_{\text{osc}} = \left(\frac{E}{\delta E} \right) L_{\text{osc}} \quad (2.18)$$

²This assumption is excellent for relativistic neutrinos, but may not be very good if one of the neutrinos is non-relativistic. We shall discuss these issues at length in the following chapter.

which is precisely the result of Eqs. (2.3) and (2.4) for the case of incoherent energy broadening. Indeed once Δr is greater than the size δ_ν of the wave packet the ν_1 and the ν_2 will have completely separated spatially. We would thus expect that they will not interfere³ when interacting locally with an electron or nucleus in a detector.

The main aim of this chapter is to study whether the two effects discussed above, namely the incoherent versus the coherent broadening, can be distinguished. They are clearly distinct physical phenomena which can be controlled (at least in principle) at the **source**. In an Atomic Physics analog the Doppler broadening can be controlled relative to the natural line width by adjusting the temperature of the system or by confining the atoms to a narrow channel transverse to the line of sight[50]. The more interesting question is: Can we distinguish these effects at the detector? In this chapter we shall show that in all physically interesting situations the answer is “no”. We shall discuss some simple cases in which this answer is clear and then we shall prove some general theorems which will show that under a wide variety of physically attainable situations these two effects cannot be distinguished.

2.2 Coherent versus Incoherent Broadening

Our goal in this section is to see whether one can distinguish an incoherent ensemble of plane waves with a mean energy E and an energy spread ΔE from an ensemble of wave packets each with the same mean energy E and the same energy width $\delta E = \Delta E$. Before proceeding we should make one point clear. Even in the “incoherent” case in which we have an ensemble of plane waves these waves certainly do not have an infinite extent in the z direction (the direction of motion). In fact even if we took each “plane wave” (with an energy in the MeV range) to have an energy uncertainty of the order of 10^{-5}eV

³We shall see below that this intuitive idea can be incorrect in some circumstances; that is, it is possible to *revive* the oscillations of neutrinos which have separated spatially.

(which is certainly a great underestimate for the solar neutrino case) the corresponding wave packet would still be only of the order of a cm in size!! Thus when discussing “plane waves” we are in fact referring to wave packets which are much larger than those discussed in the case of coherent broadening but much smaller than any macroscopic scales in the problem.

2.2.1 An Example

Our aim will be to show that the two broadening effects discussed above cannot be distinguished. We begin with a concrete suggestion for distinguishing these effects and we then show what goes wrong with this suggestion.

Let us suppose that we were able to measure the energy of a neutrino with a precision ϵ which is much better than $\delta E = \Delta E$. We then expect that for an incoherent beam of neutrinos with energies in a range ΔE about E we could recover the oscillations by measuring the neutrino energy to the precision $\epsilon \ll \Delta E$. By plotting the observed neutrino count as a function of

$$r' = r \frac{\bar{E}}{E} \quad (2.19)$$

we should see oscillations up to a new distance

$$L_\epsilon = (E/\epsilon)L_{\text{osc}} > L_{\text{max}} \quad (2.20)$$

with no loss of statistics. Note that ΔE is replaced by ϵ in Eq. (2.3).

If, on the other hand, we began with a wave packet with energy spread δE then, at a distance larger than L_{coh} (Eq. (2.18)), the wave packet of the ν_1 and the ν_2 are completely separated and one might naively expect that there will be no oscillations even if the energy could be measured more accurately.

This argument turns out to be wrong and we can understand what goes wrong in a very intuitive way. If we choose to measure the energy very accurately (to an accuracy

ϵ) we require a time $t \sim 1/\epsilon$ to make this measurement. If, during this time t , the second wave packet arrives at the detector then we will once more see the oscillations⁴. The condition for recovering the oscillations is therefore

$$t \sim 1/\epsilon > \Delta r \sim \frac{\Delta m^2}{2E^2} r \quad (2.21)$$

where Δr is the distance between the wave packets and r is the distance from the source (Eq. (2.15)). The oscillations thus persist up to a new distance L'_ϵ which is the value of r for which Eq. (2.21) breaks down.

$$L'_\epsilon = (E/\epsilon)L_{\text{osc}} \quad (2.22)$$

which is precisely the same as the result (2.20) obtained for the incoherent neutrino beam.

This behavior of the coherent beam is analogous to what occurs for a high Q oscillator hit by two successive pulses. The first pulse (in our case the ν_1 beam) comes along and sets the oscillator in motion. It then continues to oscillate for a time $t \sim 1/\epsilon$ during which time the second pulse (in our case the ν_2 beam) arrives which then causes the oscillator to be further excited. In this way coherence is maintained between the ν_1 and the ν_2 beams even when they are spatially separated. What happens is that the accurate measurement of the energy picks out the plane wave in the wave packet which has existed coherently through both pulses.

Our main goal will be to understand how general the above result is. In other words, to what extent is it true that an ensemble of plane waves will give the same result as wave packets. Although there were some initial attempts to distinguish these processes it is now widely believed that they are indistinguishable. Our goal in this paper is to prove some theorems which clarify the conditions under which this is true and to show how general the result is.

⁴This phenomenon will be demonstrated very explicitly in the next chapter when we construct a toy model for a neutrino source/detector system.

2.2.2 Measuring Observables which Commute with Momentum

Before discussing the most general situation we review here the proof that the coherently and incoherently broadened neutrino beams lead to the same total rate and energy distributions for both ν_e 's and ν_μ 's.

Oscillations in Vacuum

Let us consider two cases representing two possible **electron** neutrino beams⁵ leaving some region of the sun at time $t = 0$. In case a we have an incoherent mixture of neutrinos each of which is a nearly ideal plane wave (with some extremely small energy spread $\delta E_{\text{pw}} \ll \delta E$). In this mixture the probability of finding a neutrino of energy E is given by some probability distribution $P(E)$ which is centered about some energy E_0 with a width ΔE . In case b all the neutrinos come with the same quantum state. This state is a wave packet with amplitude $\Psi(E)$ for a plane wave component of energy E . We choose this amplitude so that the probability distribution $|\Psi(E)|^2$ precisely matches the distribution $P(E)$ of case a. Consequently the widths of the two distributions are also equal: $\delta E = \Delta E$. In this section, for simplicity, we shall treat the plane waves of case a as ideal plane waves with $\delta E_{\text{pw}} = 0$.

At $t = 0$ the wave function for the case b is given by:

$$|\psi(t = 0)\rangle = \sum_{p,i} \alpha_{p,i} |p, i\rangle \quad (2.23)$$

where the sum (which is actually an integral) is over momenta p in the z direction (the direction of motion) and over mass eigenstates $i = 1, 2$ and the $\alpha_{p,i}$ are chosen to give an electron neutrino with the appropriate wave function at $t = 0$. Since the $|p, i\rangle$ are

⁵They could, of course, be any linear combination of electron and muon neutrinos. Electron neutrinos were chosen for definiteness only.

eigenstates of the Hamiltonian, at a later time t , the wave function is given by

$$|\psi(t)\rangle = \sum_{p,i} \alpha_{p,i} e^{-i\epsilon_p^{(i)}t} |p,i\rangle \quad (2.24)$$

where $\epsilon_p^{(i)} = \sqrt{p^2 + m_i^2}$ is the energy of ν_i with momentum p .

Suppose now that at time t we measure an observable Q which *commutes with the momentum operator*. Q may, for example, be the total number of electron neutrinos in some range of momenta. This is, in fact, the most common kind of measurement which can be made. In this case Q has only diagonal matrix elements in momentum space. Therefore the expectation value of Q at time t is given by:

$$\langle\psi(t)|Q|\psi(t)\rangle = \sum_p \left[\left(\sum_j \alpha_{p,j}^* e^{i\epsilon_p^{(j)}t} \langle p,j| \right) Q \left(\sum_i \alpha_{p,i} e^{-i\epsilon_p^{(i)}t} |p,i\rangle \right) \right] \quad (2.25)$$

The expression inside the square brackets is precisely the expression for the expectation value $\langle Q \rangle_p$ of Q for a plane wave which has a total weight (i.e. normalization) $|\alpha_{p,1}|^2 + |\alpha_{p,2}|^2$ and a *relative* amplitude $\alpha_{p,1}$ and $\alpha_{p,2}$ for ν_1 and ν_2 respectively at $t = 0$. Thus

$$\langle Q \rangle = \sum_p \langle Q \rangle_p \quad (2.26)$$

which is precisely the result one obtains for the incoherent beam of case a. Thus the measurement of any observable which commutes with momentum yields the same result for case a and case b.

Although this result may seem trivial it is in fact rather powerful. From this result we can verify the result claimed in Sec. 2.1 that if we use the variation in the earth-sun distance to look for oscillations in the neutrinos from ${}^7\text{Be}$ both the coherent and the incoherent neutrino beams give the same oscillation pattern. A-priori the above theorem is not applicable since the experiment involves measuring the spatial dependence of the neutrino flux which involves the use of an operator which does not commute with momentum. This is however an example for which the conversion of spatial to temporal

dependence can be done reliably. Thus, although we measure the spatial variation in the neutrino flux, we can compute the temporal dependence of this flux by computing, for example, the total number of electron neutrinos with a given energy as a function of time. This estimate will be reliable since, as discussed previously, even the plane wave is still extremely small (certainly much less than a cm in size) relative to the relevant astronomical scales.

Oscillations in Matter

The above proof that an ensemble of plane waves cannot be distinguished, at the detector, from an ensemble of wave packets with the same energy distribution can be extended to the case of neutrino oscillations in matter (the MSW effect)[51]. To this end imagine that at $t = 0$ an electron neutrino is produced (at the origin) in matter in which the density of electrons (along the direction of motion of the neutrino) is given by $\rho_e(z)$. (This is of course an approximation in which we neglect variations of the density in the transverse directions.) The “vacuum eigenstates” $|\nu_1\rangle$ and $|\nu_2\rangle$ are no longer eigenstates of this system. Instead one can find new eigenstates of the Hamiltonian which include the full spatial variation of the density. These eigenstates will of course no longer be momentum eigenstates. For relativistic neutrinos one should, in principle, solve the Dirac Equation but for the present discussion since spin is not a crucial variable it suffices to consider the Klein–Gordon equation[52]:

$$\left(- \left(\frac{\partial}{\partial t} + iA_m \right)^2 + \nabla^2 \right) \begin{pmatrix} \psi_e \\ \psi_\mu \end{pmatrix} = M_0^2 \begin{pmatrix} \psi_e \\ \psi_\mu \end{pmatrix} \quad (2.27)$$

where M_0 is the vacuum mass matrix and the matrix A_m accounts for the effect of charged–current scattering of the ν_e off the electrons in the medium:

$$M_0^2 = \begin{pmatrix} m_1^2 \cos^2 \theta + m_2^2 \sin^2 \theta & (m_1^2 - m_2^2) \sin \theta \cos \theta \\ (m_1^2 - m_2^2) \sin \theta \cos \theta & m_1^2 \sin^2 \theta + m_2^2 \cos^2 \theta \end{pmatrix}, \quad A_m = \begin{pmatrix} \sqrt{2}G_F\rho_e(z) & 0 \\ 0 & 0 \end{pmatrix} \quad (2.28)$$

The eigenstates of this system with energy E will no longer be eigenstates of p_z (p_x and p_y are assumed to be zero) but will be labeled by some other parameter which we call γ . We shall call these eigenstates

$$|\gamma, 1\rangle \quad \text{and} \quad |\gamma, 2\rangle \quad (2.29)$$

In the regions of space where the density vanishes these eigenstates will behave as plane waves⁶ with some momentum $p_{\text{vac}}(\gamma)$. They will correspond to vacuum mass eigenstates of the system. In a region of space in which the electron density is nonzero but nearly constant the eigenstates $|\gamma, i\rangle$ will again be nearly plane waves but now corresponding to the usual neutrino eigenstates **in matter**.

Suppose now that at $t = 0$ we prepare an electron neutrino in a state described by some rather narrow wave packet $|\psi(t = 0)\rangle$. (This is the analogue of case b above.) At $t = 0$, in analogy with Eq. (2.23), this state can be expanded in the eigenstates $|\gamma, i\rangle$ described above

$$|\psi(t = 0)\rangle = \sum_{\gamma, i} \alpha_{\gamma, i} |\gamma, i\rangle \quad (2.30)$$

We now allow the state to propagate to a later time t . At this later time the state is given by

$$|\psi(t)\rangle = \sum_{\gamma, i} \alpha_{\gamma, i} e^{-i\epsilon_{\gamma}^{(i)} t} |\gamma, i\rangle \quad (2.31)$$

where $\epsilon_{\gamma}^{(i)}$ is the energy of the state $|\gamma, i\rangle$. In any reasonable case the size of the wave packet at time t will be much smaller than the scale of variations in the electron density. (This is especially true if the measurement is made in vacuum.) Thus Eq. (2.31) amounts to an expansion in the momentum eigenstates of the neutrinos in matter with density ρ equal to the density at the location of the wave packet. Every γ corresponds to some

⁶It may in fact be a superposition of an incoming and an outgoing plane wave if there is reflection.

momentum $p(\gamma)$ which depends on the density ρ . Thus

$$|\psi(t)\rangle \simeq \sum_{p,i} \hat{\alpha}_{p,i} |p, i; \rho\rangle \quad (2.32)$$

where for any given value of p and the corresponding value of γ the coefficients $\hat{\alpha}_{p,1}$ and $\hat{\alpha}_{p,2}$ are linear combinations of $\alpha_{\gamma,1}$ and $\alpha_{\gamma,2}$.

Now suppose that at time t we measure some operator Q which commutes with (the z component of the) momentum. The off-diagonal matrix elements of Q vanish in the momentum basis. Thus Q will have only diagonal matrix elements between the various $|p, i; \rho\rangle$ in Eq. (2.32). Since each of these $|p, i; \rho\rangle$ corresponds to one of the energy eigenstates $|\gamma, i\rangle$ it follows that the expectation value of Q is given by

$$\langle \psi(t) | Q | \psi(t) \rangle \sim \sum_{\gamma} \left[\left(\sum_j \alpha_{\gamma,j}^* e^{i\epsilon_{\gamma}^{(j)} t} \langle \gamma, j | \right) Q \left(\sum_i \alpha_{\gamma,i} e^{-i\epsilon_{\gamma}^{(i)} t} | \gamma, i \rangle \right) \right] \quad (2.33)$$

This expression is analogous to Eq. (2.25) in the previous subsection. Each term in the sum is precisely the result which we would have obtained for the expectation value $\langle Q \rangle_{\gamma}$ of Q for a state which was initially in an approximate momentum eigenstate corresponding to γ but with total weight $|\alpha_{\gamma,1}|^2 + |\alpha_{\gamma,2}|^2$ and a *relative* amplitude $\alpha_{\gamma,1}$ and $\alpha_{\gamma,2}$ for ν_1 and ν_2 respectively. (Recall that the realistic plane waves are actually extremely narrow on the scale of the density variations.) Thus

$$\langle Q \rangle = \sum_{\gamma} \langle Q \rangle_{\gamma} \quad (2.34)$$

which is precisely the result one obtains for the incoherent beam of case a. There is thus no difference between the wave packet (case b) and the plane wave (case a) ensemble *even in matter* when only operators which commute with momentum are measured.

2.2.3 Unrealistic Measurements which CAN Identify Wave Packets

From the above proof it seems that a keen measurement which combines a measurement of both position and momentum information might be able to distinguish an ensemble

of wave packets from an ensemble of plane waves. The simplest way of doing this would, however, require precise knowledge of the point of origin and the time of origin of the wave packet. Suppose, for example, that we **knew** that all the wave packets in our ensemble (case b) were centered at the origin ($z = 0$) precisely at time $t = 0$. Suppose also that in the alternative scenario (case a) we also knew that each (nearly ideal) plane wave (which is still a wave packet but with a much larger spatial extent than that of case b) in the ensemble was centered at the origin at $t = 0$. Under these assumptions about our previous knowledge and by a careful timing measurement at the earth to determine the duration of the neutrino pulse we **could** distinguish the two cases. (In fact in case b there may be two separated pulses.) This scenario is, of course, totally unrealistic and we shall see below that if we allow for an uncertainty in the location of the initial packets it again becomes impossible to distinguish the two cases by *any* measurement at the earth.

There is another scenario under which it is clearly possible to distinguish the two cases. Suppose we have a detailed theory for the production mechanisms of the two cases which lead to some different observable at the source. Suppose, for example, that the position or momentum distributions for the two cases are expected to differ. Then clearly such information can be used to decide which mechanism is producing the neutrinos (or, more realistically, which mechanism dominates). However in the case of level broadening we have no such information. Both the energy and the position distributions are expected to be roughly the same. The question which we are asking is: Assume we are given two “sources” of neutrinos (or production mechanisms) with the **same** position (z) and momentum (p) distributions. Is it possible to tell by measurements at the detector which of the two “sources” produced these neutrinos?

2.2.4 General Theorem

This question can be set up more precisely as follows. Consider the following two modifications of the scenarios case a and case b discussed above:

In case A we have a nearly ideal plane wave which is actually a wave packet of a fairly large size Δz . (Recall that Δz will typically be much less than a cm!). We imagine an ensemble of such “plane waves” each of which has a nearly precise momentum (in the z direction) centered about p_0 with a spread δp . Assume that each plane wave has exactly the same spatial location. (This is precisely the case a above.)

In case B we have an ensemble of wave packets. Each wave packet has a spatial size δz which is much smaller than Δz and a corresponding momentum spread $\delta p = 1/\delta z$ which is precisely equal to the δp of case A. Up to this point this looks exactly like case b above except we now allow each wave packet in our ensemble to be, at $t = 0$, at a different spatial location. We assume that the wave packets are produced in precisely the same region Δz in which the neutrinos of case A are produced with precisely the same z distribution.⁷ The two cases are shown pictorially in Fig. 2.1.

All the above information is given to the experimenter together with the additional information that the z and p distributions for both cases are equal at $t = 0$. The statement of the theorem is then the following: With only the above information the experimenter cannot distinguish the cases A and B.

Intuitively one might guess that there should exist some experiment which could distinguish the two cases. There should be some way to tell if we are dealing with wave packets or with (almost) plane waves! But in fact this is not the case. No experiment can distinguish the above two cases.

⁷In a realistic situation both the “plane waves” of case a and the wave packets of case b will be distributed over a region of space much larger than Δz . In both cases this excess spread is incoherent. It is thus sufficient to prove our result for the case when the wave packet is distributed in z by the size Δz of the plane wave of case a.

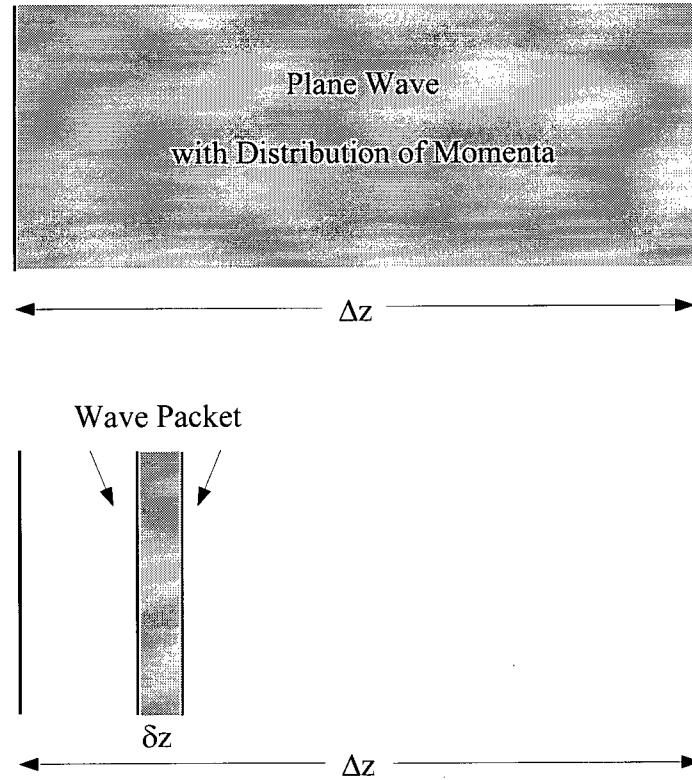


Figure 2.1: Pictorial representation of Case A and Case B in Sec. 2.2.4.

The most general proof of this statement would proceed as follows:

Step 0. Choose values for $\delta z = 1/\delta p \ll \Delta z$ and for the mean momentum p_0 which were defined above.

Step 1. Begin with an arbitrary (smooth) but fixed expression for the wave function of the nearly ideal plane wave of case A. The only constraints on this wave function will be that it is centered (say) at the origin, that its spread in position is (a fairly large) Δz with a correspondingly tiny spread in momentum about some momentum p . Then consider an ensemble of such states each with a different momentum p . Choose an arbitrary but fixed distribution for these momenta. The constraint on this distribution is that it is centered about the momentum p_0 with the given width δp .

Step 2. Construct the density matrix for the ensemble described in Step 1 above.

Step 3. One must now prove that it is always possible to construct the following, seemingly completely different ensemble, which, nonetheless, yields a density matrix identical to the one obtained in Step 2 above. We first construct a wave packet which is centered at some location z . We are free to choose the form of the wave function with the only constraint that its spread in position is approximately equal to $\delta z \ll \Delta z$ with a corresponding momentum spread $\delta p = 1/\delta z$. We then construct an ensemble of such wave packets and choose a distribution of locations z with the only constraint that this distribution be centered at the origin with a spread in position approximately equal to Δz .

The claim is that we can **always** choose the distributions in Step 3 so that the density matrix for Step 3 is identical to that of Step 2. This then implies that any measurement at all which is done on the two ensembles **at any time** t gives the same result! We also claim the converse of this theorem namely that given a “wave packet” ensemble constructed as in Step 3 it is always possible to find a “plane wave” ensemble as constructed in Step 1 with the same density matrix.

Note how the mass eigenstates ν_1 and ν_2 appear nowhere in the above discussion. The reason for this and, in our opinion, the power of this proof is that it relies entirely on properties of the system at $t = 0$ at which time the state is a pure ν_e state.

Illustration in the Simplest Case

We can show the essence of the proof by the following simple example. We model the wave packet (of case B) by a superposition of only two momentum eigenstates $|p_1\rangle$ and $|p_2\rangle$. In Step 1 above we imagine having the state $|p_1\rangle$ with probability $|\alpha|^2$ and the state

$|p_2\rangle$ with probability $|\beta|^2$; ($|\alpha|^2 + |\beta|^2 = 1$). The density matrix for this system is simply

$$|\alpha|^2 |p_1\rangle\langle p_1| + |\beta|^2 |p_2\rangle\langle p_2| \quad (2.35)$$

For implementing Step 3 we may construct an analogue of wave packets at two different locations as an ensemble consisting of these two states with equal probability:

$$|\psi_{\pm}\rangle = \alpha |p_1\rangle \pm \beta |p_2\rangle \quad (2.36)$$

The density matrix in this case

$$|\psi_+\rangle\langle\psi_+| + |\psi_-\rangle\langle\psi_-| \quad (2.37)$$

is precisely the same as the density matrix for case A in Eq. (2.35).

This completes the proof in this simple case.

Gaussian Distributions

One case in which the Steps 0-3 above can be carried out explicitly is when all distributions are Gaussian. Thus in Step 1 we choose the “plane wave” of momentum p to have a wave function

$$|p; \text{plane}\rangle = \frac{1}{(\sqrt{2\pi}\sigma)^{\frac{1}{2}}} \int dl \exp\left(-\frac{(l-p)^2}{4\sigma^2}\right) |l\rangle \quad (2.38)$$

where $\sigma \sim 1/\Delta z$. We then consider an ensemble of these states with a Gaussian distribution of momenta p

$$\frac{1}{(\sqrt{2\pi}\sigma_p)} \exp\left(-\frac{(p-p_0)^2}{2\sigma_p^2}\right) \quad (2.39)$$

where $\sigma_p \sim \delta p = 1/\delta z \gg \sigma$. The density matrix for this case (case A) is given by

$$\rho_A = \frac{1}{(\sqrt{2\pi}\sigma_p)} \frac{1}{(\sqrt{2\pi}\sigma)} \int dl dl' dp \exp\left(-\frac{(p-p_0)^2}{2\sigma_p^2} - \frac{(l-p)^2}{4\sigma^2} - \frac{(l'-p)^2}{4\sigma^2}\right) |l\rangle\langle l'| \quad (2.40)$$

We now proceed with Step 3 corresponding to case B. Consider a wave packet with mean momentum p_0 centered at some location z :

$$|z; \text{packet}\rangle = \frac{1}{(\sqrt{2\pi}\hat{\sigma}_p)^{\frac{1}{2}}} \int dl e^{-ilz} \exp\left(-\frac{(l-p_0)^2}{4\hat{\sigma}_p^2}\right) |l\rangle \quad (2.41)$$

We shall soon see that the correct choice for $\hat{\sigma}_p$ is

$$\hat{\sigma}_p^2 = \sigma_p^2 + \sigma^2 \quad (2.42)$$

which is approximately equal to $\sigma_p = 1/\delta z$ as required. We then consider an ensemble of these states with a Gaussian distribution of positions z centered at the origin of the form

$$\frac{1}{(\sqrt{2\pi}\sigma_z)} \int dz \exp\left(-\frac{2z^2}{\sigma_z^2}\right) \quad (2.43)$$

The correct choice for spread in position, σ_z , will turn out to be:

$$\sigma_z^2 = \frac{\sigma_p^2}{\sigma^2 (\sigma^2 + \sigma_p^2)} \quad (2.44)$$

This σ_z is approximately equal to $1/\sigma = \Delta z$ as required. The density matrix for this situation (case B) is given by

$$\rho_B = \frac{1}{(\sqrt{2\pi}\hat{\sigma}_p)} \frac{2}{(\sqrt{2\pi}\sigma_z)} \int dl dl' dz \left[\exp\left(-\frac{2z^2}{\sigma_z^2} - \frac{(l-p_0)^2}{4\hat{\sigma}_p^2} - \frac{(l'-p_0)^2}{4\hat{\sigma}_p^2}\right) \right] e^{-i(l-l')z} |l\rangle \langle l'| \quad (2.45)$$

With the choices we have made for $\hat{\sigma}_p$ and σ_z in Eqs. (2.42) and (2.44) it turns out that the density matrices ρ_A and ρ_B are **precisely equal**. The calculation is straightforward and most easily done by computing the matrix elements $\langle l|\rho_{A,B}|l'\rangle$. In order to compute the matrix elements of ρ_A only the integral over p must be done. This is a Gaussian integral. For ρ_B only the integral over z must be done. This is simply the Fourier Transform of a Gaussian. The result is the same for ρ_A and ρ_B and is given by:

$$\langle l|\rho_{A,B}|l'\rangle = \frac{1}{(\sqrt{2\pi}\hat{\sigma}_p)} \exp\left(-\frac{(l-p_0)^2}{4\hat{\sigma}_p^2} - \frac{(l'-p_0)^2}{4\hat{\sigma}_p^2} - \frac{(l-l')^2\sigma_p^2}{8\sigma^2\hat{\sigma}_p^2}\right) \quad (2.46)$$

We thus establish, for the Gaussian case, that the two ensembles are identical.

General Proof

In the Gaussian case described above we did not use the fact that $\delta z \ll \Delta z$. In the case of a more general shape for the “plane wave” and the wave packet we shall present a proof which does rely on this approximation. We conjecture that it is possible to slightly modify the theorem ⁸ so that it will be valid for general values of δz and Δz but we do not have a proof at this time.

We begin again with Step 1 for which we choose a “plane wave” of momentum p to have a wave function

$$|p; \text{plane}\rangle = \int dl f_\sigma(l - p)|l\rangle \quad (2.47)$$

where the function $f_\sigma(l - p)$ has a width $\sigma \sim 1/\Delta z$. We then consider an ensemble of these states with a distribution of momenta p given by some function $g_{\sigma_p}(p - p_0)$ with a width $\sigma_p \sim \delta p = 1/\delta z \gg \sigma$. The density matrix for this case (case A) is given by

$$\rho_A = \int dl dl' dp \left[f_\sigma^*(l' - p) f_\sigma(l - p) g_{\sigma_p}(p - p_0) \right] |l\rangle \langle l'| \quad (2.48)$$

We now proceed with Step 3 corresponding to case B. Consider a wave packet with mean momentum p_0 centered at some location z :

$$|z; \text{packet}\rangle = \int dl e^{-ilz} \alpha_{\sigma_p}(l - p_0) |l\rangle \quad (2.49)$$

which has *approximately* a width σ_p . We then consider an ensemble of these states with a distribution of positions z centered at the origin given by some function $h_{\sigma_z}(z)$ with a width σ_z which is approximately equal to $1/\sigma = \Delta z$. The density matrix for this situation (case B) is given by

$$\rho_B = \int dl dl' dz \left[\alpha_{\sigma_p}^*(l' - p_0) \alpha_{\sigma_p}(l - p_0) h_{\sigma_z}(z) \right] e^{-i(l-l')z} |l\rangle \langle l'|$$

⁸The modification we have in mind is to relax the unnecessary restriction that the shape of the wave packet is independent of z . It is reasonable to consider an ensemble of wave packets all of which have the same width but with slightly different shapes. The same could be done for the “nearly plane waves”.

$$= \int dl \, dl' \left[\alpha_{\sigma_p}^*(l' - p_0) \alpha_{\sigma_p}(l - p_0) \tilde{h}_\sigma(l - l') \right] |l\rangle\langle l'| \quad (2.50)$$

where $\tilde{h}_\sigma(l - l')$ is the Fourier transform of $h_{\sigma_z}(z)$ which has a width approximately equal to σ .

The requirement that the two density matrices are equal is now simply stated as:

$$\alpha_{\sigma_p}^*(l' - p_0) \alpha_{\sigma_p}(l - p_0) \tilde{h}_\sigma(l - l') = \int dp \, f_\sigma^*(l' - p) f_\sigma(l - p) g_{\sigma_p}(p - p_0) \quad (2.51)$$

(It is now clear why the theorem, as stated, cannot be true in general. Given arbitrary smooth functions g_{σ_p} and f_σ with the restrictions described previously it is certainly not possible, in general, to find functions α_{σ_p} and \tilde{h}_σ which satisfy Equation (2.51) since the integral in (2.51) will not always factorize in the required form.) The result is however valid when the width σ_p of g_{σ_p} is much larger than the width σ of f_σ . If $\sigma \ll \sigma_p$ and if the function g_{σ_p} is sufficiently smooth

$$\begin{aligned} f_\sigma^*(l' - p) f_\sigma(l - p) g_{\sigma_p}(p - p_0) = \\ f_\sigma^*(l' - p) f_\sigma(l - p) \sqrt{g_{\sigma_p}(l - p_0)} \sqrt{g_{\sigma_p}(l' - p_0)} + O\left(\frac{\sigma}{\sigma_p}\right) \end{aligned} \quad (2.52)$$

Thus

$$\int dp \, f_\sigma^*(l' - p) f_\sigma(l - p) g_{\sigma_p}(p - p_0) \sim \sqrt{g_{\sigma_p}(l - p_0)} \sqrt{g_{\sigma_p}(l' - p_0)} \times \int dq \, f_\sigma^*(q) f_\sigma(l - l' + q) \quad (2.53)$$

Thus if we identify the function α_{σ_p} with the square root of g_{σ_p} and the function $h_{\sigma_z}(z)$ with the square of the Fourier transform of $f_\sigma(p)$ then the equality in Eq. (2.51) is satisfied to order $\delta z / \Delta z$ as required.

2.2.5 Consequences

Although the result proven above is not entirely general it is sufficient for all cases of practical interest. The reason for this is that we have actually proven three things. The

result that measurements which commute with momentum could not distinguish coherent from incoherent broadening was completely general and did not depend on the shape of the wave packet nor on its width. Secondly the proof that for Gaussian wave packets the two effects could not be distinguished with **any** measurement was also general and it did not depend on the width of the Gaussians. Thirdly our extension of the proof to arbitrary wave packet shapes was possible in the limit $\delta z \ll \Delta z$. A practical attempt to distinguish the two mechanisms of broadening would likely begin with a theoretical calculation which assumes Gaussian wave packets for simplicity. Furthermore it would likely compare the wave packets to actual plane waves for which $\Delta z \rightarrow \infty$. We have **shown** that any such attempt is doomed to failure. We conjecture that the result is more general so that for an arbitrary shape of wave packet it is possible to find an ensemble of nearly plane waves which mimic its behavior exactly.

An interesting corollary to the result proven in the previous section is that one cannot tell, on an event by event basis, whether one has a wave packet or a “plane wave”. The proof is as follows: Suppose it were possible, on an event by event basis, to distinguish a wave packet from a plane wave. It would then be trivially possible to distinguish the cases A and B above since in one case we are presented with a plane wave and in the other case with a wave packet. In fact in just one event we would know with which case we are dealing. But, as we saw in the previous section we cannot do this since the density matrices for the two cases are identical. It follows that no such determination can be made on an event by event basis.

This result does not contradict the recent work of several authors[53] on the ability to measure the wave function of a single particle via a “protective measurement”. There are at least two requirements for such a measurement to be possible. The first is that the system needs an energy gap so that successive (soft) measurements keep the particle in the same state. The second requirement is that it is known a-priori that the system is in

an eigenstate of the Hamiltonian. Thus, for example, it is in principle possible to measure the ground state wave function of a typical atom even on a single atom but, if we do not know whether the atom is in an eigenstate of the Hamiltonian or in a superposition of eigenstates then this cannot be determined on a single atom. An argument very similar to that in the previous paragraph can be used to prove this result. In our case neither of these conditions are satisfied. We do not have a gap and we certainly are not in an eigenstate of the Hamiltonian when we are dealing with a wave packet and/or we start with a pure flavor state such as a $|\nu_e\rangle$.

The theorem presented in the previous section also provides a general tool for understanding how the size of a quantum mechanical wave packet affects physical results in various circumstances. In fact the style of our proof which relies on the *initial* properties of the system rather than on the details of its time evolution is extremely useful. There have been several instances in which either careless approximations or faulty logic have lead to conclusions which disagree with our very general result. To illustrate this point imagine, instead of using our general proof, that we evolve each of the two ensembles to a later time t and **then** compared them. We must, by our theorem, get the same density matrix for each ensemble. But in doing this calculation we might make several approximations to simplify the calculation. We might, for example, neglect the longitudinal spreading of the wave packet. It turns out that even when this spreading is negligible compared to the size of the wave packet it has a significant effect on the final density matrices and we would find significant differences between the two ensembles. We know from our theorem that this cannot be the case. Indeed when the effect of longitudinal spreading is included all results computed with ρ_A and ρ_B agree.

2.3 Summary and Conclusions

The main focus of this chapter was the question of our ability experimentally (even in principle) to distinguish incoherent broadening of a neutrino line (such as the ${}^7\text{Be}$ solar neutrino line) from coherent broadening of such a line. Of particular interest was whether these two types of broadening would have different effects on neutrino oscillations and the MSW effect. We began by identifying processes which contribute to these mechanisms of broadening. Coherent broadening results from several processes including the natural width of the emitting nucleus, pressure broadening caused by collisions of this nucleus and the finite size of the wave packet of the captured electron. We argued that this last process leads to the smallest estimate for the spatial size of the neutrino wave packet ($\sim 6 \times 10^{-8}\text{cm}$). Incoherent broadening results mainly from the thermal energy spread of the captured electron as well as from the Doppler shift due to the thermal motion of the emitting nucleus.

We then began to present our argument that although the two forms of broadening were distinct physical processes which could be controlled at the source they could not be distinguished at the detector. We first showed that if the detector had an excellent energy resolution not only could oscillations due to an incoherent ensemble of (nearly) monoenergetic neutrinos be restored but oscillations of a coherent neutrino beam could also be restored despite the physical separation of the ν_1 and the ν_2 at the detector. We then proved that the measurement of any operator which commuted with momentum could never distinguish a wave packet from a plane wave. We extended the proof of this result to the case in which the neutrino propagates in matter (the MSW effect).

The next stage was to show that if we had no a-priori knowledge of any difference in the properties of the coherent versus the incoherent neutrino “beams” there was *no* measurement which could distinguish them. Our method was to show that it was possible

to construct two ensembles, one corresponding to “nearly plane waves” and the other to wave packets which had the same density matrix at $t = 0$. This would imply that the density matrices were equal at all later times and that no measurements could distinguish the two cases. We presented a complete proof in the case of Gaussian wave packets by showing that the density matrix at the source for an ensemble of plane waves with a given (Gaussian) energy distribution was **equal** to that of an ensemble of wave packets each with a much narrower z distribution but distributed, incoherently, over the same range of positions as the “incoherent” ensemble. We extended this proof to the case of non-Gaussian wave packets in the limit that the spatial size of the wave packet was much smaller than the spatial size of the “nearly plane wave”. We conjectured that the result is even more general and that given any ensemble of “nearly plane waves” with a given energy and position distribution we can construct an ensemble of wave packets which has precisely the same density matrix.

There have been claims in the literature that wave packets could give different results than plane waves with the same momentum distribution. These differences show up either when the neutrinos are nearly nonrelativistic or when their momentum distribution is extremely broad so that $\delta p \sim p$. This of course implies that some of the components of the neutrino wave function are nonrelativistic and that some of the neutrinos are moving “backwards”. In all these cases it is essential to include the longitudinal spreading of the neutrino wave packet. If this is done one confirms the results of our theorem that there are no differences between the two scenarios.

Although we have chosen to focus on neutrinos and neutrino oscillations it is clear that the result is much more general. It applies to any particle for which the question of the distinguishability of a wave packet from plane waves is relevant. Some examples include neutral Kaon oscillations and the effect of wave packets in scattering theory.

Chapter 3

Neutrino Oscillations in a Model with a Source and Detector

In this chapter we present a rigorous field theoretic derivation of the neutrino oscillation probability as a function of the distance between an idealized “source” and “detector.” Our calculation may be contrasted with the conventional (plane wave) treatment, in which an oscillation probability is derived which is a function of the *time* between the production and detection of the neutrino. Since in any realistic experiment one expects to measure only the distance between the source and detector and not the time between the production and detection of the neutrino, the conventional treatment needs to employ some sort of ad hoc prescription to convert the time-dependent oscillation probability into a distance-dependent one. Some of the ambiguities associated with such a procedure have already been discussed in Chapter. 1.

One of the first calculations to take the time-versus-distance issue seriously was performed by Giunti, Kim and Lee [54], who modeled the neutrino mass eigenstates by wavepackets and derived an oscillation probability which was dependent on both distance and time. This expression was then integrated over time in order to obtain an expression as a function only of distance. Subsequent papers have improved on this calculation by incorporating explicitly the interactions through which the neutrino is produced and detected [55, 56, 57].

Lately there has been renewed interest in the time-versus-distance question in particle oscillations. This interest is due primarily to two recent papers concerned with the oscillations of neutral mesons, the first by Lipkin [39] and the second by Srivastava,

Widom and Sassaroli [40]. Lipkin argues that there exists some ambiguity as to what is the “correct” prescription for converting a probability as a function of time into one as a function of distance. Different prescriptions lead to results which differ quite significantly from each other; in fact, in the example considered by Lipkin it was found that setting $t_i = x/v_i$ (v_i is the mass eigenstate velocity) independently for the mass eigenstates gave a relative factor of “2” in the oscillation length compared to the usual result. As we discussed in Sec. 1.3.2, however, the apparent ambiguity in that case can be resolved by thinking in terms of wave packets. The second paper, by Srivastava, *et al.*, has actually been somewhat controversial. They considered the process $\pi^- p \rightarrow \Lambda K^0$ and derived an expression for the $K^0 - \bar{K}^0$ oscillation length (and hence for $\delta m \equiv m_{K_L} - m_{K_S}$) which differs by a factor of *at least* 2 from the usual result. A subsequent analysis of their calculation by Lowe, *et al.* [42], shows that their result follows from the same sort of reasoning which led to the problem in the case which Lipkin discussed. Finally, a recent calculation by Ancochea, *et al.* [58], has avoided the necessity of converting time probabilities into distance probabilities by deriving a probability *current* which can plausibly be integrated over time to arrive at the probability as a function of distance. In this manner they arrive at the conventional result for the oscillation length, with *no* factor of “2”.

A quick calculation in the neutrino case reveals that there, too, an anomalous factor of two shows up in the oscillation length if the “wrong” prescription of converting times into distances is followed in the conventional treatment. As we discussed in Sec. 1.3.2, the problem in the calculation which leads to the factor of two is that it attempts to model wave packet behaviour, namely that the mass eigenstates arrive at the detector at different times, using plane waves. In this chapter we present a calculation which accounts correctly for the localization of the source and detector (and hence of the neutrino “wave packets”) and yields a rigorous approach to computing the neutrino oscillation probability.

We begin in Sec. 3.1 by providing a summary of the wave packet approach presented in Refs. [54, 59, 22]. In this approach the source and detector are not explicitly incorporated into the calculation. We point out some of the insights which this calculation gives as well as some its difficulties. The main problem in this approach is that there appears to be no real justification for one of the steps in the calculation, in which a probability density is integrated over *time* to yield an oscillation probability as a function of distance. Indeed, as we shall see, this procedure leads to some rather provocative results when one or more of the mass eigenstates is non-relativistic.

It would be more appropriate to instead integrate a *current density* over time in order to obtain a distance probability. This is the approach which was taken in the kaon system in the recent calculation of Ancochea, *et al.* [58], and it appears to have cleared up the ambiguities in that case. Thus, in Sec. 3.2 we consider whether there might exist a current density, defined without reference to any specific process for the production or detection of the neutrinos, which satisfies some minimum requirements and which may be reliably integrated over time in order to yield a distance probability. In the analogous calculation in the kaon system, one may use a current which is closely related to the regular quantum mechanical current, $\text{Im}(\psi^* \vec{\nabla} \psi)/m$, since the kaons may be taken to be non-relativistic. In our case we wish to allow the neutrino mass eigenstates to be either relativistic *or* non-relativistic, so that the above approach does not work. Nonetheless, we shall find that it is possible to construct a current density which does satisfy some minimum formal requirements. A closer investigation reveals, however, that the probability density to which the current is related (by the continuity equation) is not positive semi-definite. We shall thus be forced to abandon this approach.

Sec. 3.3 contains our main calculation. Having found no clear and self-consistent way of defining distance probabilities independent of the neutrino production and detection

processes¹, we turn to a calculation in which the neutrino fields are explicitly coupled to an idealized “source” and “detector,” modeled in our case by harmonic oscillators². For convenience, we first model the neutrinos by complex scalar fields, leaving a more realistic treatment using fermionic neutrinos for the next section. In the source/detector approach, the neutrinos themselves are never “observed.” Rather, a source is observed to decay into its ground state and a detector is observed to be excited into its first excited state.

There are many advantages to treating neutrino oscillations from the point of view of a source and detector. First of all, the quantities which we calculate will have clear physical interpretations. That is, we calculate the amplitude for the source to decay and for the detector to subsequently be excited. From this amplitude we may give a clear *physical* definition of the oscillation probability. This is to be contrasted with the “wave packet” and “current” approaches, in which the formal quantities which are calculated do not have any clear physical significance³. Furthermore, the requisite (in order to observe oscillations) localization of the source and detector in space is easily accomplished in our approach. This approach also allows for a *temporal* localization of the source and detector. Recall from our discussion in Sec. 2.2.1 that we expect a long coherent measurement in time to “revive” the oscillations of neutrinos even after the mass eigenstate wave packets have separated spatially. Our simple model will allow us to demonstrate this phenomenon very explicitly.

¹See, however, the recent calculation of Grossman and Lipkin [43], in which the imposition of an appropriate boundary condition allows one to calculate “distance” probabilities. Their calculation assumes that the neutrino mass eigenstate wave packets have nearly 100% overlap at the detection point and that the neutrinos are relativistic. We are interested in the general case in which the wave packets may have separated and in which one or more of the neutrinos may be non-relativistic.

²Analogous approaches have been used to successfully resolve ambiguities in other areas of physics. For example, Unruh and Wald used a similar idealized detector to study the “Rindler particles” detected by an accelerated detector [60].

³The problems with calculating probability densities and currents in relativistic field theories are well-known [61].

Another advantage of explicitly coupling the neutrino to a source and detector is that it allows for a careful study of the efficiency with which neutrinos of different masses are produced and detected. It turns out that in the “wave packet” approach, the oscillation probabilities are skewed by factors of $1/v$, so that non-relativistic mass eigenstates tend to dominate the expression, if they are present. This is justified by the authors by noting that “Non-relativistic mass eigenstates dominate . . . because they move very slowly and spend more time in the detector” [22, p. 214]. Yet this comment is made without anywhere including the detector in the calculation. It is thus important to determine whether this effect is observed when the neutrino is explicitly coupled to the source and detector. In our model we *will* find that the efficiency for producing and detecting neutrinos can depend on the detector. The origin of this dependence in our case, however, will be quite different than is suggested in [22]. Furthermore, for a suitable choice of parameters the dependence disappears entirely.

Another motivation for considering the neutrinos in a given interaction as being exchanged between a source and a detector is that it completely avoids the problem, pointed out by Giunti, *et al.* (and discussed in Sec. 1.1), that there do not exist weak neutrino eigenstates⁴ [30]. The flavour neutrinos do not have well-defined dispersion relations and it is thus inappropriate to consider them as being the asymptotic initial or final states in an interaction. This problem is avoided in a natural way in our formulation, since there is never any need to refer to neutrino “flavour” eigenstates. The only eigenstates which appear are the “mass” eigenstates, which are each produced and detected with an amplitude dictated by the experimental set-up and which propagate between the source and detector with well-defined dispersion relations as “on-shell” particles (over macroscopic

⁴For a competing point of view see Refs. [62, 63]. There it is claimed that one *can* construct such eigenstates. While their states do formally satisfy the required relations (they are able to construct “flavour” creation and annihilation operators which satisfy canonical anti-commutation relations), we believe that their subsequent derivation of corrections to the neutrino oscillation formula is incorrect.

distances.) This brings us to the final point which we would like to make concerning our source/detector system. Once the characteristics of the source and detector are fixed, there is no longer any flexibility regarding the “wave packets” of the neutrino mass eigenstates. In the “wave packet” approach one has to decide, for example, whether or not the packets corresponding to each of the mass eigenstates will have the same width in momentum space. In our approach these sorts of questions simply don’t arise.

An analogous point of view to that which we advocate has also been adopted by Giunti, Kim, Lee and Lee [55], Rich [56] and Grimus and Stockinger [57]. The calculation in Ref. [56] is performed essentially using second order perturbation theory in ordinary quantum mechanics and is confined to relativistic neutrinos, while the calculations in Refs. [55, 57] are performed using field theoretic techniques and appear to treat non-relativistic neutrinos much more appropriately. The principle feature which distinguishes our calculation from theirs is that we have chosen to study a model which is *completely solvable* so that the response of the detector to the source may be studied explicitly without making any approximations (for example, with respect to the spreading of the wave packet in the case of non-relativistic neutrinos.) As we shall see, in order to derive an expression for the oscillation probability, it is very useful to have a thorough understanding of how efficient the source/detector system is at producing and detecting neutrinos of different masses. Furthermore, our simple model will allow us to examine the dependence of the oscillation probability on the time resolution of the detector.

In Sec. 3.4 we present a somewhat more realistic – and less transparent – model of a neutrino source/detector system which accounts correctly for the neutrino helicities and the $V - A$ nature of the production and detection interactions. This final calculation will bear some similarities to those discussed in Refs. [55, 57] but will be simpler and in principle more amenable to numerical study. Finally, in Sec. 3.5 we provide a brief summary of our main results.

3.1 A Wave Packet Approach

Our goal is to derive a neutrino oscillation formula which is a function of distance, not time, and which deals appropriately with both relativistic *and* non-relativistic neutrinos. The simplest approach which manages to take into account the required spread in the neutrino's energy or momentum is to model the neutrino state by a wave packet which is evolved in time by the Hamiltonian. The main limitations of this approach are that the form for the initial (and final) state is ambiguous and that the probability density which is initially derived is a function of distance *and* time. With respect to the former point, it is unclear for example what the relative "widths" of the wave packets corresponding to different mass eigenstates should be. Should they be the same? Furthermore, should the wave packets be separately normalized (implying that all mass eigenstates are produced with the same efficiency) or should there be just one normalization condition which sums over the wave packets? Regarding the latter limitation, i.e., that the probability density which is derived is a function of distance *and* time, we note that in the standard quantum mechanical interpretation, this probability density, when multiplied by Δx , gives the probability to detect a neutrino of a given flavour between x and $x + \Delta x$ (in $1 + 1$ dimensions.) Thus, integrating this object over x would, in the standard approach, yield the probability at a given instant in time to detect a neutrino of a given flavour. But how to convert this into a probability as a function of distance?

In order to find the oscillation probability at location x after a long time has elapsed, one would expect that a more fruitful starting point would in fact be to calculate the probability *current* and to integrate it over time, as was done by Ancochea, *et al*, in the kaon system [58]. We will examine this approach in the next subsection and see that this seemingly simple idea has several problems.

In this subsection we will sketch the wave packet approach presented in Ref. [54] (see

also [22, pp. 206-215].) Note that the calculation in Ref. [54] is performed in one spatial dimension and ignores the different helicities of the neutrinos (which may sometimes be a good approximation, even for non-relativistic neutrinos.)

Suppose a neutrino with flavour α ($=e, \mu, \tau, \dots$) is produced at the origin at time $t=0$. This neutrino is actually a superposition of mass eigenstates, which will each be taken to have a gaussian shape in momentum space. Thus we set

$$|\psi_i(x, t; \langle p_i \rangle)\rangle = (\sqrt{2\pi}\sigma_p)^{-1/2} \int \frac{dp}{(2\pi)^{1/2}} \exp \left[i(px - E_i(p)t) - \frac{(p - \langle p_i \rangle)^2}{4\sigma_p^2} \right] |\nu_i\rangle, \quad (3.1)$$

where

$$\langle \nu_i | \nu_j \rangle = \delta_{ij}, \quad (3.2)$$

$$E_i(p) \equiv \sqrt{p^2 + m_i^2}, \quad (3.3)$$

and where σ_p is the width of the gaussian in momentum space. The flavour state may then be defined to be

$$|\psi_\alpha(x, t)\rangle = \sum_i \mathcal{U}_{\alpha i}^* |\psi_i(x, t; \langle p_i \rangle)\rangle, \quad (3.4)$$

where the mean momenta $\langle p_i \rangle$ of the various mass eigenstates are allowed to be different (they could in principle be determined by looking at the specific production process), but the widths of the various packets are taken to be equal⁵. The probability density to detect a neutrino with flavour β is then given by

$$\begin{aligned} P_{\alpha \rightarrow \beta}(x, t) &= \left| \sum_j \mathcal{U}_{\beta j} \langle \nu_j | \psi_\alpha(x, t) \rangle \right|^2 \\ &= \sum_{i,j} \mathcal{U}_{\alpha i}^* \mathcal{U}_{\beta i} \mathcal{U}_{\alpha j} \mathcal{U}_{\beta j}^* (\sqrt{2\pi}\sigma_p)^{-1} \end{aligned} \quad (3.5)$$

⁵This assumption is somewhat suspect. If a source emits a neutrino wave train for a fixed time interval Δt , then the various mass eigenstate wave packets would be expected to have sizes of the order $\sigma_{x_i} \sim v_i \Delta t$, where v_i is the associated neutrino's velocity. Thus, more relativistic neutrinos would be expected to have broader wave packets in space. This discussion illustrates the ambiguity inherent in discussing neutrino wave packets without reference to some type of source.

$$\times \int \frac{dp dp'}{2\pi} \exp \left[i(p - p')x - i(E_i - E'_j)t - \frac{(p - \langle p_i \rangle)^2}{4\sigma_p^2} - \frac{(p' - \langle p_j \rangle)^2}{4\sigma_p^2} \right].$$

As mentioned above, the conventional interpretation of this probability density is as follows: given that a neutrino of flavour α was produced at the origin at time $t=0$, the probability to detect a neutrino of flavour β between x and $x + \Delta x$ at some later time t is given by $P_{\alpha \rightarrow \beta}(x, t)\Delta x$. Indeed, as it stands, this probability density is properly normalized over x , since one may easily show that

$$\int dx \sum_{\beta} P_{\alpha \rightarrow \beta}(x, t) = 1. \quad (3.6)$$

The authors of Ref. [54] integrate Eq. (3.5) over time instead of over space in order to obtain some sort of oscillation probability as a function of distance. We shall see below the approximation that they make before doing the integral, but let us note for the moment that the time integral may, in fact, be done directly, since the only time dependence in (3.5) is in the oscillating exponential. Proceeding in this way yields

$$\frac{1}{2\pi} \int dt e^{-i(E_i - E'_j)t} = \delta(E'_j - E_i) \quad (3.7)$$

$$\begin{aligned} &= \theta(m_i^2 - m_j^2) \frac{E'_j}{|p'|} \left[\delta \left(p' - \sqrt{p'^2 + \Delta_{ij}} \right) + \delta \left(p' + \sqrt{p'^2 + \Delta_{ij}} \right) \right] \\ &+ \theta(m_j^2 - m_i^2) \frac{E_i}{|p|} \left[\delta \left(p - \sqrt{p^2 + \Delta_{ij}} \right) + \delta \left(p + \sqrt{p^2 + \Delta_{ij}} \right) \right], \end{aligned} \quad (3.8)$$

where $\theta(z)$ is the usual Heaviside function (with the convention that $\theta(0) \equiv 1/2$) and where we have defined

$$\Delta_{ij} \equiv |m_i^2 - m_j^2|. \quad (3.9)$$

One may use Eq. (3.8) to reduce the time integral of the probability density to a single integration over momentum, but there does seem to be some problem for the terms with $i=j$, since one is left with a piece which goes like $1/|p|$ and which therefore diverges at the origin.

Instead of performing the time integral directly, the authors of Ref. [54] choose to approximate the expression (3.1) for the wavefunction to obtain

$$|\psi_i(x, t; \langle p_i \rangle)\rangle \simeq (\sqrt{2\pi}\sigma_x)^{-1/2} \exp \left[i(\langle p_i \rangle x - \langle E_i \rangle t) - \frac{(x - v_i t)^2}{4\sigma_x^2} \right] |\nu_i\rangle, \quad (3.10)$$

where

$$\sigma_x \equiv \frac{1}{2\sigma_p}, \quad (3.11)$$

$$v_i \equiv \left. \frac{\partial E_i}{\partial p} \right|_{p=\langle p_i \rangle} = \frac{\langle p_i \rangle}{\langle E_i \rangle}. \quad (3.12)$$

The above approximation ignores the spreading of the wave packet in time, which is often a reasonable approximation for sufficiently relativistic wave packets⁶. Inserting the expression (3.12) into Eq. (3.5) allows one to perform the time integral⁷ to obtain

$$\begin{aligned} \tilde{P}_{\alpha \rightarrow \beta}(x) &\simeq \left[\sum_k \frac{|\mathcal{U}_{\alpha k}|^2}{|v_k|} \right]^{-1} \sum_{i,j} \mathcal{U}_{\alpha i}^* \mathcal{U}_{\beta i} \mathcal{U}_{\alpha j} \mathcal{U}_{\beta j}^* \exp \left[i \left(\langle p_i \rangle - \langle p_j \rangle - \frac{(\langle E_i \rangle - \langle E_j \rangle)(v_i + v_j)}{v_i^2 + v_j^2} \right) x \right] \\ &\times \left(\frac{2}{v_i^2 + v_j^2} \right)^{1/2} \exp \left[-\frac{x^2}{4\sigma_x^2} \frac{(v_i - v_j)^2}{v_i^2 + v_j^2} - \frac{(\langle E_i \rangle - \langle E_j \rangle)^2}{4\sigma_p^2(v_i^2 + v_j^2)} \right], \end{aligned} \quad (3.13)$$

in which the factor

$$\left[\sum_k \frac{|\mathcal{U}_{\alpha k}|^2}{|v_k|} \right]^{-1} \quad (3.14)$$

has been put in by hand in order to ensure that

$$\sum_{\beta} \tilde{P}_{\alpha \rightarrow \beta}(x) = 1. \quad (3.15)$$

⁶It is also shown in Ref. [54] how to incorporate some spreading should some of the mass eigenstates be non-relativistic.

⁷The singularity noted above has disappeared due to the approximation which has been made and the integral is now convergent. Also note that the “cross-term” corresponding to the contributions of the i^{th} and j^{th} mass eigenstate combination receives its main contribution from the time $t=t_{ij} \approx (v_i + v_j)x/(v_i^2 + v_j^2)$. Thus, as we noted in Sec. 1.3.2, the pieces with $i=j$ get their main contributions from x/v_i , while those with $i \neq j$ get their main contributions from some weighted average of the times for the i^{th} and j^{th} mass eigenstates.

The damping factor for $i \neq j$

$$\exp \left[-\frac{x^2}{4\sigma_x^2} \frac{(v_i - v_j)^2}{v_i^2 + v_j^2} \right] \quad (3.16)$$

is due to the fact that the wave packets corresponding to different mass eigenstates travel at different velocities and hence separate spatially as they propagate. The coherence length is then given by

$$L_{ij}^{\text{coh}} = 2\sigma_x \sqrt{\frac{v_i^2 + v_j^2}{(v_i - v_j)^2}} \quad (3.17)$$

which agrees in the relativistic limit with the intuitive result $L_{ij}^{\text{coh}} \sim \sigma_x / |v_i - v_j|$ originally obtained by Nussinov [47].

It is instructive to consider the limit of Eq. (3.13) as $x \rightarrow \infty$. For very large x , all of the interference terms are damped out, leaving only the terms with $i=j$. Thus,

$$\lim_{x \rightarrow \infty} \tilde{P}_{\alpha \rightarrow \beta}(x) = \left[\sum_k \frac{|\mathcal{U}_{\alpha k}|^2}{|v_k|} \right]^{-1} \sum_i |\mathcal{U}_{\alpha i}|^2 |\mathcal{U}_{\beta i}|^2 |v_i|^{-1}, \quad (3.18)$$

which differs from the usual result, which is gotten by setting $v_i=1$ in the above expression,

$$\lim_{x \rightarrow \infty} \tilde{P}_{\alpha \rightarrow \beta}(x) = \sum_i |\mathcal{U}_{\alpha i}|^2 |\mathcal{U}_{\beta i}|^2. \quad (3.19)$$

When all of the mass eigenstates are relativistic, the two results coincide. If one or more of the mass eigenstates are non-relativistic, however, a substantial departure from the usual result occurs. This phenomenon, if it were true, would actually be quite spectacular, for it would have the potential to substantially enhance the regular vacuum oscillations. Suppose we consider the two-neutrino case, with the two neutrinos being ν_e and ν_τ , and with $\sin \theta$ quite small and m_3 quite large (so that ν_3 is non-relativistic.) In this case (3.18) becomes

$$\tilde{P}_{\nu_e \rightarrow \nu_\tau} = \left(\frac{\cos^2 \theta}{|v_1|} + \frac{\sin^2 \theta}{|v_3|} \right)^{-1} \left(\frac{1}{|v_1|} + \frac{1}{|v_3|} \right) \sin^2 \theta \cos^2 \theta \simeq \cos^2 \theta, \quad (3.20)$$

compared to the usual result, which is

$$\tilde{P}_{\nu_e \rightarrow \nu_\tau} \simeq \frac{1}{2} \sin^2(2\theta). \quad (3.21)$$

Thus even a small coupling to a heavy neutrino would seem to be able to produce quite a large flavour-changing probability.

The end result in Eq. (3.20) is due entirely to the fact that the contributions of the various mass eigenstates to the oscillation probability are weighted by $1/v$, which in turn arises from the fact that the probability density has been integrated over time.

3.2 An Approach Using a Current

Since the response of a detector is typically assumed to be proportional to the *flux* of incoming particles, the correct approach to calculating the oscillation probability would be to integrate an appropriate *current* density, rather than a probability density, over time. Furthermore, as we shall see, employing a conserved two-current (in $1 + 1$ dimensions) has the desirable result that once the zero-th component is normalized over space, the spatial component is automatically normalized over time and thus, in contradistinction with the wave packet approach, no normalization factors need to be put in by hand. It turns out however that this method, while in some sense correct in spirit, is not without its own difficulties.

It is not apriori obvious how best to define a current corresponding to the probability density in Eq. (3.5). In some sense it should reduce to multiplying the various terms of the probability density by appropriate factors of v , but which “ v ” does one use in the cross-terms? It turns out that there is a somewhat “natural” candidate for the appropriate current if we work within the context of quantum field theory. In order to simplify our calculation, it is convenient to disregard the neutrinos’ helicity degrees of freedom, as

was also done above, and to model the neutrinos by free complex scalar fields, $\phi_\alpha(x)$ ⁸. If we take as a requirement that our probability and current densities be the zero-th and first components of a conserved two-current, then a plausible candidate is given by

$$J_{\alpha \rightarrow \beta}^\mu(x, t) \equiv \langle \tilde{\phi}_\alpha(t) | j_\beta^\mu(x, 0) | \tilde{\phi}_\alpha(t) \rangle, \quad (3.22)$$

which is the expectation value of the current operator

$$j_\beta^\mu(x, t) \equiv: i \phi_\beta^\dagger(x, t) \overleftrightarrow{\partial}^\mu \phi_\beta(x, t) :, \quad (3.23)$$

in the wave packet state

$$|\tilde{\phi}_\alpha(t)\rangle \equiv \sum_k \mathcal{U}_{\alpha k}^* \int_0^\infty d\tilde{q}_k e^{-iE_k(q)t} f_k(q) a_q^{k\dagger} |0\rangle. \quad (3.24)$$

(The reader is referred to Appendix B for a more detailed derivation of the results of this section.)

This current has several attractive formal properties. First of all, it is conserved when summed over β

$$\partial_\mu \sum_\beta J_{\alpha \rightarrow \beta}^\mu(x, t) = 0. \quad (3.25)$$

Furthermore, once the zero-th component is normalized over space, the first component is automatically normalized over time. That is,

$$\int dx \sum_\beta J_{\alpha \rightarrow \beta}^0(x, t) = 1 \quad \Rightarrow \quad \int dt \sum_\beta J_{\alpha \rightarrow \beta}^1(x, t) = 1, \quad (3.26)$$

in contradistinction with the case considered in the previous section, in which a new normalization constant needed to be inserted by hand.

We may then use this current to define a probability as a function of distance as follows

$$P_{\alpha \rightarrow \beta}(x) \equiv \int dt J_{\alpha \rightarrow \beta}^1(x, t) \quad (3.27)$$

⁸We are modeling Dirac neutrinos, so the “charge” in this case is lepton number.

$$\begin{aligned}
&= \sum_{i,j} \mathcal{U}_{\alpha i}^* \mathcal{U}_{\alpha j} \mathcal{U}_{\beta i} \mathcal{U}_{\beta j}^* \theta(m_i^2 - m_j^2) \\
&\quad \times \int \frac{dp}{8\pi E_i} \frac{(p + p'_{ij})}{p'_{ij}} f_i(p) f_j^*(p'_{ij}) e^{i(p-p'_{ij})x} + \text{c.c.}, \quad (3.28)
\end{aligned}$$

where

$$p'_{ij} \equiv \sqrt{p^2 + \Delta_{ij}}. \quad (3.29)$$

This current appears to be well-behaved. It is straightforward, for example, to evaluate this expression in the limit as $x \rightarrow \infty$. For large x all of the oscillations damp out, leaving only the diagonal contributions, so that

$$\lim_{x \rightarrow \infty} P_{\alpha \rightarrow \beta}(x) = \sum_i |\mathcal{U}_{\alpha i}|^2 |\mathcal{U}_{\beta i}|^2, \quad (3.30)$$

in which we have made use of the normalization condition

$$\int d\tilde{p}_i |f_i(p)|^2 = 1. \quad (3.31)$$

Thus, integrating a current density, rather than a probability density, over time appears to give the usual result, Eq. (3.19), instead of that obtained in the previous section, Eq. (3.18). Indeed, this is as one might expect since, roughly speaking, the current is the product of the probability density and the velocity; the extra factors of v thus cancel the factors of $1/v$ which came up in the wave packet approach.

This approach is not without its own difficulties, however. While it appears that the current density itself may be well-behaved, the probability density to which it is associated through the continuity equation can have quite strange behaviour. As an example, let us consider the two-neutrino case with one relativistic and one non-relativistic neutrino, taking

$$f_i(p) = \left(\frac{2\sqrt{2\pi}E_i}{\sigma_p} \right)^{1/2} \exp \left[-\frac{(p - \bar{p})^2}{4\sigma_p^2} \right], \quad i = 1, 2, \quad (3.32)$$

with $\sigma_p \ll \bar{p}$ and $m_2 \gg m_1 \sim \bar{p}$. Then one finds for the probability

$$P_{e \rightarrow \mu}(x) \simeq \frac{1}{2} \sin^2 2\theta, \quad \forall x. \quad (3.33)$$

The results for the corresponding probability density are, however, quite strange. Integrating the flavour-changing probability density over x , for example, we find

$$\begin{aligned} \int dx J_{e \rightarrow \mu}^0(x, t) &\simeq \frac{1}{2} \sin^2 2\theta \left(1 - \frac{1}{2} \frac{\langle E_1 \rangle + \langle E_2 \rangle}{\sqrt{\langle E_1 \rangle \langle E_2 \rangle}} \right) \\ &\simeq \frac{1}{2} \sin^2 2\theta \left(1 - \frac{1}{2} \sqrt{\frac{m_2}{\sqrt{p^2 + m_1^2}}} \right), \end{aligned} \quad (3.34)$$

which is *negative*. Furthermore, the first of the normalization conditions in Eq. (3.26) implies that for the flavour-conserving piece we have

$$\int dx J_{e \rightarrow e}^0(x, t) > 1. \quad (3.35)$$

It thus appears that this approach should be abandoned, despite its formal appeal.

3.3 A Toy Model for a Neutrino Source and Detector

From the discussion in the previous two subsections it is clear that the formal quantities, such as the probability density and probability current, which one might attempt to manipulate in order to derive an appropriate oscillation formula do not give reliable results. It is for this reason that we wish to improve upon such calculations by presenting a simple model for a neutrino source/detector system. As we shall see, framing the neutrino oscillation problem directly in terms of the source and detector has the advantage that the manipulations which we do (such as integrating some expression over time, for example) will be related in a clear way to the “experiment” itself. Furthermore, this approach removes all ambiguities concerning the relative shapes and sizes of the initial wave packets for the various mass eigenstates, since everything is completely determined by the initial and final configurations of the source and detector. Finally, in the model which we present, almost all of the calculations may be done by hand with no approximation. This will allow for a very thorough understanding of the system.

In our toy model, we shall couple the neutrino field to two harmonic oscillators, one of which is the “source,” and the other of which is the “detector.” In this section we will model the neutrinos by complex scalar fields, which will simplify the calculations considerably ⁹; in Sec. 3.3 we consider some of the complications which arise in a more realistic calculation with fermionic neutrinos. The physical picture which we have in mind is the following. We imagine the “source” and “detector” to be microscopic on the scale of some macroscopic “bulk” source and detector, but to also be very massive compared to the energy of the exchanged neutrino (so that the dynamical degrees of freedom of the source and detector may be ignored.) Thus, the source (detector) could represent some nucleus inside a bulk sample which undergoes beta decay (inverse beta decay). The spatial “widths” of the source and detector in our calculation are then widths appropriate to, say, nuclear or atomic dimensions. In principle, the oscillation probability which we calculate here should subsequently be averaged incoherently over the physical dimensions of the source and detector, although we do not perform this average. If the size of the macroscopic source and detector are much smaller than the neutrino oscillation length (which they need to be in order to observe oscillations), then this averaging would have only a very small effect.

The interactions at the source and detector will be made explicitly time dependent so that they may be turned “on” and “off.” This is in keeping with our physical picture. In general the source and detector will be in an environment which is “noisy,” so that the coherent emission or absorption of a neutrino gets cut off after some time due to the interactions of the source or detector with its surrounding environment. This phenomenon was discussed at some length in Sec. 2.1 (see also Ref. [22, pp.203-206].) The explicit turning on and off of the source and detector violates energy conservation microscopically,

⁹The main drawback of this approach is that it ignores the neutrino’s spin and the characteristic $V - A$ nature of neutrino interactions.

but that is natural since the interactions of the source and detector with their respective environments involve the exchange of energy. If we choose to look at the source or detector in isolation, this exchange of energy appears as energy non-conservation. Note as well that although we will first study a single (microscopic) detector which turns on and off at a given time, our calculation needs somehow to reflect the fact that the bulk detector is always “on.” That is, at any given point in time, many of the microscopic detectors may be “off,” but many will also be “on.” We shall consider this question in detail once we have first performed the calculation for a single detector.

Our calculation proceeds as follows. We take the initial state of the system to have the source in its first excited state and the detector in its ground state. We then calculate the probability that, at some time far in the future, the source is found to be in its ground state and the detector in its first excited state. We will construct our model in such a way that this interaction will correspond to exactly one neutrino being exchanged between the source and detector (to first non-vanishing order in perturbation theory.) In this approach, then, the neutrinos themselves are not observed, but are simply the exchange particles in the source-detector interaction. In Sec. 3.3.1 we study the case with a single neutrino coupled to the source and detector. This will allow for a careful analysis of the efficiency of our system at producing and detecting neutrinos of different masses. Furthermore, it will allow us to derive a self-consistent formalism which models the fact that the bulk detector stays “on” even though the microscopic detectors may always be turning on and off. In Sec. 3.3.2 we couple several neutrino fields to the source and detector. This will give rise in a natural way to oscillations (as a function of the distance between the source and detector) in the probability for the source to decay and the detector to be excited. These are “neutrino oscillations,” but the neutrino itself is never observed! Sec. 3.3.3 contains a brief analysis of the non-relativistic case.

3.3.1 A Single Species of Neutrino

In order study the characteristics of our source and detector, we first consider the case in which they are coupled to only one neutrino field. This will enable us to study, in particular, the efficiency of our source and detector at producing and detecting neutrinos of different masses. Our model is defined by the following action

$$S = \int d^4x \left(\mathcal{L}_\phi^0 + \mathcal{L}_{\text{int}} \right) + \int dt L_q^0, \quad (3.36)$$

where

$$\mathcal{L}_\phi^0 = -\phi^\dagger(x) \left(\square + m^2 \right) \phi(x), \quad (3.37)$$

$$L_q^0 = \dot{q}_1^\dagger(t) \dot{q}_1(t) - \Omega_1^2 q_1^\dagger(t) q_1(t) + \dot{q}_2^\dagger(t) \dot{q}_2(t) - \Omega_2^2 q_2^\dagger(t) q_2(t), \quad (3.38)$$

$$\begin{aligned} \mathcal{L}_{\text{int}} = & -\epsilon_1(t) \left(\phi^\dagger(x) q_1(t) h_1(\mathbf{x}) + \phi(x) q_1^\dagger(t) h_1^*(\mathbf{x}) \right) \\ & -\epsilon_2(t) \left(\phi^\dagger(x) q_2(t) h_2(\mathbf{x}) + \phi(x) q_2^\dagger(t) h_2^*(\mathbf{x}) \right), \end{aligned} \quad (3.39)$$

and in which $\phi(x)$, $q_1(t)$ and $q_2(t)$ represent the neutrino, source and detector fields, respectively¹⁰. The functions $\epsilon_i(t)$ are explicit functions of time which allow us to “turn on” and “turn off” the interactions, and the functions $h_1(\mathbf{x})$ ($h_2(\mathbf{x})$) are smooth functions of \mathbf{x} which vanish outside the source (detector.) Note that we are now working in $3 + 1$ dimensions. The time-dependent functions $\epsilon_i(t)$ are useful for modelling the real-world situation since the nuclei which emit and absorb neutrinos do not do so coherently over infinitely long time periods. Rather, the coherent emission and detection is typically truncated due to the interactions of the nucleus with its surroundings.

We quantize the (free) fields in the usual way, requiring

$$[\phi(\mathbf{x}, t), \pi(\mathbf{y}, t)] = i\delta^3(\mathbf{x} - \mathbf{y}), \quad (3.40)$$

$$[q_i(t), p_i(t)] = i. \quad (3.41)$$

¹⁰Here we are using the word “field” rather loosely, since $q_1(t)$ and $q_2(t)$ are not actually fields.

All other commutators are taken to vanish. The field operators may then be expressed in terms of creation and annihilation operators as follows

$$\phi(x) = \int d\tilde{k} \left(a(k) e^{-ik \cdot x} + b^\dagger(k) e^{ik \cdot x} \right), \quad (3.42)$$

$$q_i(t) = \frac{1}{2\Omega_i} \left(A_i e^{-i\Omega_i t} + B_i^\dagger(k) e^{i\Omega_i t} \right), \quad (3.43)$$

where

$$d\tilde{k} \equiv \frac{d^3k}{(2\pi)^3 2E} \quad (3.44)$$

and where the annihilation and creation operators satisfy the usual commutation relations

$$[a(k), a^\dagger(k')] = [b(k), b^\dagger(k')] = (2\pi)^3 2E \delta^3(\mathbf{k} - \mathbf{k}'), \quad (3.45)$$

$$[A_i, A_i^\dagger] = [B_i, B_i^\dagger] = 2\Omega_i. \quad (3.46)$$

We interpret $a^\dagger(k)$ and $a(k)$ in the usual way as the operators which create and annihilate, respectively, a neutrino state with four-momentum k . $b^\dagger(k)$ and $b(k)$ act similarly with respect to the anti-neutrino states. The operators A_i^\dagger and A_i and B_i^\dagger and B_i interpolate between the energy levels of the harmonic oscillators¹¹.

We take as our initial state

$$|s, -\infty\rangle = |0; 1; 0\rangle \equiv |0\rangle_\phi \otimes |1\rangle_1 \otimes |0\rangle_2 \quad (3.47)$$

in which

$$|1\rangle_i \equiv A_i^\dagger |0\rangle_i \quad (3.48)$$

represents the first excited state of the oscillator i and in which $|0\rangle_\phi$ is the neutrino vacuum state. We wish to calculate the amplitude for the process in which the source de-excites to its ground state and the detector is excited to its first excited state. That

¹¹Note that we have allowed the q_i to be complex. Had we not done this, the source would have emitted both neutrinos and anti-neutrinos when it decayed.

is,

$$\mathcal{A} \equiv \langle 0; 0; 1 | s, \infty \rangle = \langle 0; 0; 1 | T \exp \left[-i \int_{-\infty}^{\infty} H^S(t') dt' \right] | s, -\infty \rangle, \quad (3.49)$$

in which H^S represents the Hamiltonian in the Schrödinger picture. The modulus squared of this amplitude is the probability for the transition to take place.

We shall assume the couplings in the interaction Hamiltonian to be sufficiently small that the amplitude in Eq. (3.49) is always much less than unity. This is of course always the case in the real-world situation which we are attempting to model – neutrino interactions are so weak that perturbation theory is always valid. It is then straightforward to evaluate (3.49) using standard techniques to obtain, up to an over-all unobservable phase,

$$\mathcal{A} = -\frac{1}{2} \langle 0; 0; 1 | T \left[\int_{-\infty}^{\infty} dt' dt'' H_{\text{int}}^H(t') H_{\text{int}}^H(t'') \right] | 0; 1; 0 \rangle, \quad (3.50)$$

where $H_{\text{int}}^H(t)$ refers to the interaction Hamiltonian evaluated in terms of the free fields in the Heisenberg picture at time t . The above expression may be evaluated explicitly in terms of neutrino propagators [55, 57] for arbitrary turn-on/off functions $\epsilon_i(t)$. We find it simpler, however, to require that the source and detector turn-on/off functions are never on at the same time, and to furthermore require that the source function always turns on first, and then the detector function; this is essentially a trick which allows us to use only one of the time orderings in the propagator. If the detector were allowed to be turned on before the source, there would in fact be some amplitude for the detector to become excited by emitting an anti-neutrino, but this amplitude would be very small, since it would violate energy conservation. In our calculations, then, we shall always be very insistent that the detector turns on after the source so that our calculation is simplified. Under the above assumptions, \mathcal{A} may be evaluated using Eqs. (3.42), (3.43), (3.45), (3.46) and (3.48) to obtain

$$\mathcal{A} = -\langle 0; 0; 1 | \int dt' dt'' d^3x' d^3x'' \epsilon_1(t') \epsilon_2(t'')$$

$$\times \phi(x'') q_2^\dagger(t'') h_2^*(\mathbf{x}'') \phi^\dagger(x') q_1(t') h_1(\mathbf{x}') |0; 1; 0\rangle \quad (3.51)$$

$$= - \int dt' dt'' d^3 x' d^3 x'' d\tilde{k} \epsilon_1(t') \epsilon_2(t'') h_1(\mathbf{x}') h_2^*(\mathbf{x}'') \\ \times \exp[-i(E - \Omega_2)t'' + i(E - \Omega_1)t' + i\mathbf{k} \cdot (\mathbf{x}'' - \mathbf{x}')] . \quad (3.52)$$

Since the amplitude is proportional to $\langle 0 | \phi(x'') \phi^\dagger(x') | 0 \rangle$, it is clear from Eq. (3.42) that this interaction corresponds to the creation and subsequent annihilation of a single neutrino. It is convenient to choose h_1 , h_2 and ϵ_1 all to be gaussians since this allows many of the integrals to be evaluated exactly. Setting

$$h_1(\mathbf{x}) = (\sqrt{2\pi}\sigma_{x_1})^{-3} e^{-|\mathbf{x}|^2/2\sigma_{x_1}^2}, \quad (3.53)$$

$$h_2(\mathbf{x}) = (\sqrt{2\pi}\sigma_{x_2})^{-3} e^{-|\mathbf{x}-\mathbf{x}_D|^2/2\sigma_{x_2}^2}, \quad (3.54)$$

$$\epsilon_1(t) = \epsilon_1^0 e^{-t^2/2\sigma_{t_1}^2} \quad (3.55)$$

we obtain

$$\mathcal{A} = -\sqrt{2\pi}\epsilon_1^0\sigma_{t_1} \int dt'' d\tilde{k} \epsilon_2(t'') \exp \left[-i(E - \Omega_2)t'' - \frac{1}{2}(E - \Omega_1)^2\sigma_{t_1}^2 \right. \\ \left. - \frac{1}{2}(E^2 - m^2)(\sigma_{x_1}^2 + \sigma_{x_2}^2) + i\mathbf{k} \cdot \mathbf{x}_D \right] \quad (3.56)$$

$$= - \left(\frac{\sqrt{2\pi}\epsilon_1^0\sigma_{t_1}}{4\pi^2 x_D} \right) \int_{-\infty}^{\infty} dt'' \epsilon_2(t'') \int_m^{\infty} dE \exp \left[-i(E - \Omega_2)t'' - \frac{1}{2}(E - \Omega_1)^2\sigma_{t_1}^2 \right. \\ \left. - \frac{1}{2}k^2(\sigma_{x_1}^2 + \sigma_{x_2}^2) \right] \sin(kx_D), \quad (3.57)$$

where

$$k \equiv \sqrt{E^2 - m^2}. \quad (3.58)$$

Before choosing an explicit form for $\epsilon_2(t'')$, there are several features of the above expression for the amplitude which we may note. First of all, for large x_D , the amplitude decreases like x_D^{-1} so that the probability falls like x_D^{-2} , as one might expect on geometric grounds in three dimensions. At the origin, however, the amplitude does not diverge

(despite the $1/x_D$ factor), due to the sine function in the integrand. A second point which we note is that conservation of energy at the source and of momentum at both the source and detector are governed by the relative sizes of σ_{t_1} , σ_{x_1} and σ_{x_2} . This situation is in accordance with the uncertainty principle (and is in fact necessary, as discussed above, in order to observe oscillations.) In general, neither energy nor momentum need be conserved exactly if the source and detector are localized in space and time. The specific set-up which we have chosen favours energies close to the energy of the excited source, Ω_1 , and momenta close to zero. This latter point is due to the fact that our source and detector have no dynamical degrees of freedom – they cannot recoil when a neutrino is emitted or absorbed – and thus the neutrino gets all of its momentum from the uncertainties in the positions of the source and detector. In order to avoid the problem that low momenta are favoured, we shall typically choose to set $\sigma_{t_1} \gg \sigma_{x_{1,2}}$ in our numerical work below¹². When several neutrino fields are coupled to the source and detector, this will mean that the energies of the mass eigenstates will be approximately equal, while their momenta will be determined by their energies. Furthermore, the sizes of the neutrino wave packets will then be determined more by the amount of time for which the source emits an uninterrupted wave-train than by the localization of the source-field interaction in configuration space. In Sec. 3.4, when we extend our analysis to fermionic neutrinos, we will allow the source to decay by emitting both a neutrino and its associated lepton. In this case the neutrino's momentum will no longer be centered about $k \approx 0$.

It will be useful in what follows to consider two different forms for the time-dependent function ϵ_2 . An obvious choice, given the forms we have chosen for ϵ_1 , h_1 and h_2 , is to take ϵ_2 to be a gaussian. This choice is indeed a useful one in many circumstances, and

¹²This is a “trick” which we use to get sensible results, but it is also not unreasonable on physical grounds. According to our discussion in Sec. 2.1, for example, this condition is satisfied by several orders of magnitude if σ_x is taken to be on the order of nuclear sizes. The reader is also referred to the discussion of Lipkin [39], where this same point is emphasized.

we thus define

$$\epsilon_2^{\text{gauss}}(t'') \equiv \epsilon_2^0 e^{-(t''-t_D)^2/2\sigma_{t_2}^2}. \quad (3.59)$$

Another useful choice is to take ϵ_2 to be simply a step function; that is,

$$\epsilon_2^{\text{step}}(t'') \equiv \epsilon_2^0 \theta(t_2 - t'') \theta(t'' - t_1), \quad (3.60)$$

where $\theta(t)$ is the Heaviside function. The gaussian detector is thus turned on and off gradually at a time centered around t_D , and the step function detector is turned on abruptly at t_1 and off again abruptly at time t_2 . The reader might worry about the abruptness with which the step function detector is turned on and off¹³. We shall address such concerns once we have studied the detector more carefully.

It is straightforward to evaluate the amplitudes for both types of detectors and we obtain

$$\begin{aligned} \mathcal{A}_{\text{gauss}} = & \tilde{N} \sqrt{2\pi} \sigma_{t_2} \int_m^\infty dE \exp \left[-\frac{1}{2}(E - \Omega_1)^2 \sigma_{t_1}^2 - \frac{1}{2}(E - \Omega_2)^2 \sigma_{t_2}^2 \right. \\ & \left. - \frac{1}{2}k^2(\sigma_{x_1}^2 + \sigma_{x_2}^2) - i(E - \Omega_2)t_D \right] \sin(kx_D), \end{aligned} \quad (3.61)$$

$$\begin{aligned} \mathcal{A}_{\text{step}} = & \tilde{N}(t_2 - t_1) \int_m^\infty dE \frac{\sin[(E - \Omega_2)(t_2 - t_1)/2]}{[(E - \Omega_2)(t_2 - t_1)/2]} \exp \left[-\frac{i}{2}(E - \Omega_2)(t_1 + t_2) \right. \\ & \left. - \frac{1}{2}(E - \Omega_1)^2 \sigma_{t_1}^2 - \frac{1}{2}k^2(\sigma_{x_1}^2 + \sigma_{x_2}^2) \right] \sin(kx_D), \end{aligned} \quad (3.62)$$

where

$$\tilde{N} \equiv -\frac{\epsilon_1^0 \epsilon_2^0 \sigma_{t_1}}{(2\pi)^{3/2} x_D}. \quad (3.63)$$

It is not possible in general to obtain an analytic closed-form solution of these integrals, but they are simple to evaluate numerically. In so doing, we obtain exact¹⁴ solutions

¹³It is well-known that turning on the detector too quickly can result in the excitation of the detector without its absorbing a particle. In our case, the detector would actually emit an anti-neutrino (which we cannot observe). This process is usually forbidden by energy conservation, but when the detector is turned on too quickly the energy distribution becomes very broad.

¹⁴“Exact” to second order in perturbation theory, that is. As we have argued above, however, second order perturbation theory is nearly exact for neutrino interactions.

to the problem which we are studying, including all effects due to the spreading of the neutrino wave packets.

As indicated above, it is important to understand the efficiency with which our source/detector system produces and detects neutrinos, since this has a direct bearing on whether or not some of the mass eigenstates will dominate the oscillation probability. We are also interested in examining effects due to the time resolution of the detector (in order to see if oscillations may truly be “revived” after the wave packets have separated) and in providing a self-consistent formalism which models the fact that the bulk detector stays “on” even though the microscopic detectors may always be turning on and off. In order to understand these issues, it is convenient to fix most of the parameters of the theory and to vary the neutrino mass and the various parameters having to do with when and for how long the detector is turned on. For the purposes of the numerical work below, then, we fix the following parameters

$$\Omega_1 = \Omega_2 = 10, \quad (3.64)$$

$$\sigma_{x_1} = \sigma_{x_2} = .1, \quad (3.65)$$

$$\sigma_{t_1} = 1, \quad (3.66)$$

where the units are arbitrary, but may be taken to be fixed by, for example, the value of Ω . Later on we shall also consider the effects of varying σ_{x_i} .

Let us study the step function detector first. Recall that the step function detector turns on at t_1 and off at t_2 . We define a modified “probability” associated with the amplitude in Eq. (3.62) as follows

$$\mathcal{P}_{\text{step}}(x_D, t_1, t_2) \equiv |\mathcal{A}_{\text{step}}(x_D, t_1, t_2)|^2 / \tilde{N}^2, \quad (3.67)$$

where we have divided through by \tilde{N}^2 because the value of that constant (including the fall-off as x_D^{-2}) is not really of interest to us – in any calculation of the oscillation

probability \tilde{N}^2 always factors out. We will use the step-function detector to model a very long “coherent” detection process. That is, each of the microscopic detectors in the bulk detector stays “on” for the entire time that the neutrino wave packet passes by. This is straightforward to model: we simply fix $t_1 > 0$ to be some time before the first bit of neutrino flux arrives ($t_1 < x_D - \sigma_{t_1}$) and allow t_2 to go to infinity. We will refer to this type of a detector as a “coherent” detector, to be distinguished from the “incoherent” detector which we shall discuss below.

Fig. 3.1 shows a plot of the probability in Eq. (3.67) as a function of $t_2 - t_1$, which is the amount of time for which the detector is turned on. In this figure, the energy of the neutrino is fixed to be $\sim \Omega_1 = \Omega_2 = 10$ and the momentum of the neutrino is determined by its mass. The various curves correspond to masses $m = 1, 2, \dots, 9$, with $m = 9$ being quite close to threshold. Also, the detector is positioned at $x_D = 10$ and is turned on at time $t_1 = 5$. We may make several observations concerning this figure. First of all, the curves each approach a constant as $t_2 \rightarrow \infty$. This is as one would hope: after a sufficiently long period of time, the entire wave packet has passed the detector and so the probability to find the detector in an excited state no longer changes (the subsequent decay of the detector would be a higher-order process which we do not consider here.) Two other characteristics of these curves which are obvious from the figure are that the curves corresponding to higher masses begin their ascent at later times and that the asymptotic values of the curves as $t_2 \rightarrow \infty$ are larger for larger masses. This latter point shows that this source/detector system is *more efficient* at producing and detecting heavier neutrinos. The first property is easy to understand. The more massive neutrinos travel more slowly and hence take longer to get to the detector. In order to understand the second property, it is convenient to appeal to an approximate form of the limit of Eq. (3.62) as $t_2 \rightarrow \infty$ (the reader is referred to Appendix C.) This approximation is valid

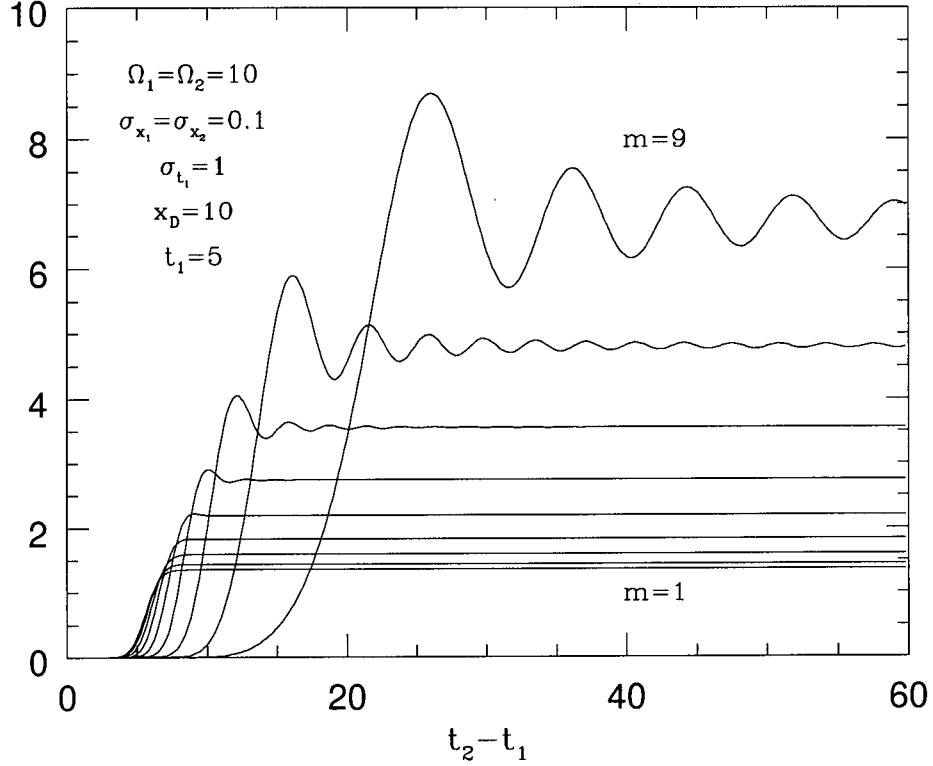


Figure 3.1: Plot of the (unnormalized) probability $\mathcal{P}_{\text{step}}$ (Eq. (3.67)) in the case of a single neutrino. The probability is plotted as a function of $t_2 - t_1$, which is the amount of time for which the detector is left on. The various curves correspond to the probabilities to detect different mass neutrinos, with $m=1, 2, \dots, 9$, as indicated in the figure. This detector is more efficient at detecting heavier neutrinos.

for masses not too close to the production and detection thresholds ($m \ll \Omega_i - 1/\sigma_{t_1}$) and for t_1 corresponding to a time before any appreciable amount of flux has arrived at the detector and yields

$$\lim_{t_2 \rightarrow \infty} \mathcal{A}_{\text{step}}(x_D, t_1, t_2) \simeq -i\tilde{N}\pi \exp \left[i\bar{k}x_D - \frac{1}{2}(\Omega_2 - \Omega_1)^2 \sigma_{t_1}^2 - \frac{1}{2}(\Omega_2^2 - m^2)(\sigma_{x_1}^2 + \sigma_{x_2}^2) \right], \quad (3.68)$$

where $\bar{k} \equiv (\Omega_2^2 - m^2)^{1/2}$. Note that the coherent detector “picks out” momenta corresponding to the energy Ω_2 . From the above expression it follows that

$$\frac{\mathcal{P}_{\text{step}}(m; x_D, t_1, \infty)}{\mathcal{P}_{\text{step}}(m'; x_D, t_1, \infty)} \simeq \exp \left[(m^2 - m'^2)(\sigma_{x_1}^2 + \sigma_{x_2}^2) \right], \quad (3.69)$$

demonstrating that indeed the system is more efficient at producing and detecting higher-mass neutrinos. It has been found numerically that the ratios of the asymptotic values (as $t_2 \rightarrow \infty$) of the curves in Fig. 3.1 are in excellent agreement with the expression in Eq. (3.69).

The mass-dependence of the source/detector system arises due to the fact that our source and detector favour neutrino states with momenta close to zero. This feature was predicted already in the discussion following Eq. (3.57) and is due to the fact that the source and detector in our model cannot “recoil” and thus the neutrino gets all of its momentum from the uncertainty in the positions of the source and detector. Thus the upper limit on the neutrino’s momentum is given by $k_{\text{max}} \sim 1/\sigma_{x_{1,2}}$. Note that the preference for non-relativistic neutrinos is essentially a quirk of our model and is *not* due to the fact that non-relativistic neutrinos “spend more time in the detector.” The mass-dependence of the system can be minimized by setting $\sigma_{x_{1,2}}$ to be much less than $\Omega_{1,2}^{-1}$. In such cases, the step function detector becomes nearly “ideal;” that is, it detects neutrinos of different masses with nearly the same efficiency.

Let us return briefly to the question of the abruptness with which the step function detector is turned on and off. Since the probability which is measured by the step function detector does not depend on the actual values chosen for t_1 and t_2 (provided that t_1 corresponds to a time before the first bit of neutrino flux arrives and that t_2 corresponds to a time after the last bit has passed) we could actually consider t_1 and t_2 to be smeared out, and the abruptness with which the detector is turned on and off need not concern us.

We now turn to the gaussian detector and define a modified probability in analogy with Eq. (3.67)

$$\mathcal{P}_{\text{gauss}}(x_D, t_D, \sigma_{t_2}) \equiv |\mathcal{A}_{\text{gauss}}(x_D, t_D, \sigma_{t_2})|^2 / \tilde{N}^2. \quad (3.70)$$

This expression gives the probability that a given microscopic detector – turned on for a time σ_{t_2} centered around the time t_D – is excited. We need to convert this expression into one giving the probability that the bulk detector “detects” the neutrino (i.e., that one of the microscopic detectors is excited.) We assume that the bulk detector is “on” for all $t_D > 0$ – in the sense that at any given time many of the microscopic detectors are “on” – but that the microscopic detectors themselves turn on and off randomly, so that the number which are “on” at any given time is roughly constant. Then the probability that the bulk detector “detects” the neutrino is proportional to the integral of Eq. (3.70) over t_D ¹⁵. We thus refer to this type of bulk detector as an “incoherent” detector, since we sum the probability incoherently over different times.

Before integrating Eq. (3.70), let us examine its behaviour as a function of m and t_D . Fig. 3.2 shows a plot of this expression as a function of t_D for a fixed width $\sigma_{t_2}=1$. We have again placed the detector at $x_D=10$ and the various curves correspond to neutrino masses $m=1, 2, \dots, 9$, as before. As one might expect, the curves corresponding to higher-mass neutrinos are displaced to the right since they travel more slowly. We

¹⁵Consider first a simpler case in which there are N detectors, turning on and off at times centered about $t_1 < t_2 < \dots < t_N$. Each of them has probability ϵ to detect the neutrino, but *only* if one of the previous detectors has not already detected it. Then the probability that none of them detects the neutrino is $(1 - \epsilon)^N$, that the last one detects it is $(1 - \epsilon)^{N-1}\epsilon$, that the second last one detects it is $(1 - \epsilon)^{N-2}\epsilon$, and so on. The probabilities for the $N + 1$ distinct possibilities sum to unity, as required. The probability that the neutrino is detected is then $1 - (1 - \epsilon)^N = N\epsilon - N! \epsilon^2 / (N - 2)! + \dots \simeq N\epsilon$ if $N\epsilon \ll 1$, that is, if the probability of detecting the neutrino in the bulk detector is much less than one, which is certainly the case. In the case at hand suppose that t_1 corresponds to a time before any appreciable flux has arrived at the detector and $t_N = t_1 + T$ to a time after all of the flux has passed. Then

$$\sum_{i=1}^N \mathcal{P}(x_D, t_i) \equiv \frac{(N-1)}{T} \sum_{i=1}^N \mathcal{P}(x_D, t_i) \Delta t \simeq \frac{(N-1)}{T} \int_{t_1}^{t_1+T} dt_D \mathcal{P}(x_D, t_D). \quad (3.71)$$

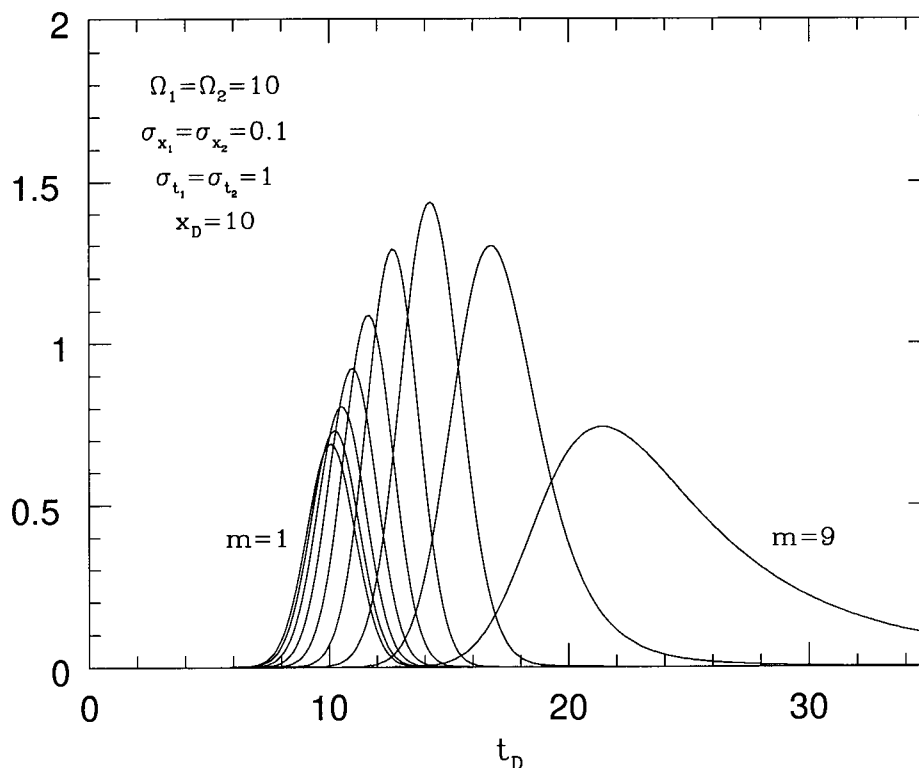


Figure 3.2: Plot of the “modified probability” $\mathcal{P}_{\text{gauss}}$ (Eq. (3.70)) for the case of a single neutrino. The probability is plotted as a function of t_D , for a fixed value of the width, $\sigma_{t_2}=1$. The various curves correspond to $m=1, 2, \dots, 9$, as indicated in the figure.

also note that the area under the curves appears to increase for higher masses. For the “incoherent” measurements which we have described, this would correspond to having a higher probability to detect more massive neutrinos. Finally, note that the probability is negligibly small at the origin, as required.

The time integral of Eq. (3.70) may actually be done explicitly, as we shall now show. Let us define the following unnormalized time-integrated probability

$$\mathcal{P}_{\text{incoh}}(x_D, \sigma_{t_2}) \equiv \int_0^\infty dt_D \mathcal{P}_{\text{gauss}}(x_D, t_D, \sigma_{t_2}). \quad (3.72)$$

Since the integrand is symmetric under $t_D \rightarrow -t_D$, we may formally extend the integration

to negative infinity and divide by two. The time integral then reduces to a delta function in energy and allows us to perform one of the energy integrals. As a result, we obtain

$$\mathcal{P}_{\text{incoh}}(x_D, \sigma_{t_2}) = 2\pi^2 \sigma_{t_2}^2 \int_m^\infty dE \exp \left[-(E - \Omega_1)^2 \sigma_{t_1}^2 - (E - \Omega_2)^2 \sigma_{t_2}^2 - k^2(\sigma_{x_1}^2 + \sigma_{x_2}^2) \right] \sin^2(kx_D). \quad (3.73)$$

If $m \ll \Omega - \sigma_{t_{1,2}}$ and $\sigma_{t_{1,2}} \gg \sigma_{x_{1,2}}$ (the latter condition is always assumed) then we may approximate the above expression by setting $\sin^2(kx_D) \approx 1/2$ to yield

$$\begin{aligned} \mathcal{P}_{\text{incoh}}(x_D, \sigma_{t_2}) \simeq & \frac{\pi^{3/2} \sigma_{t_2}^2}{(\sigma_{t_1}^2 + \sigma_{t_2}^2 + \sigma_{x_1}^2 + \sigma_{x_2}^2)^{1/2}} \exp \left[m^2(\sigma_{x_1}^2 + \sigma_{x_2}^2) \right] \\ & \times \exp \left[\frac{(\Omega_1 \sigma_{t_1}^2 + \Omega_2 \sigma_{t_2}^2)^2}{(\sigma_{t_1}^2 + \sigma_{t_2}^2 + \sigma_{x_1}^2 + \sigma_{x_2}^2)} - \Omega_1^2 \sigma_{t_1}^2 - \Omega_2^2 \sigma_{t_2}^2 \right]. \end{aligned} \quad (3.74)$$

Thus, under the above conditions the “incoherent” gaussian detector has the same mass-dependence as the step function detector does (c.f. Eq. (3.69))

$$\frac{\mathcal{P}_{\text{incoh}}(m; x_D, \sigma_{t_2})}{\mathcal{P}_{\text{incoh}}(m'; x_D, \sigma_{t_2})} \simeq \exp \left[(m^2 - m'^2)(\sigma_{x_1}^2 + \sigma_{x_2}^2) \right]. \quad (3.75)$$

This fact is rather remarkable and shows again that it is correct to perform the time integral in Eq. (3.72).

Fig. 3.3 shows a plot of the time-integrated probability, Eq. (3.73), as a function of the neutrino mass for the same set of parameters as in Fig. 3.2, as well as for the case in which $\sigma_{x_{1,2}} = 0.05$. This probability may be regarded as giving a measure of the *efficiency* with which the system produces and detects a neutrino of a given mass. For convenience, the probabilities have been normalized to their values at $m=0$. In each case, the solid line gives the exact result and the dashed line shows the approximation for non-threshold masses derived in Eq. (3.74). Clearly the approximation is quite good if the mass is not too close to the neutrino production and detection thresholds. Furthermore, it is clear that this detector can be made “ideal” (that is, the probability to detect a

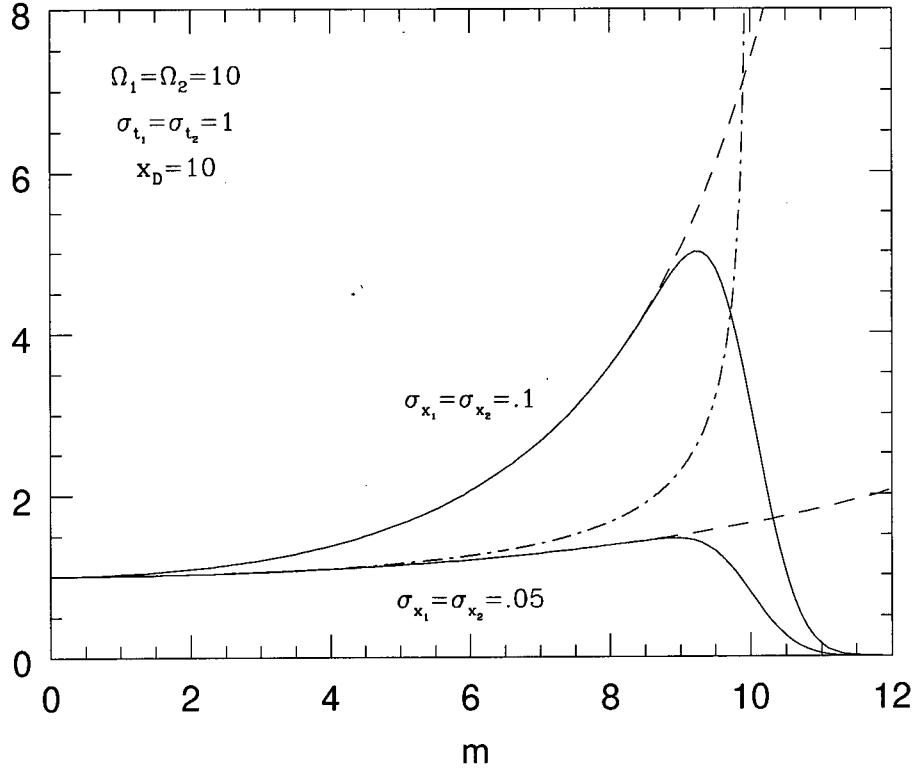


Figure 3.3: Plot of the “incoherent probability” $\mathcal{P}_{\text{incoh}}$ (Eq. (3.73), normalized to its value at $m=0$) as a function of mass for the case of a single neutrino, taking $\sigma_{x_{1,2}}=0.1, 0.05$. In each case, the solid line shows the exact result and the dashed line shows the result obtained in the approximation of Eq. (3.74). The dash-dotted line shows a plot of $1/v(m)$ for comparison.

neutrino may be made mass-independent) by using suitably small values for $\sigma_{x_{1,2}}$. The mass-dependence for large $\sigma_{x_{1,2}}$ occurs for the same reason as in the case of the step function detector and is due to the fact that the source and detector in our model cannot recoil (c.f. the discussion following Eq. (3.69).) For sufficiently small $\sigma_{x_{1,2}}$, neutrinos of different masses are detected with nearly the same efficiencies and the detector becomes “ideal.” The dash-dotted line shows a plot of $1/v(m)$, which would be the analogous efficiency inferred from the calculation in Ref. [54].

Before coupling more neutrino fields to the source and detector, let us first summarize our results for the single-neutrino case. We have coupled the neutrino field to two harmonic oscillators, one of which acts as a neutrino “source” and the other of which acts as a neutrino “detector.” These are understood as being microscopic constituents of larger macroscopic “bulk” sources and detectors. We have shown that the system is easily solved in second-order perturbation theory, which is perfectly adequate when considering neutrino interactions. The neutrino in this system is never “observed” directly; rather it is the exchange particle which mediates the source-detector interaction. We have taken the source and detector to be localized both in space and in time. The uncertainties in the turn on/off times and in the spatial couplings of the source and detector lead naturally to uncertainties in the energy and momentum of the exchanged neutrino; that is, the neutrino is produced as a wave packet, whose characteristics are *completely determined* by the source and detector configurations. This fact will be extremely important when we consider neutrino oscillations because the relative characteristics of the wave packets corresponding to the various mass eigenstates will be completely determined and need not be put in by hand.

We have considered two different types of macroscopic “bulk” detectors. The first type we have called a “coherent” detector, since each of its microscopic constituents makes a long coherent measurement of the neutrino wave packet. The second type we have called an “incoherent” detector, since in our calculation we have summed incoherently over a large number of (microscopically coherent) detection events. In our study of these two types of detectors, we have noted that they are not in general “ideal” detectors, since they are generally more efficient at detecting low-momentum neutrinos. This effect is well-understood and is simply due to the fact that our source and detector are “fixed” in the lab system and thus tend to favour neutrino momenta close to zero. Put another way, since the neutrino is the only decay particle in this model, all of its momentum comes

from the uncertainties in the positions of the source and detector; that is, $k < 1/\sigma_{x_{1,2}}$. It turns out that it is easy to tune the parameters of the theory in such a way that this effect is negligible and thus we do not generically get the $1/v$ dependence suggested by the calculation in Ref. [54]. Nevertheless, this simple calculation demonstrates the important point that for non-relativistic neutrinos the production and detection efficiencies might in general be expected to be mass-dependent. Such a mass dependence could in principle skew the oscillation probability such as occurred in Ref. [54]. Finally, we note that the formalism which we have developed for the incoherent detector (of integrating over t_D) yields the same mass-dependence of the detection efficiency as is found for the coherent detector and this gives us additional confidence that this method is indeed justified.

3.3.2 Several Neutrinos

Now that we have studied the characteristics of the source/detector system in the single-neutrino case, we turn to the case in which there are several neutrino fields coupled to the source and detector. Suppose that there are N different neutrino mass eigenstates. Then, in order to model the real-life situation, we suppose that there are also several different types of sources and detectors, each of which couple to a given unitary linear combination of the neutrino mass eigenstates. The action of Eq. (3.36) is then generalized to

$$S = \int d^4x \left(\mathcal{L}_\phi^0 + \mathcal{L}_{\text{int}} \right) + \int dt L_q^0, \quad (3.76)$$

where

$$\mathcal{L}_\phi^0 = - \sum_i \phi_i^\dagger(x) \left(\square + m_i^2 \right) \phi_i(x), \quad (3.77)$$

$$L_q^0 = \sum_\alpha \left[\dot{q}_1^{\alpha\dagger}(t) \dot{q}_1^\alpha(t) - \Omega_1^{\alpha 2} q_1^{\alpha\dagger}(t) q_1^\alpha(t) + \dot{q}_2^{\alpha\dagger}(t) \dot{q}_2^\alpha(t) - \Omega_2^{\alpha 2} q_2^{\alpha\dagger}(t) q_2^\alpha(t) \right], \quad (3.78)$$

$$\mathcal{L}_{\text{int}} = - \sum_{\alpha,i} \left[\epsilon_1(t) \left(\mathcal{U}_{\alpha i}^* \phi_i^\dagger(x) q_1^\alpha(t) h_1(\mathbf{x}) + \mathcal{U}_{\alpha i} \phi_i(x) q_1^{\alpha\dagger}(t) h_1^*(\mathbf{x}) \right) \right]$$

$$+\epsilon_2(t) \left(\mathcal{U}_{\alpha i}^* \phi_i^\dagger(x) q_2^\alpha(t) h_2(\mathbf{x}) + \mathcal{U}_{\alpha i} \phi_i(x) q_2^{\alpha\dagger}(t) h_2^*(\mathbf{x}) \right) \Big], \quad (3.79)$$

and in which \mathcal{U} is a unitary matrix. Note that the subscripts “1” and “2” on the functions ϵ and h and on the fields q refer, respectively, to the source and detector. These should not be confused with the subscripts on the fields ϕ which refer to the mass eigenstates. Also note that we have taken ϵ and h to be independent of the flavour or mass eigenstate in question. In principle there could be such a dependence, but including it would unnecessarily complicate our analysis. In what follows, we shall also set $\Omega_i^\alpha = \Omega_i$, $\forall \alpha$, in order to “idealize” our sources and detectors.

The experimental set-up which we wish to consider is a simple generalization of that given in the previous section. In this case we imagine that the initial state of the system has an α -flavour “source” oscillator in its first excited state and that the final state has a β -flavour “detector” oscillator in its first excited state. The amplitude for this process may then be calculated as in the single-neutrino case and we find

$$\begin{aligned} \mathcal{A}_{\alpha \rightarrow \beta} &= - \sum_{i,j} \mathcal{U}_{\beta j} \mathcal{U}_{\alpha i}^* \langle 0; 0; 1_\beta | \int dt' dt'' d^3 x' d^3 x'' \epsilon_1(t') \epsilon_2(t'') \\ &\quad \times \phi_j(x'') q_2^{\beta\dagger}(t'') h_2^*(\mathbf{x}'') \phi_i^\dagger(x') q_1^\alpha(t') h_1(\mathbf{x}') | 0; 1_\alpha; 0 \rangle \end{aligned} \quad (3.80)$$

$$\begin{aligned} &= - \sum_i \mathcal{U}_{\beta i} \mathcal{U}_{\alpha i}^* \int dt' dt'' d^3 x' d^3 x'' d\tilde{k}_i \epsilon_1(t') \epsilon_2(t'') h_1(\mathbf{x}') h_2^*(\mathbf{x}'') \\ &\quad \times \exp[-i(E_i - \Omega_2)t'' + i(E_i - \Omega_1)t' + i\mathbf{k} \cdot (\mathbf{x}'' - \mathbf{x}')], \end{aligned} \quad (3.81)$$

in which we have defined

$$d\tilde{k}_i \equiv \frac{d^3 k}{(2\pi)^3 2E_i}, \quad (3.82)$$

$$E_i \equiv \sqrt{k^2 + m_i^2}. \quad (3.83)$$

Taking h_1 , h_2 and ϵ_1 to be gaussians with widths σ_{x_1} , σ_{x_2} and σ_{t_1} as in the single-neutrino case (see Eqs. (3.53), (3.54) and (3.55)), we may further simplify this expression

$$\mathcal{A}_{\alpha \rightarrow \beta} = - \left(\frac{\sqrt{2\pi} \epsilon_1^0 \sigma_{t_1}}{4\pi^2 x_D} \right) \sum_i \mathcal{U}_{\beta i} \mathcal{U}_{\alpha i}^* \int_{-\infty}^{\infty} dt'' \epsilon_2(t'') \int_{m_i}^{\infty} dE \exp[-i(E - \Omega_2)t'']$$

$$-\frac{1}{2}(E - \Omega_1)^2 \sigma_{t_1}^2 - \frac{1}{2}k_i^2(\sigma_{x_1}^2 + \sigma_{x_2}^2) \Big] \sin(k_i x_D), \quad (3.84)$$

where

$$k_i \equiv \sqrt{E^2 - m_i^2}. \quad (3.85)$$

This expression is clearly just a simple generalization of Eq. (3.57). The final step in our calculation is to substitute in the expressions (3.59) and (3.60) for $\epsilon_2(t'')$ in the gaussian and step function detector cases. This yields

$$\begin{aligned} \mathcal{A}_{\alpha \rightarrow \beta}^{\text{gauss}} &= \tilde{N} \sqrt{2\pi} \sigma_{t_2} \sum_i \mathcal{U}_{\beta i} \mathcal{U}_{\alpha i}^* \int_{m_i}^{\infty} dE \exp \left[-\frac{1}{2}(E - \Omega_1)^2 \sigma_{t_1}^2 - \frac{1}{2}(E - \Omega_2)^2 \sigma_{t_2}^2 \right. \\ &\quad \left. - \frac{1}{2}k_i^2(\sigma_{x_1}^2 + \sigma_{x_2}^2) - i(E - \Omega_2)t_D \right] \sin(k_i x_D), \end{aligned} \quad (3.86)$$

$$\begin{aligned} \mathcal{A}_{\alpha \rightarrow \beta}^{\text{step}} &= \tilde{N}(t_2 - t_1) \sum_i \mathcal{U}_{\beta i} \mathcal{U}_{\alpha i}^* \int_{m_i}^{\infty} dE \frac{\sin[(E - \Omega_2)(t_2 - t_1)/2]}{[(E - \Omega_2)(t_2 - t_1)/2]} \sin(k_i x_D) \\ &\quad \times \exp \left[-\frac{i}{2}(E - \Omega_2)(t_1 + t_2) - \frac{1}{2}(E - \Omega_1)^2 \sigma_{t_1}^2 - \frac{1}{2}k_i^2(\sigma_{x_1}^2 + \sigma_{x_2}^2) \right], \end{aligned} \quad (3.87)$$

where \tilde{N} is defined in (3.63).

We are finally in a position to define the oscillation probability as a function of distance for the two cases. In both cases our definition of the probability is a “physical” one. We imagine that the source produces neutrinos of type α ($\alpha=e, \mu, \tau, \dots$) and that we set a β -neutrino detector at some distance x_D from the source. We prepare the source (or an ensemble of identically prepared sources) in an excited state, wait a long period of time, and then check to see if the detector has been excited. After repeating this experiment enough times to get good statistics, we repeat the procedure with a β' -neutrino detector, and so on. The probability to observe a β neutrino is then simply the number of events observed in “ β -mode” divided by the total number of events in all modes. Since we have attempted to make our source/detector system as “ideal” as possible, there are no further corrections for detector efficiencies or anything of that nature. The normalized coherent

and incoherent oscillation probabilities may then be defined as

$$\mathcal{P}_{\alpha \rightarrow \beta}^{\text{coh}}(x_D) = \lim_{t_2 \rightarrow \infty} \frac{|\mathcal{A}_{\alpha \rightarrow \beta}^{\text{step}}(x_D, t_1, t_2)|^2}{\sum_{\beta} |\mathcal{A}_{\alpha \rightarrow \beta}^{\text{step}}(x_D, t_1, t_2)|^2}, \quad (3.88)$$

$$\mathcal{P}_{\alpha \rightarrow \beta}^{\text{incoh}}(x_D, \sigma_{t_2}) = \frac{\int_0^\infty dt_D |\mathcal{A}_{\alpha \rightarrow \beta}^{\text{gauss}}(x_D, t_D, \sigma_{t_2})|^2}{\sum_{\beta} \int_0^\infty dt_D |\mathcal{A}_{\alpha \rightarrow \beta}^{\text{gauss}}(x_D, t_D, \sigma_{t_2})|^2}. \quad (3.89)$$

It is understood in the first expression that t_1 is taken to be some time before the first bit of neutrino “flux” arrives at the detector.

The expressions which we have derived for our two types of detectors are in forms which are amenable to numerical calculation. The coherent probability may be found after a single integration over energy and the incoherent probability requires two integrations, one over energy and one over time. In the two-neutrino case, the time integral in Eq. (3.89) may be done by hand, but this is not possible in general for more neutrinos. The reason for this is that the integrand is no longer symmetric under $t_D \rightarrow -t_D$ due to the possible presence of phases in the mixing matrix \mathcal{U} .

Let us examine the case for two flavours in some detail. In that case, the matrix \mathcal{U} may be taken to be a real orthogonal matrix parametrized by one angle, θ . The time integral in the numerator of (3.89) may be performed explicitly and we find

$$\begin{aligned} \int_0^\infty dt_D |\mathcal{A}_{\alpha \rightarrow \beta}^{\text{gauss}}(x_D, t_D, \sigma_{t_2})|^2 &= \\ 2\pi^2 \sigma_{t_2}^2 \tilde{N}^2 \sum_{i,j} \mathcal{U}_{\beta i} \mathcal{U}_{\beta j} \mathcal{U}_{\alpha i} \mathcal{U}_{\alpha j} \int_{\max(m_i, m_j)}^\infty dE \sin(k_i x_D) \sin(k_j x_D) \\ &\times \exp \left[-(E - \Omega_1)^2 \sigma_{t_1}^2 - (E - \Omega_2)^2 \sigma_{t_2}^2 - (E^2 - (m_i^2 + m_j^2)/2)(\sigma_{x_1}^2 + \sigma_{x_2}^2) \right]. \end{aligned} \quad (3.90)$$

Fig. 3.4 shows several plots of the flavour-conserving probability $\mathcal{P}_{e \rightarrow e}(x_D)$ as a function of x_D for two relativistic neutrinos, using both the “coherent” and the “incoherent” detector. The various parameters chosen for the plot are as indicated in the figure. Recall that Ω_1 and Ω_2 (set equal here) are the energies of the excited source and detector,

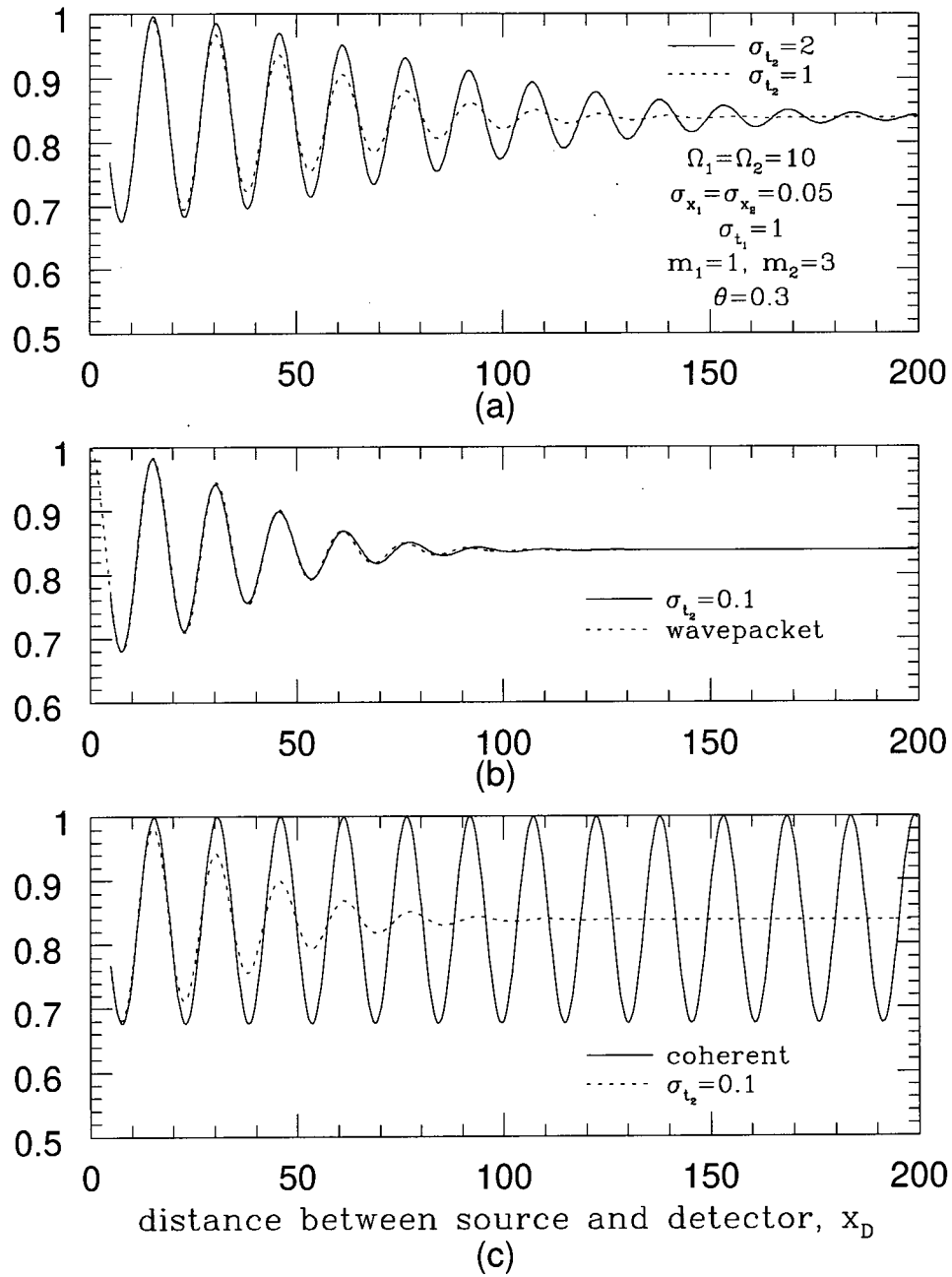


Figure 3.4: Oscillation probabilities as a function of distance. The two curves in (a) correspond to the "incoherent" detector with time resolutions $\sigma_{t_2}=1, 2$. The solid curve in (b) gives the "incoherent" probability for $\sigma_{t_2}=0.1$. The dotted curve shows the analogous result obtained in the wave packet approach. The solid curve in (c) shows the probability measured by the "coherent" detector.

respectively. Since we have chosen to set $\sigma_{x_i} \ll \sigma_{t_i}$, the energies of the mass eigenstates are approximately equal to Ω and their momenta are determined by their energies.

The values employed here for θ , m_1 and m_2 are chosen merely for the purpose of illustration. Note that the curves do not go all the way to $x_D=0$, since our formalism is not valid for very small x_D . The expressions themselves are mathematically well-defined but they have no physical meaning¹⁶.

Figs. 3.4(a) and (b) show plots of the probability for detecting the same-flavour neutrino as emitted in the case of an “incoherent” detector (see Eq. (3.89)) for several different values of the time resolution of the detector, σ_{t_2} . The dotted curve in (b) is the analogous result derived using the wave packet approach of Sec. 3.1. This appears to be a good approximation to our result in the limit as $\sigma_{t_2} \rightarrow 0$. It is clear from these plots that the coherence length of the oscillations is dependent on the time resolution of the detector; that is, as we discussed in the previous chapter, a long coherent measurement in time is capable of “reviving” oscillations of neutrinos whose mass eigenstate wave packets have become physically separated. This effect is particularly striking in the case of the probability detected by the coherent detector, shown by the solid curve in Fig. 3.4(c). In this case the oscillations appear to have been *completely revived* even after, according to an “incoherent” measurement (dotted curve), the wave packets have completely separated.

We have already discussed to some extent in Sec. 2.2.1 how it is possible for a long coherent measurement in time to revive the oscillations of neutrinos even after the mass eigenstates have separated spatially. Essentially, the accurate measurement of the energy picks out the plane wave in the wave packet which has existed coherently through both pulses. Our present approach allows for a complementary way to view the situation. The idea that “the mass eigenstates have separated spatially” is based upon the notion that

¹⁶Recall that we require the source to turn off before the detector turns on in order that we may drop one of the time-orderings in the neutrino propagator. The reader is referred to the discussion following Eq. (3.50) for more details on this point.

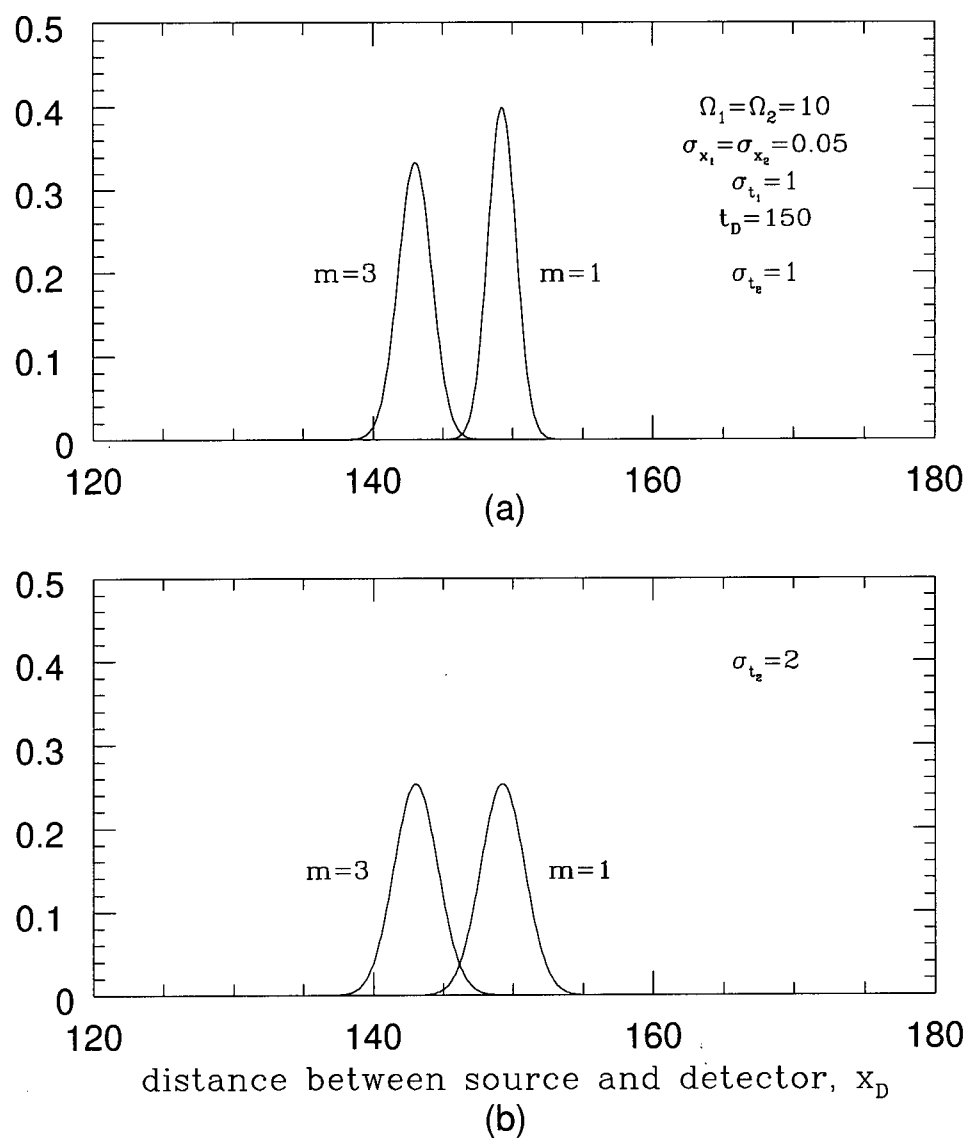


Figure 3.5: “Snapshots” of two mass eigenstate wave packets using incoherent detectors with different time resolutions. The wave packets have been individually normalized over x_D . In (a) the time resolution of the detector is such that the wave packets appear to be nearly separated, while in (b) the same wave packets appear to overlap due to the broader temporal resolution in that case.

the characteristics of the neutrino wave packets are determined at some initial time and then are propagated forward in time. In our case, however, there is no need to regard the *production* of the neutrinos as somehow being special compared to their *detection*. Indeed, a cursory examination of the expression for the incoherent probability (see Eqs. (3.89) and (3.90)) reveals that it is completely symmetric in the parameters describing the production and the detection of the neutrino! There is thus no need in our calculation to refer to the neutrino “wave packets” as being objects which have some significance on their own, independent of their detection. If indeed we wish to refer to a neutrino wave packet, however, we could define it as being what the detector measures in the limit as $\sigma_{t_2}, \sigma_{x_2} \rightarrow 0$. In this limit the detector sees the wave packets “as they are.” For non-zero values of σ_{x_2} and σ_{t_2} , the widths of the detector are “folded in” and the detector sees wave packets which have been broadened somewhat. Thus, whether the wave packets corresponding to two mass eigenstates have separated or not depends on the temporal and spatial resolution of the detector. We may demonstrate this effect by way of an example. To do this, it is instructive to take a “snapshot” of the wave packets corresponding to two different mass eigenstates at a fixed time $t_D=150$ using the incoherent detector with different widths, σ_{t_2} . Figs. 3.5(a) and (b) show the detection probabilities (given by Eq. (3.70), but separately normalized over x_D) for the two mass eigenstates. In (a), the time resolution of the detector is taken to be $\sigma_{t_2}=1$ and there is almost no overlap between the two wave packets. Indeed, comparison with Fig. 3.4(a) shows that, for $x_D \approx 150$, the oscillations have been almost completely damped out. If the detector is taken to have a broader time resolution as in Fig. 3.5(b), however, the wave packets appear to have a non-negligible overlap. In this case the width due to the finite time resolution of the detector has been added to the original widths of the wave packets. Comparison with Fig. 3.4(a) shows that in this case the oscillations have not yet been wiped out for $x_D \approx 150$. From this point of view, then, the fact that the conventional “wave

packet” approach for relativistic neutrinos agrees with the source/detector approach (see Fig. 3.4(b)) for very small σ_{t_2} is not that surprising. The wave packet approach simply ignores the finite time resolution of the detector.

The “incoherent” and “coherent” probabilities, Eqs. (3.89) and (3.88) may both be reliably approximated in the relativistic limit. Setting $\Omega \equiv \Omega_1 = \Omega_2$ for convenience, we obtain ¹⁷

$$\mathcal{P}_{\alpha \rightarrow \beta}^{\text{coh}}(x_D) \simeq \frac{1}{\mathcal{N}} \sum_{i,j} \mathcal{U}_{\beta i} \mathcal{U}_{\alpha i} \mathcal{U}_{\beta j} \mathcal{U}_{\alpha j} \exp \left[i(\bar{k}_i - \bar{k}_j)x_D + (m_i^2 + m_j^2)(\sigma_{x_1}^2 + \sigma_{x_2}^2)/2 \right] \quad (3.91)$$

and

$$\begin{aligned} \mathcal{P}_{\alpha \rightarrow \beta}^{\text{incoh}}(x_D, \sigma_{t_2}) &\simeq \frac{1}{\mathcal{N}} \sum_{i,j} \mathcal{U}_{\beta i} \mathcal{U}_{\alpha i} \mathcal{U}_{\beta j} \mathcal{U}_{\alpha j} \exp \left[i(\bar{k}_i - \bar{k}_j)x_D + (m_i^2 + m_j^2)(\sigma_{x_1}^2 + \sigma_{x_2}^2)/2 \right] \\ &\times \exp \left[-\frac{x_D^2 (1/v_i - 1/v_j)^2}{4(\sigma_{t_1}^2 + \sigma_{t_2}^2)} \right] \end{aligned} \quad (3.92)$$

for the coherent and incoherent cases, respectively, where we have defined

$$\mathcal{N} = \sum_i \mathcal{U}_{\alpha i}^2 \exp \left[m_i^2(\sigma_{x_1}^2 + \sigma_{x_2}^2) \right] \quad (3.93)$$

$$\bar{k}_i = \sqrt{\Omega^2 - m_i^2}, \quad (3.94)$$

$$v_i = \bar{k}_i/\Omega. \quad (3.95)$$

These expressions are identical except for the damping of the cross-terms which occurs in the approximation for the “incoherent” case, Eq. (3.74). Note that the oscillation length which may be extracted from either of these expressions is exactly what one finds in the usual approach, with no spurious factor of “2.” The approximation for the “coherent” case contains no damping whatsoever, demonstrating that an infinitely long coherent measurement does indeed completely revive the oscillations of the neutrinos! We also note

¹⁷We have used the approximate form of $\mathcal{A}^{\text{step}}$ given in Eq. (3.68) in order to derive Eq. (3.91). Also, in deriving Eq. (3.92) we have dropped the highly oscillatory terms in the integrand since they are strongly damped for $x_D > \sigma_{t_1} + \sigma_{t_2}$. Recall that our calculation is only sensible for $x_D < \sigma_{t_1} + \sigma_{t_2}$.

that, while our expression for the incoherent case, Eq. (3.74), bears some resemblance to the analogous expression obtained in the wave packet approach, Eq. (3.13), our expression has an intrinsic dependence on the temporal and spatial resolution of the detector which is ignored in the wave packet approach. Finally, we note the absence of factors of $1/v_i$ pre-multiplying the exponentials such as occurred in the wave packet approach.

3.3.3 The Non-relativistic Case

It is worthwhile to consider briefly the oscillations of non-relativistic neutrinos in our toy model. Let us assume that one of the mass eigenstates is relatively light and let us study the behaviour of the oscillation probability as the mass of the other neutrino (in the two-neutrino case) is varied. Furthermore, let us restrict our attention to the case of the incoherent detector, which is the more realistic of the two detector types. As the mass of the heavier neutrino increases, the packets separate more quickly and, for sufficiently non-relativistic neutrinos, the oscillations are damped out almost immediately. It is convenient, then, to simply study the asymptotic expression

$$\mathcal{P}_{\alpha \rightarrow \beta}^{\infty}(\sigma_{t_2}) \equiv \lim_{x_D \rightarrow \infty} \mathcal{P}_{\alpha \rightarrow \beta}^{\text{incoh}}(x_D, \sigma_{t_2}). \quad (3.96)$$

The main non-relativistic effect in our toy model is the effect due to the model's dependence on $\sigma_{x_{1,2}}$. Recall from our discussion in Sec. 3.3.1 that our source and detector are more efficient at producing and detecting non-relativistic neutrinos (see also Fig. 3.3.) This dependence skews the results for the oscillations, as one might expect.

In Fig. 3.6 we have plotted the probability for a ν_e to be detected as a ν_e in the limit as $x_D \rightarrow \infty$ ($\mathcal{P}_{e \rightarrow e}^{\infty}$ in Eq. (3.96)) as a function of the mass of the heavier neutrino. The various curves correspond to different values of $\sigma_{x_{1,2}}$, the spatial resolution of the source and detector. For larger values of $\sigma_{x_{1,2}}$, this probability is indeed skewed quite dramatically due to the fact that the heavier mass eigenstate starts to dominate the

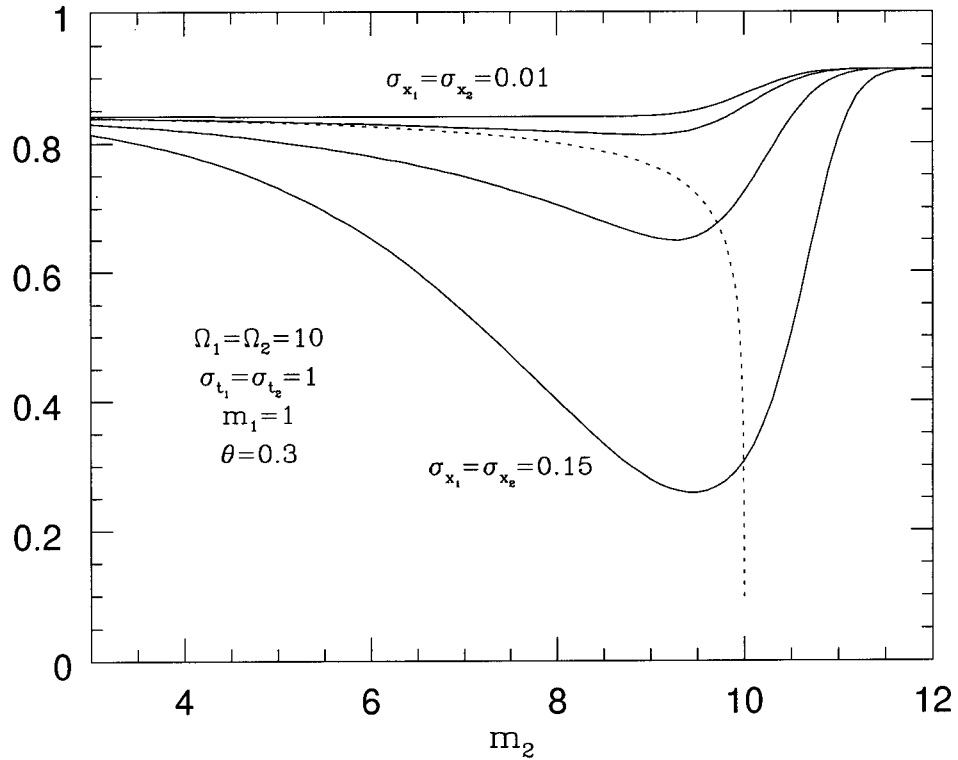


Figure 3.6: Plot of the constant flavour-conserving probability, $\mathcal{P}_{e \rightarrow e}^\infty$, defined in Eq. (3.96) as a function of the mass of the heavier neutrino. The solid lines correspond to spatial widths $\sigma_{x_{1,2}} = 0.01, 0.05, 0.1, 0.15$ and the dotted line shows the value obtained in the wave packet approach (c.f. Eq. (3.18).)

probability distribution. Recall our earlier explanation as to why this occurs in our model. Since our source and detector do not “recoil” when the neutrino is emitted or absorbed, the upper limit on the neutrino’s momentum is given by $k_{\max} \sim 1/\sigma_{x_{1,2}}$ (the reader is referred to the discussion following Eq. (3.69).) We emphasize, however, that this effect is an artifact of our model and would not be expected to occur in more realistic models. We shall discuss this point further below when we consider how our approach might be extended to the more realistic case in which the neutrino is not the only decay particle emitted. Note also that as m_2 increases above the production/detection threshold

all of the solid curves approach the same value of $\cos^2 \theta$. (How abrupt the threshold is depends on how large σ_{t_1} and σ_{t_2} are, of course.) The dotted curve gives the generic result derived in the wave packet approach [54]. We see no evidence in our model for this type of $1/v$ behaviour.

3.4 Towards a More Realistic Calculation

In this section we show how the bosonic model of the previous section may be modified to account correctly for the fermionic nature of the neutrinos (which we shall assume to be Dirac neutrinos) and for the $V - A$ nature of neutrino interactions. Once again the source and detector will be modelled by harmonic oscillators. This time, however, the oscillators will be coupled to the usual $V - A$ leptonic current rather than simply to the neutrino field. As a result, the interactions at the source and detection points will involve both the neutrino and its associated charged lepton. It is convenient to take the initial state to consist only of the source and detector, both in their first excited states. The source decays by emitting a neutrino and its associated charged anti-lepton, and the detector decays by absorbing the neutrino and emitting another charged lepton:

$$\begin{aligned} (\text{source})^* &\rightarrow \nu(k) + l_\alpha^+(p_1) + (\text{source}) \\ &\hookrightarrow \nu(k) + (\text{detector})^* \rightarrow l_\beta^-(p_2) + (\text{detector}). \end{aligned} \quad (3.97)$$

This sequence of events is illustrated schematically in Fig. 3.7. The system may be described by the following action

$$S = \int d^4x \left(\mathcal{L}_\nu^0 + \mathcal{L}_{\text{int}} \right) + \int dt L_q^0, \quad (3.98)$$

where

$$\mathcal{L}_\nu^0 = \sum_i \bar{\nu}_i(x) (i\rlap{\not{D}} - m_i) \nu_i(x), \quad (3.99)$$

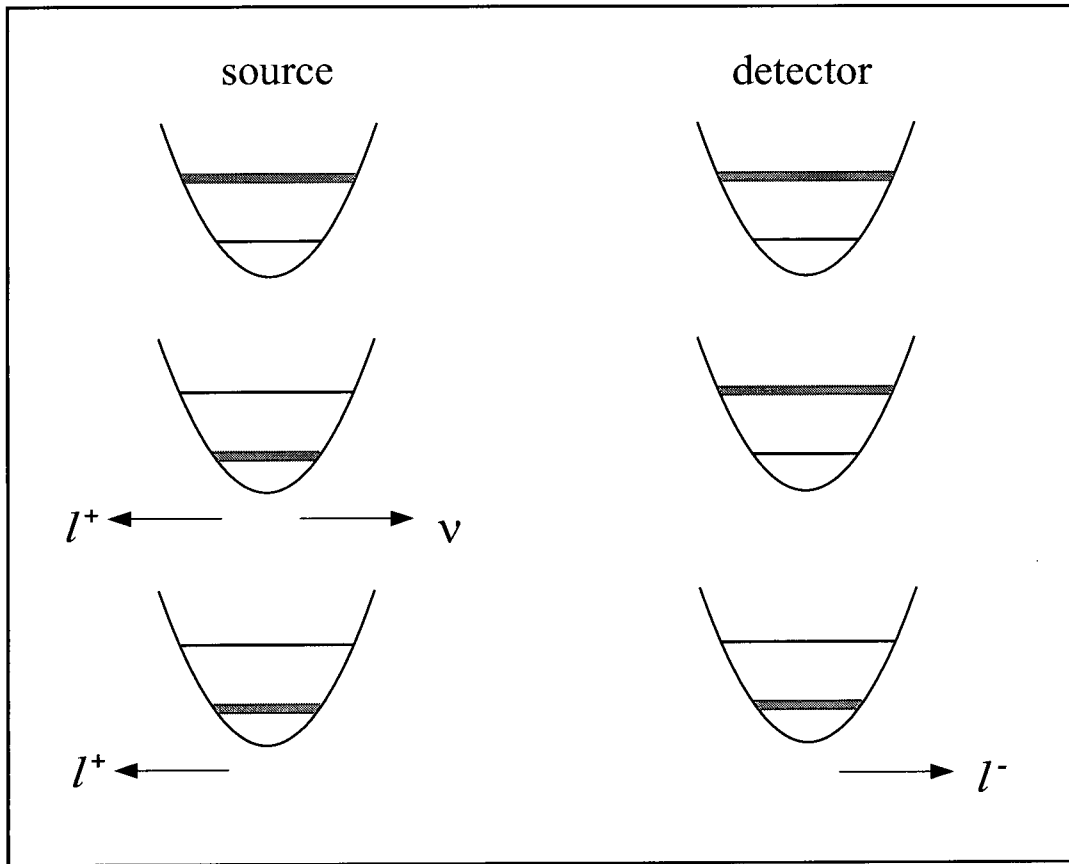


Figure 3.7: A schematic illustration of the sequence of events in the source/detector system for fermionic neutrinos considered in Sec. 3.4. The excited source decays by emitting a neutrino and its associated anti-lepton. The detector subsequently absorbs the neutrino and emits a lepton.

$$L_q^0 = \sum_{\alpha} \left[\dot{q}_1^{\alpha\dagger}(t) \dot{q}_1^{\alpha}(t) - \Omega_1^2 q_1^{\alpha\dagger}(t) q_1^{\alpha}(t) + \dot{q}_2^{\alpha\dagger}(t) \dot{q}_2^{\alpha}(t) - \Omega_2^2 q_2^{\alpha\dagger}(t) q_2^{\alpha}(t) \right], \quad (3.100)$$

$$\mathcal{L}_{\text{int}} = - \sum_{\alpha} \left[\epsilon_1(t) q_1^{\alpha}(t) h_1(\mathbf{x}) j_{\alpha}^0(x) + \epsilon_2(t) q_2^{\alpha}(t) h_2(\mathbf{x}) j_{\alpha}^{0\dagger}(x) + \text{h.c.} \right], \quad (3.101)$$

and where $j_{\alpha}^0(x)$ is the zeroth¹⁸ component of the leptonic $V - A$ current

$$j_{\alpha}^{\mu}(x) \equiv \sum_i \mathcal{U}_{\alpha i} \bar{l}_{\alpha} \gamma^{\mu} P_L \nu_i(x), \quad l_{\alpha} = e, \mu, \tau, \dots, \quad (3.102)$$

¹⁸In a more realistic calculation, one might perhaps couple the $V - A$ current to a current representing the initial and final nucleus. If these nuclei are sufficiently non-relativistic then it is a good approximation to consider only the zeroth component of the current.

with $P_L \equiv (1 - \gamma^5)/2$. Once again, $\epsilon_{1(2)}$ and $h_{1(2)}$ are functions which parametrize the temporal and spatial couplings of the neutrino and lepton fields to the source (detector).

The calculation of the amplitude proceeds in complete analogy with the calculation for the bosonic case and we shall omit most of the details. As above, we take $\epsilon_1(t)$ ($\epsilon_2(t)$) to be a gaussian of width σ_{t_1} (σ_{t_2}) centered at $t=0$ ($t=t_D$) and $h_1(\mathbf{x})$ ($h_2(\mathbf{x})$) to be a gaussian of width σ_{x_1} (σ_{x_2}) centered at $\mathbf{x}=0$ ($\mathbf{x}=\mathbf{x}_D$) (see Eqs. (3.53), (3.54), (3.55) and (3.59).) Thus, we omit here the case of the (coherent) “step function” detector and consider only the (incoherent) “gaussian” detector. Also, recall that the energies of the source and detector are Ω_1 and Ω_2 , respectively. The amplitude to detect a neutrino of flavour β given that a neutrino of flavour α was emitted at the source is then given by

$$\begin{aligned} \mathcal{A}_{\alpha \rightarrow \beta} = & (2\pi)\epsilon_1\epsilon_2\sigma_{t_1}\sigma_{t_2} \sum_i \mathcal{U}_{\beta i} \mathcal{U}_{\alpha i}^* \int \frac{d^3k}{(2\pi)^3 2E_i} \exp \left[-\frac{1}{2}(\Omega_1 - E(p_1) - E_i)^2 \sigma_{t_1}^2 \right. \\ & \left. -\frac{1}{2}(\Omega_2 + E_i - E(p_2))^2 \sigma_{t_2}^2 - \frac{1}{2}|\mathbf{k} + \mathbf{p}_1|^2 \sigma_{x_1}^2 - \frac{1}{2}|\mathbf{k} - \mathbf{p}_2|^2 \sigma_{x_2}^2 - iE_i t_D + i\mathbf{k} \cdot \mathbf{x}_D \right] \\ & \times \bar{u}_\beta(p_2) \gamma^0 P_L (\not{k} + m_i) \gamma^0 P_L v_\alpha(p_1), \end{aligned} \quad (3.103)$$

in which the subscripts on the u and v spinors refer to their flavours; the spinors also have an implicit spin index which has been omitted.

The above expression for the amplitude is qualitatively similar to the analogous expression, Eq. (3.86), derived previously in the bosonic model, with a few notable exceptions. On a technical note, we see first that it is no longer possible to perform the angular parts of the \mathbf{k} integral exactly as was done in the previous case. This occurs because of the presence of the momenta of the charged leptons, \mathbf{p}_1 and \mathbf{p}_2 , which complicate the integrand somewhat. A related point is that now the neutrinos' momenta are not centered around zero, as was the case above. Rather, we have for the momenta

$$\mathbf{k} \approx -\mathbf{p}_1, \quad (3.104)$$

$$\mathbf{k} \approx \mathbf{p}_2 \quad (3.105)$$

and for the energies

$$\Omega_1 \approx E(p_1) + E_i, \quad (3.106)$$

$$E_i + \Omega_2 \approx E(p_2), \quad (3.107)$$

where E_i is the energy of the i^{th} neutrino mass eigenstate. The relations (3.104)–(3.107) are only approximate equalities since the degree to which each of them holds is determined by the relative sizes of $\sigma_{x_1}, \dots, \sigma_{t_2}$. The fact that the neutrinos' momenta are not centered about the origin is rather encouraging because it indicates that this model would not be expected to have the (unphysical) feature that it favours non-relativistic neutrinos, as was the case in the bosonic model of the previous section. The final difference, compared to the bosonic case, is the presence of the matrix element, $\bar{u}_\beta \dots v_\alpha$, which contains all of the information regarding the neutrinos' spin. It is interesting to note the presence of the factor

$$\frac{(\not{k} + m_i)}{2E_i}, \quad (3.108)$$

which arises in this case from the sum over spins of the neutrino u spinors, $\sum_s u^s(k_i) \bar{u}^s(k_i)$. This same factor appears in the field theoretic calculation of Ref. [55], but in that case is due to an integral in the complex k_0 plane which extracts the pole of the propagator [64]. We need not do any such integration since we always insist that our source be turned “off” before our detector is turned “on.” This forces the neutrinos to always be on-shell.

It would be possible at this point to proceed as we did in the previous section. First we could examine the response of the detector to the source by looking very carefully at the case in which there is only one neutrino. Armed with this knowledge we could define the probability in analogy with the bosonic case and study its behaviour as a function of the various parameters of the theory. While this program might be deserving of future study, for now we shall content ourselves with a more qualitative examination of the generic features of this model.

As we have noted, two of the main qualitative differences between this model and our former bosonic model are the different energy-momentum conservation equations and the presence of the matrix element in the integrand. A further difference is that in order to obtain the oscillation probability, we now need to integrate over the momenta of the two outgoing charged leptons. Since the \mathbf{k} integral in the expression for the amplitude is expected to be dominated by values of \mathbf{k} which are parallel to \mathbf{x}_D , the \mathbf{p}_1 and \mathbf{p}_2 integrals would similarly be dominated by values anti-parallel and parallel, respectively, to \mathbf{x}_D , due to the damping terms in the exponential of Eq. (3.103). In order to get some idea of the effect of the matrix element as a function of the neutrino's mass, then, let us evaluate it when all of the momenta are parallel (or anti-parallel) to \mathbf{x}_D . Choosing an explicit representation for the gamma matrices and adopting the normalization conditions of Itzykson and Zuber [61, pp. 57, 145-6, 201], we find that only two of the four helicity combinations of the leptons survive, yielding

$$\mathcal{M}_{\alpha \rightarrow \beta}^{++}(m_i) = -(E_i - k) \frac{(E(p_1) + m_\alpha + p_1)(E(p_2) + m_\beta - p_2)}{2 [4m_\alpha m_\beta (E(p_1) + m_\alpha)(E(p_2) + m_\beta)]^{1/2}}, \quad (3.109)$$

$$\mathcal{M}_{\alpha \rightarrow \beta}^{--}(m_i) = -(E_i + k) \frac{(E(p_1) + m_\alpha - p_1)(E(p_2) + m_\beta + p_2)}{2 [4m_\alpha m_\beta (E(p_1) + m_\alpha)(E(p_2) + m_\beta)]^{1/2}}, \quad (3.110)$$

where $k \equiv |\mathbf{k}|$, etc., and where the “++” and “--” superscripts refer to the helicities of the lepton and anti-lepton. In the limit as the neutrino mass goes to zero, only the combination in which both leptons have negative helicity survives, since the exchanged neutrino can only have negative helicity in that limit. For non-zero masses it becomes possible to also produce lepton pairs with positive helicity.

The quantities which will occur in the oscillation probability are the squares of the matrix elements. Let us define

$$h_{\alpha \rightarrow \beta}^+(m_i) = |\mathcal{M}_{\alpha \rightarrow \beta}^{++}(m_i)|^2 / |\mathcal{M}_{\alpha \rightarrow \beta}^{--}(0)|^2, \quad (3.111)$$

$$h_{\alpha \rightarrow \beta}^-(m_i) = |\mathcal{M}_{\alpha \rightarrow \beta}^{--}(m_i)|^2 / |\mathcal{M}_{\alpha \rightarrow \beta}^{--}(0)|^2. \quad (3.112)$$

Then h^+ (h^-) gives some measure of the probability that the source/detector interaction gives rise to two leptons with positive (negative) helicity. Since the efficiency of the system at producing and detecting neutrinos of a given mass is determined to some extent by the functions h^\pm , it is useful to plot them as a function of the mass of the exchanged neutrino.

It turns out that the energy-momentum conservation equations, Eqs. (3.104)–(3.107), are over-complete. Thus, for given values of the charged lepton and neutrino masses, for example, Ω_1 and Ω_2 may be found such that all of the conditions are met, but when the neutrino mass is varied, at least one of the conditions needs to be violated. This problem is related to the difficulty which occurred in the bosonic model (where momenta close to zero were favoured) and has its root in the fact that our source and detector are fixed and do not recoil. For the purposes of our plot, let us require that Eqs. (3.104), (3.106) and (3.107) hold exactly – so that energy and momentum are conserved at the source and energy is conserved at the detector – and allow the momentum conservation at the detector, Eq. (3.105), to be violated. As in our previous model, this can again be allowed by setting σ_{x_2} to be somewhat small¹⁹. For the plot let us take $\alpha=\beta=e$, so that both the source and detector are sensitive to electron neutrinos. We then set

$$\begin{aligned}\Omega_1 &= 0.6\text{MeV}, \quad \Omega_2 = 0.5\text{MeV} \\ m_\alpha &= m_\beta = m_e = 0.511\text{MeV}.\end{aligned}\tag{3.113}$$

Fig. 3.8 shows a plot of $h_{e\rightarrow e}^+(m)$ and $h_{e\rightarrow e}^-(m)$ as a function of the neutrino mass. The “threshold” in this case is determined by the condition $\Omega_1=m_e+m$, where m is the neutrino mass. The upper curve corresponds to the negative helicity case and approaches

¹⁹On physical grounds we would prefer to allow momentum conservation to be violated somewhat rather than energy conservation. The reason for this is that in the former case, the small value required for σ_x is still of a reasonable magnitude compared to nuclear scales (it is on the order of several hundred fm in the example considered here), but the value which would be required for σ_t would be far too small compared to any time scales in the physical problem.

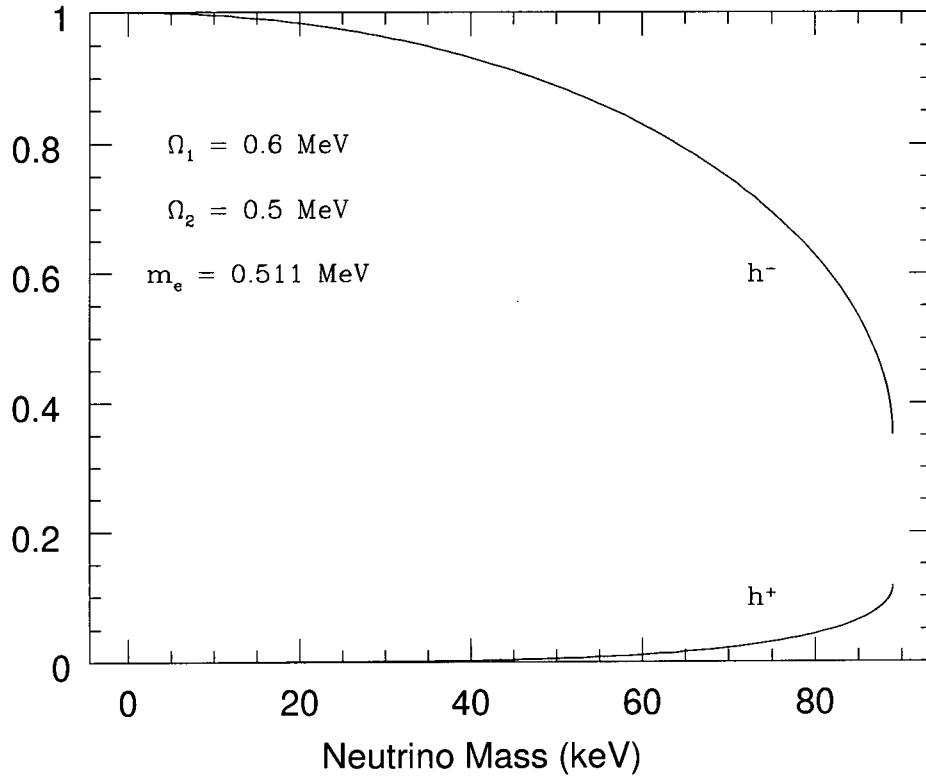


Figure 3.8: Plot of the two functions $h_{e \rightarrow e}^+$ and $h_{e \rightarrow e}^-$ as a function of the neutrino mass. These provide a measure of the probability to produce electrons and positrons of helicity +1 and -1, for h^+ and h^- , respectively.

unity as $m \rightarrow 0$. The lower curve disappears in the same limit. For neutrino masses closer to threshold, fairly substantial deviations from the $m=0$ case are observed to occur.

The plot in Fig. 3.8 should of course be treated with some caution, since it shows only the square of the matrix element evaluated at some “optimal” energy and momentum configuration. In general, the oscillation probability will also receive contributions due to energy and momentum configurations which are non-optimal. Furthermore, it has been found that the procedure which we have followed can lead to non-sensical results if the neutrino mass is taken to be large compared to the lepton mass ²⁰. In any case,

²⁰This occurs because, in our prescription, k and p_2 need not be the same. For very heavy neutrinos

however, the plot *does* demonstrate something which might be regarded as “typical”: for non-relativistic neutrinos there will be a non-zero probability to produce charged leptons in the final state which have the “wrong” helicity configurations. Thus, particularly if the spin of the leptons were to be measured in a certain experiment, one could expect there to be quite strong mass effects for non-relativistic neutrinos. In our case, for example, there is a suppression of the negative helicity final states for large mass and a mild enhancement of the positive helicity ones.

Since in this model the neutrinos no longer have their momenta centered about the (unphysical) value of “zero,” one would expect in this case that the non-relativistic neutrinos would not be favoured, as was found to be the case in the bosonic model studied above. In fact, it is possible that there would be a suppression for non-relativistic neutrinos due to the phase space suppression of the final state leptons, for small momenta. This question could really only be answered by performing a thorough numerical analysis of the model, which we shall not do at this time.

3.5 Summary and Conclusions

In this chapter we have presented a rigorous derivation of the neutrino oscillation probability as a function of the distance between an idealized “source” and “detector.”

In order to motivate our main calculation, we first examined some of the options which one might consider which do not make any reference to a source or detector. We first considered a fairly standard approach using wave packets, but found that a key step in the calculation, in which a probability density was integrated over time, appeared to be completely unjustified. Furthermore, this procedure led to some rather provocative

this starts to cause problems in this approach.

behaviour when one or more of the mass eigenstates involved in the interaction were non-relativistic. In Sec. 3.2 we attempted instead to construct a current density which could plausibly be integrated over time in order to arrive at a distance-dependent probability. The current which we derived appeared formally to satisfy the minimum requirements which we might impose. A closer examination revealed, however, that the probability density to which the current was related by a continuity equation was not positive semi-definite. We were thus forced to abandon this approach as well, despite its formal appeal.

Our main calculation was presented in Sec. 3.3, in which we studied the oscillations of “bosonic” neutrinos coupled to an idealized source and detector. It was found that the source/detector approach to studying neutrino oscillations had several advantages compared to approaches which do not involve the source and detector explicitly. The first and most obvious advantage was found to be that the oscillation probability had a very clear “physical” definition which could be related directly to the “experiment” which was being studied. It was also found that it was quite natural in this approach to localize the source and detector both in space and in time. It is well-known that without such localization neutrino oscillations cannot be observed. Another advantage of this approach was found to be that there was no ambiguity concerning the “initial state” of the neutrino wave packet: the relative sizes and shapes of the wave packets corresponding to the various mass eigenstates were completely determined by the configurations of the source and detector.

In our investigation of this model we were able to gain some interesting insights into the phenomenon of neutrino oscillations. We studied two different types of macroscopic detectors, both of which were assumed to be composed of a large number of microscopic constituent detectors. In the case of the “coherent” detector, the constituent detectors were each taken to make long coherent measurements and in the case of the “incoherent” detector, the constituent detectors were each taken to make microscopically coherent

measurements of some finite temporal resolution which were subsequently summed. It was found that both of these detectors were not in general ideal in the sense that their detection efficiency was found to be mass-dependent. This behaviour was studied closely and the mass-dependence for the two types was found to be the same. Furthermore, the mass-dependence of the efficiency was found to be easily understood and was seen to be due a quirk in our model which was that the source and detector were “fixed” and could not recoil when a neutrino was emitted or absorbed. It was found that it was quite straightforward to tune the parameters of the theory in such a way that the mass-dependence completely disappeared.

When the two detector types were used to study neutrino oscillations, it was found that they had quite different behaviour. The coherent detector was found never to have its oscillations damped. The incoherent detector did have its oscillations damped, but the coherence length was found to depend on the temporal resolution of the detector. This served as an explicit demonstration of an effect which we discussed in Sec. 2.2.1, namely that the oscillations of neutrinos could be revived by a long coherent measurement even after the various mass eigenstates had separated spatially. In fact we found that this toy model allowed for some insights into this problem as well. In our case it was found that the oscillation probability depended in a symmetric way on the parameters of the source and of the detector. From this point of view, it appeared that the concept of the neutrino’s “wave packet” was somewhat of an artificial one, since both the source and detector contributed to the “width” of the exchanged neutrino.

We investigated neutrino oscillations, both for relativistic and non-relativistic neutrinos, in our model. In the relativistic case the results were in agreement with what one might expect. The oscillation length was found, not surprisingly, to be given by the usual result, with no spurious factor of “2.” Furthermore, in the limit as $\sigma_{t_2} \rightarrow 0$, it was noted that our result agreed with the wave packet result. For finite values of σ_{t_2} , however, it was

found that our result would always differ from a wave packet result, since that approach ignores the resolution of the detector. In the non-relativistic case we examined the effects due to the mass-dependence of our source/detector system. It was found that in fact the probability could be skewed quite dramatically. As we have mentioned, however, this is to be understood as a quirk of our model which can be controlled by suitably tuning its parameters.

In Sec. 3.4 we constructed a more realistic source/detector model in which the neutrinos were taken to be Dirac fermions and in which the source and detector were each coupled to the usual charged lepton current. We did not solve this model to the extent that we did in the bosonic case, but we did derive an explicit expression for the amplitude for the interaction to occur and we were able to make some general comments as to how the fermionic nature of the neutrino might modify the results obtained above in the bosonic case. This model was also more realistic in the sense that non-relativistic neutrinos were not favoured, as occurred in the bosonic case.

Chapter 4

Coherent Neutrino Interactions in a Dense Medium

4.1 Introduction

Motivated by the effect of matter on neutrino oscillations (the MSW effect), there have been several works in recent years aimed at understanding in a more complete way the propagation of one or more flavours of massive neutrinos in matter. One of the first papers along these lines was the paper of Mannheim in 1987 [65] whose main purpose was to show that the MSW effect could be derived from a Field Theoretic starting point. Mannheim used second quantization techniques to derive the wave functions and dispersion relations of two flavours of both Dirac and Majorana neutrinos propagating in a medium in which there was a finite density of electrons. Mannheim then analyzed his result in the ultrarelativistic regime and recovered the standard MSW results.

Both the work of Mannheim and the work of Nieves [66] and of Nötzold and Raffelt [67] showed that the entire MSW effect could be reliably analyzed with a modified Dirac (or Majorana) equation by adding to the frequency of the electron neutrino a term proportional to the density ($\sqrt{2}G_F\rho$ in the standard MSW scenario). This term is analogous to a chemical potential term for the electron neutrino.

In 1991 Panteleone [68] used such a modified Dirac equation to study the behaviour of neutrinos in supernova cores. He first analyzed the case of only one neutrino flavour for all neutrino momenta. At this point he discovered a very unusual behaviour of the neutrino dispersion relation. The dispersion relation had a minimum at a nonzero

neutrino momentum. Thus for a range of neutrino momentum the neutrino's phase velocity and group velocity are in opposite directions! Panteleone later analyzed the case of two and three flavours of neutrinos. He noticed that the neutral currents did not decouple in general though he analyzed his equations only in the high energy regime in which they do cancel.

In this chapter we provide a synthesis of many of the above results. We are particularly interested in the effects due to the minimum of the dispersion relation at nonzero momentum. We begin in Section 4.2 by examining a simple model with only a single neutrino flavour in which the neutrino propagates in a background of electrons. We will take the neutrino-electron interaction to be mediated only by neutral current interactions. This model will allow for a careful analysis of the Field Theory aspects of neutrino propagation in a medium. We pay special attention to the minimum of the dispersion relation which occurs at non-zero momentum and analyze its effects on neutrino interactions. We will find that the minimum energy for Dirac neutrinos in the medium will generically be *less* than the rest mass of the neutrino in the vacuum so that very low energy neutrinos are effectively *trapped* by the medium. A similar effect has been studied from a different point of view in the work of Loeb ¹[69]. Our analysis of the trapping of neutrinos will bring up many interesting questions and puzzles which will need to be resolved in order to have a complete understanding of the problem. We will also examine the case of Majorana neutrinos and find that in general Majorana neutrinos cannot be trapped.

In Sec. 4.3 we extend our analysis to a more realistic model which has two neutrino flavours and in which there are both neutral and charged current interactions. In this

¹Loeb studies the problem from the point of view of the neutrino's "index of refraction" in the medium. He then uses optics arguments to show that neutrinos can have bound orbits in the medium. The index of refraction approach gives slightly different results compared to ours. (In particular, the dispersion relation gotten from Loeb's Eq. (4) is centered about $p=0$. As a result, Loeb's trapping condition is slightly different than ours.)

case the dispersion relations are governed by quartic equations for Dirac neutrinos and quadratic equations for Majorana neutrinos. We will again be most interested in examining the form of the dispersion relations in the medium and their effects on neutrino propagation. Again we will find that the Dirac case leads quite generically to neutrino trapping while the Majorana case can have no trapping. We will also make a few remarks regarding the oscillations of neutrinos in a medium, noting that even for a *single* neutrino there could in principle be oscillations in the probability to detect the neutrino, due to the differing phase velocities of the helicity eigenstates.

We conclude in Sec. 4.4 with a brief discussion of our results and some concluding remarks.

4.2 A Simple Model with One Neutrino Flavour

Many of the interesting effects which we will discuss, namely those due to the minimum of the dispersion relation which occurs at non-zero momentum, occur already in a simple model with only a single neutrino flavour. It is useful, then, to first consider a simplified model in which a Dirac neutrino propagates in an electron “gas” to which it couples only via the neutral current interaction. The case of a Majorana neutrino is somewhat more subtle and will be considered subsequently. Our model may be described by the following Lagrangian ²

$$\mathcal{L} = \bar{\psi}_\nu (i\not{D}^+ - m_\nu) \psi_\nu + \bar{\psi}_e (i\not{D}^- - m_e) \psi_e - \frac{1}{4}F^2 + \frac{m_Z^2}{2}Z^2 - \mu_e \psi_e^\dagger \psi_e, \quad (4.1)$$

where

$$D_\mu^\pm = \partial_\mu \pm igZ_\mu(1 - \gamma^5), \quad (4.2)$$

²Our simple model is not renormalizable, but this does not affect our calculation of the neutrino dispersion relations, which are the same as would be obtained in a model similar to the standard model in which the masses are generated by a Higgs mechanism and in which only neutral currents are present.

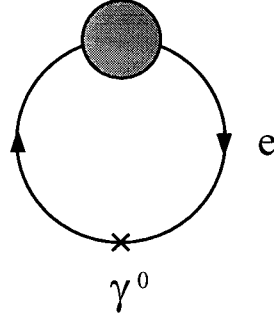


Figure 4.1: Feynman diagram corresponding to the electron density, $\rho_e = \langle \psi_e^\dagger \psi_e \rangle$.

$$F_{\mu\nu} = \partial_\mu Z_\nu - \partial_\nu Z_\mu. \quad (4.3)$$

The chemical potential term in the Lagrangian is included in order to give a non-zero value to the electron density; that is

$$\rho_e = \langle \psi_e^\dagger \psi_e \rangle \neq 0. \quad (4.4)$$

The diagram corresponding to $\langle \psi_e^\dagger \psi_e \rangle$ is shown in Fig. 4.1.

In order to study the propagation of a neutrino in this medium, we compute the neutrino self-energy. To one loop there are three diagrams, shown in Fig. 4.2. All effects due to the non-zero electron density come from the electron loop in Fig. 4.2(a) which is easily calculated and yields

$$\Sigma = -\sqrt{2}G\rho_e\gamma^0(1 - \gamma^5), \quad (4.5)$$

in which we have defined $G = g^2/\sqrt{2}m_Z^2$ in analogy with the usual Fermi coupling constant, G_F . From the self-energy one may obtain the neutrino propagator in the usual way by summing a geometric series. For constant ρ_e the resulting expression is given in momentum space by

$$G_\nu(p) = \frac{1}{\not{p} - m_\nu - \Sigma}. \quad (4.6)$$

If ρ_e depends explicitly on x the propagator may still be formally written in position space as

$$G_\nu(x) = \frac{1}{i\rlap{\not{\partial}} - m - \Sigma(x)}. \quad (4.7)$$

The effective action is then given, to this order, by

$$S_{\text{eff}} = \int d^4x \bar{\psi}_\nu [G_\nu^{-1}(x)] \psi_\nu \quad (4.8)$$

$$= \int d^4x \bar{\psi}_\nu [i\rlap{\not{\partial}} - m + \sqrt{2}G\rho_e\gamma^0(1 - \gamma^5)] \psi_\nu. \quad (4.9)$$

Variation of the effective action leads finally to an effective “Dirac equation,” given by

$$[i\rlap{\not{\partial}} - m + \alpha\gamma^0(1 - \gamma^5)] \psi_\nu = 0, \quad (4.10)$$

in which we have defined $\alpha = \sqrt{2}G\rho_e$. For constant electron density, the presence of the “chiral potential” in this expression leads to a *shift* in the frequency by α , but only for the left-handed (chiral) piece. This shift in the frequency is precisely the “index of refraction” familiar from the MSW effect. Once we have derived the dispersion relations, it will be clear that the shift in energy for the neutrino is opposite that for the anti-neutrino. If the neutrino is “repelled” by the medium, then the anti-neutrino is “attracted” by it.

We have noted above that the chemical potential μ_e in the Lagrangian (4.1) gives rise to a non-zero electron density, $\rho_e \equiv \langle \psi_e^\dagger \psi_e \rangle$. A similar calculation of $\rho_\nu \equiv \langle \psi_\nu^\dagger \psi_\nu \rangle$ for the effective Lagrangian defined by Eq. (4.9) shows that, at least naively, there appears also to be a non-zero density of *neutrinos* in this medium. It is clear that this arises due to the potential term proportional to γ^0 in the effective Lagrangian, since this term looks exactly like a chemical potential for the neutrinos. How one handles this apparent density of neutrinos, however, can drastically affect the MSW effect. Suppose, for example, that we were to insist that in the sun $\rho_\nu \equiv \langle \psi_\nu^\dagger \psi_\nu \rangle = 0$. In order to implement this, we would have to introduce a “counter” chemical potential into the original Lagrangian which would exactly cancel the neutrino density generated by the interactions with the electrons in the

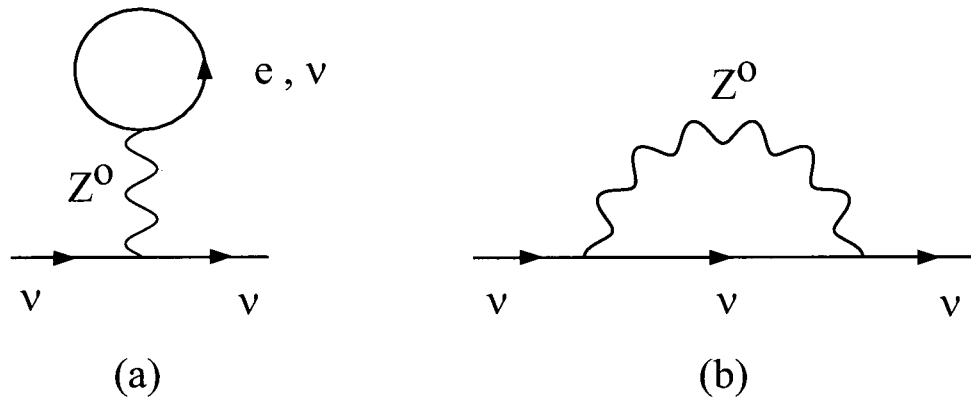


Figure 4.2: One-loop diagrams contributing to the neutrino self-energy in the model of Sec. 4.2.

medium. It turns out, however, that this would change the MSW result quite drastically. In fact, if our theory had a “vector” instead of a “chiral” potential, we would kill the entire MSW effect by doing this. It would seem more appropriate to accept the fact that in equilibrium there is a non-zero density of neutrinos of very low momentum.

Further insight into the physics of our model can be gained by examining the equations of motion following from the Lagrangian in Eq. (4.1). Varying the Lagrangian with respect to the Z^μ field leads to

$$\partial_\nu F^{\nu\mu} + m_Z^2 Z^\mu = -gJ^\mu, \quad (4.11)$$

where

$$J^\mu = \bar{\psi}_e \gamma^\mu (1 - \gamma^5) \psi_e - \bar{\psi}_\nu \gamma^\mu (1 - \gamma^5) \psi_\nu. \quad (4.12)$$

If $\rho_e = \langle \psi_e^\dagger \psi_e \rangle$ is constant, then (4.11) leads to

$$\langle Z^0 \rangle = -\frac{g\rho_e}{m_Z^2}, \quad (4.13)$$

that is, the Z^0 field has gained a vacuum expectation value. The equation of motion for

the neutrino field is then given by

$$\left[i\not{\partial} - m - g\langle Z^0 \rangle \gamma^0 (1 - \gamma^5) \right] \psi_\nu = 0, \quad (4.14)$$

which is equivalent to the effective Dirac equation of (4.10) once the value for the Z^0 expectation value, Eq. (4.13), is inserted. From this point of view, then, the left-handed neutrino sees a mean (coherent) “scalar potential,” $\langle Z^0 \rangle$. From the point of view of the field theoretic calculation above, it is clear why the Z^0 field has developed a vacuum expectation value. The one-loop diagram corresponding to $\langle Z^0 \rangle$ is simply the electron loop in Fig. 4.1 with a Z propagator attached. This coherent Z^0 field is similar to the electric field which surrounds a static charge distribution and is due to the net weak charge of the medium.

4.2.1 Solution to the Dirac Equation

In order to study the propagation of neutrinos over macroscopic distances, it suffices to study the effective Dirac equation given in Eq. (4.10). The propagator defined in Eq. (4.7) contains the same information, but also encodes the off-shell behaviour of the neutrino.

For a medium with constant density, it is straightforward to solve the Dirac equation in momentum space by employing the chiral representation, so that

$$\psi = \begin{pmatrix} \chi_L \\ \chi_R \end{pmatrix}, \quad (4.15)$$

in which the upper and lower components correspond to the left and right chiral projections, respectively. In this representation, the Dirac equation becomes

$$\begin{pmatrix} -m & \omega - \vec{\sigma} \cdot \vec{p} \\ \omega + 2\alpha + \vec{\sigma} \cdot \vec{p} & -m \end{pmatrix} \begin{pmatrix} \chi_L \\ \chi_R \end{pmatrix} = 0. \quad (4.16)$$

Without loss of generality we may choose $\vec{p}=p\hat{z}$, so that $\chi_{L,R}$ (and hence also ψ) may be chosen to be eigenstates of σ_3 , the spin projection in the z direction. That is,

$$\sigma_3 \chi_{L,R} = s \chi_{L,R}, \quad (4.17)$$

where $s=\pm 1$. Solving for the energy yields four solutions

$$\omega = -\alpha \pm \sqrt{(p + \alpha s)^2 + m^2}. \quad (4.18)$$

These dispersion relations are plotted in Fig. 4.3 both for $m=0$ (dashed curves) and $m \neq 0$ (solid curves.) Several key features of these plots should be noted. First of all, the “negative energy” states are, in this case, those which are unbounded from below as the momentum is increased. In the second quantized theory the correct energy of such a state is just the negative of its energy eigenvalue. We also note that when $m=0$ there are “level crossings.” These are avoided for $m \neq 0$ by level repulsion due to the mixing of the levels.

The most noteworthy feature of these dispersion relations (discussed previously by Pantaleone) is the fact that the minima of the dispersion relations occur at non-zero values of the momentum, $p=\pm\alpha$, instead of at the origin. One interesting consequence of this fact is that the neutrino can have a vanishing group velocity at non-zero momenta. Furthermore, for $|p|<|\alpha|$, the neutrino’s group velocity, $d\omega/dp$, is in a direction opposite to its momentum! Another interesting feature of these curves is that the minimum energy $\omega_{\min}=-\alpha + m$ is *less than* the neutrino mass. Thus it is possible to produce a neutrino in the medium which has $\omega < m$. Such a neutrino will not have enough energy to survive in the vacuum and will thus be *trapped* by the medium. We shall examine these peculiar features of the neutrino dispersion relations in detail below.

Finally, we note that for high momentum, the solution corresponding to spin (and

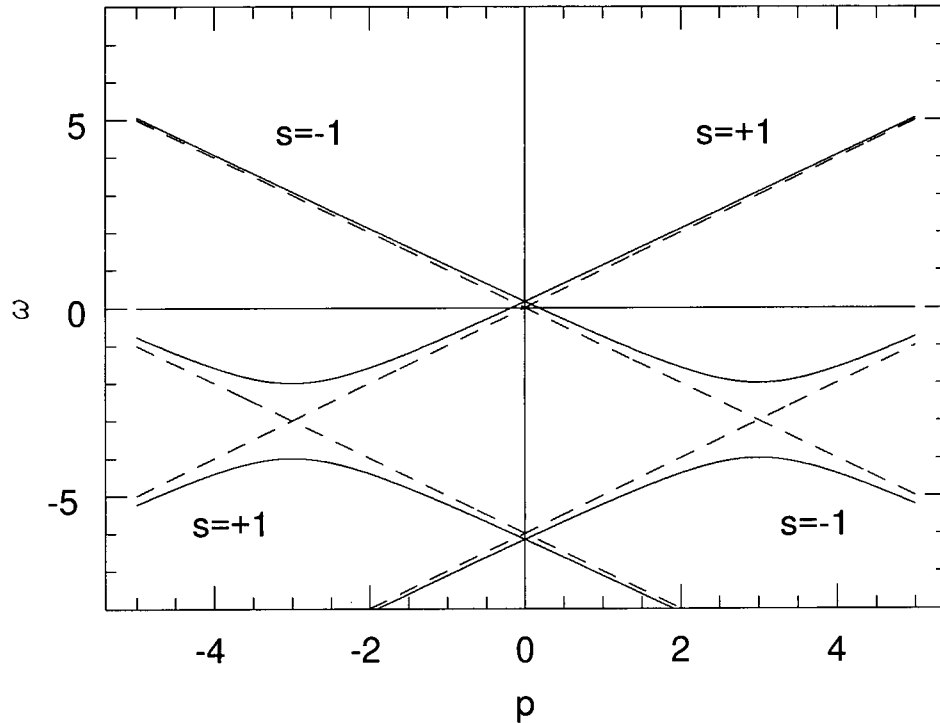


Figure 4.3: Dispersion relations for the model considered in Sec. 4.2.1, with $\alpha=3$ and $m=0, 1$, in arbitrary units. The dashed and solid curves correspond, respectively, to the $m=0$ and $m \neq 0$ cases.

hence helicity) -1 has energy

$$\omega \approx p + \frac{m^2}{2p} - 2\alpha, \quad (4.19)$$

which is just the usual MSW result. By way of contrast, the positive helicity solution approaches its vacuum value of $\omega \approx p + m^2/2p$. This illustrates the spin-dependence of the interaction. For high momentum, the left-handed (chiral) states are nearly equivalent to the negative helicity eigenstates, so the potential (which is left-handed) affects only the negative, and not the positive, helicity eigenstates.

4.2.2 Neutrino Trapping

Let us first consider the criterion which must be met in order that a neutrino be trapped. We shall assume here for definiteness that $\alpha > 0$, which leads to the trapping of neutrinos. One could just as easily suppose that $\alpha < 0$, in which case anti-neutrinos would be trapped. The analysis in that case would be perfectly analogous. The dispersion relation for a negative spin (relative to \hat{z}) neutrino is given by

$$\omega = -\alpha + \sqrt{(p - \alpha)^2 + m^2}, \quad (4.20)$$

so that the condition for trapping is

$$-\alpha + \sqrt{(p - \alpha)^2 + m^2} < m \quad (4.21)$$

or

$$p < p_{\text{trap}} \equiv \alpha + \sqrt{\alpha^2 + 2\alpha m}. \quad (4.22)$$

Thus, neutrinos produced in this medium with momentum $p < p_{\text{trap}}$ will not have enough energy to survive in the vacuum and will be trapped. The derivation of p_{trap} is illustrated graphically in Fig. 4.4. The solid and dashed curves correspond in this case to the dispersion relations in matter and in vacuum, respectively.

Before examining some of the subtler issues involved in the coherent trapping of neutrinos, let us first get some idea of the overall magnitude of the effect. Setting $G \approx G_F$ and $m \approx 10^{-3} \text{eV}$ (which is a mass relevant for the MSW-resolution of the solar neutrino problem), we find that $p_{\text{trap}} \sim 10^{-8} \text{eV}$ in the sun (for which $\alpha \sim 10^{-12} \text{eV}$) and $p_{\text{trap}} \sim 100 \text{eV}$ in a supernova (for which $\alpha \sim 100 \text{eV}$.) The phenomenon of trapping is quite remarkable when we consider that the mean free path (which increases with decreasing momentum) of a neutrino with $p \sim 10^{-8} \text{eV}$ in the sun is on the order of 10^{20} solar radii. Such a neutrino would thus have no chance of being “incoherently” trapped in the sun (say by

back-scattering from nuclei), but would still be trapped by the coherent process which we are discussing. We note furthermore that in the case of incoherent trapping the scattering cross section is typically dependent on the mass of the target particle, whereas for coherent trapping this is not the case. Loeb has discussed a similar effect for neutron stars and has estimated that in general this effect will add an extra 30 kg to the mass of the star [69].

In order to study the trapping of neutrinos in more detail, let us consider a situation in which the background varies with position, setting

$$\alpha(z) = \begin{cases} \alpha, & z > 0 \\ 0, & z < 0. \end{cases} \quad (4.23)$$

In the following, we shall treat the Dirac equation as a single-particle wave equation and solve for its “classical” solutions. It is well-known that such an approach can lead to difficulties, for example in the Klein paradox, which can only be resolved by a more complete field-theoretic treatment. The field theory resolution of the Klein paradox still employs the classical solutions of the Dirac equation, however, so these solutions are useful to have in hand. Nonetheless, one must always exercise caution when interpreting the classical solutions of the Dirac equation when a potential term is included.

The simple density profile which we have chosen allows for an exact solution of the Dirac equation. Since the energy and transverse momentum are both good quantum numbers, we may set

$$\psi(t, \vec{x}) = \exp(-i\omega t + i\vec{p}_\perp \cdot \vec{x}_\perp) \tilde{\psi}(z), \quad (4.24)$$

where \vec{p}_\perp denotes the momentum transverse to the z direction. The Dirac equation then becomes

$$\begin{pmatrix} -m & \omega - \vec{\sigma}_\perp \cdot \vec{p}_\perp + i\sigma_3 \partial_z \\ \omega + 2\alpha(z) + \vec{\sigma}_\perp \cdot \vec{p}_\perp - i\sigma_3 \partial_z & -m \end{pmatrix} \begin{pmatrix} \tilde{\chi}_L(z) \\ \tilde{\chi}_R(z) \end{pmatrix} = 0. \quad (4.25)$$

For the moment, let us neglect the transverse momentum and set $\vec{p}_\perp=0$. In that case, $\chi_{L,R}$ may again be chosen as eigenstates of σ_3 , which implies that there is no spin-flip induced at the boundary. We study the case in which the spin is in the $-z$ direction, so that the incident neutrino has negative helicity. For a given energy ω in the medium, there are then two solutions for the momentum, given by

$$p^\pm = \alpha \pm \sqrt{(\omega + \alpha)^2 - m^2}. \quad (4.26)$$

If we set $p \equiv p^+ > \alpha$, then

$$p^- = 2\alpha - p. \quad (4.27)$$

These solutions may be used to form an incident wave, $\tilde{\psi}_{\text{inc}} \sim \exp(ipz)$, and a reflected wave, $\tilde{\psi}_{\text{ref}} \sim \exp(ip^-z)$. Note that in some cases the reflected wave can have its momentum in the *same* direction as the incident wave, since it is possible to have $p^- > 0$. The group velocity corresponding to such a value of the momentum is still negative, however, so that wave packets reflected from the boundary always travel in the $-z$ direction. This may also be seen by looking at the current

$$\vec{j} \equiv \bar{\psi} \vec{\gamma} \psi, \quad (4.28)$$

since $\text{sign}(j_z) = \text{sign}(p - \alpha)$. A related point to note is that the reflected neutrino has its helicity “flipped” depending on whether or not $p^- > 0$. This flipping of the helicity is a somewhat artificial concept, however, since the spin of the neutrino is conserved in the interaction, as we have noted above.

The solution of the Dirac equation corresponding to a neutrino with spin -1 incident from the left is then given by

$$\psi(z) = \theta(-z) (\tilde{\psi}_{\text{inc}} + \tilde{\psi}_{\text{ref}}) + \theta(z) \tilde{\psi}_{\text{trans}}, \quad (4.29)$$

in which

$$\tilde{\psi}_{\text{inc}} = \begin{pmatrix} 0 \\ \frac{\omega+p}{m} \\ 0 \\ 1 \end{pmatrix} e^{ipz}, \quad \tilde{\psi}_{\text{ref}} = \begin{pmatrix} 0 \\ \frac{\omega+p^-}{m} \\ 0 \\ 1 \end{pmatrix} \rho e^{ip^-z}, \quad \tilde{\psi}_{\text{trans}} = \begin{pmatrix} 0 \\ \frac{\omega+\tilde{p}}{m} \\ 0 \\ 1 \end{pmatrix} \tau e^{i\tilde{p}z}, \quad (4.30)$$

and where ³

$$\tilde{p} \equiv \sqrt{\omega^2 - m^2}. \quad (4.31)$$

The reflection and transmission coefficients, R and T , may then be defined in terms of the incident, reflected and transmitted currents as follows

$$R = \frac{j_{\text{ref}}}{j_{\text{inc}}} = \frac{-[(\omega + p^-)^2 - m^2] |\rho|^2}{[(\omega + p)^2 - m^2]}, \quad (4.32)$$

$$T = \frac{j_{\text{trans}}}{j_{\text{inc}}} = \frac{-[\omega + \tilde{p}]^2 - m^2 |\tau|^2}{[(\omega + p)^2 - m^2]}, \quad (4.33)$$

in which ρ and τ may be determined by matching the solutions in Eq. (4.29) across the boundary, yielding

$$\rho = \frac{p - \tilde{p}}{\tilde{p} - p^-}, \quad \tau = \frac{p - p^-}{\tilde{p} - p^-}. \quad (4.34)$$

One may then show that the current is conserved across the boundary, that is

$$R + T = 1. \quad (4.35)$$

There are three cases which we may consider for the neutrino incident on the boundary. The following list enumerates the three cases according to the condition on the incident neutrino's momentum (energy)

- (i) $p > p_{\text{trap}} \ (\omega > m)$,

³If $\omega^2 < m^2$, the positive imaginary root should be taken, so that the transmitted solution corresponds to a decaying exponential.

$$(ii) \ p_{\text{Klein}} < p < p_{\text{trap}} \ (\omega < m, \ \omega^2 < m^2),$$

$$(iii) \ \alpha < p < p_{\text{Klein}} \ (\omega < m, \ \omega^2 > m^2),$$

where p_{trap} was defined in Eq. (4.22) and where p_{Klein} is defined by the condition $\omega = -m$:

$$p_{\text{Klein}} = \alpha + \sqrt{\alpha^2 - 2\alpha m}. \quad (4.36)$$

Case (i), in which $p > p_{\text{trap}}$, corresponds to the “regular” situation in which the neutrino’s energy is greater than its rest mass in the vacuum. In this case the transmitted wave is oscillatory and the incident neutrino is primarily transmitted. One should of course interpret the reflection coefficients T and R with some caution, even in this case, since they are derived from the classical solutions of the Dirac equation. Cases (ii) and (iii) both correspond to the “trapping” of the neutrino. Recall that for $p < p_{\text{trap}}$, the neutrino is completely reflected at the boundary since it doesn’t have enough energy to exist in the vacuum, that is, $\omega < m$. The difference between the two cases is that in case (ii), $\omega^2 < m^2$, while in case (iii), $\omega^2 > m^2$. The case (iii) only occurs if the medium is sufficiently dense that $\alpha > 2m$. Let us first look at the “regular” case of perfect reflection which occurs in (ii). In that case, since $\omega^2 < m^2$, the momentum of the transmitted wave, \tilde{p} , is purely imaginary and the transmitted wave is a damped exponential. Furthermore, since

$$|\omega + \tilde{p}|^2 - m^2 = 0 \quad (4.37)$$

we see from Eq. (4.33) that $T=0$ and $R=1$. It is clear from the classical solution, then, that the wave is perfectly reflected at the boundary. In the third case, case (iii), we have $\omega < m$, but *also* $\omega^2 > m^2$, so that the transmitted momentum \tilde{p} is *real*, even though the neutrino is supposed to be trapped. Furthermore, calculation of the reflection coefficient yields $R > 1$, which would seem to imply that the flux of reflected neutrinos is greater than that of incident neutrinos! This is of course the classic signal of the famous “Klein

paradox" [70]. The oscillatory solution in this case corresponds to a negative energy state in the vacuum, which is supposed to be "filled" in the Dirac picture. Clearly we are entering here into a many-particle problem. The analogy of our situation with Klein's paradox is actually quite close since the Dirac equation which we are solving is quite similar to the one originally examined by Klein, the only real difference being the $(1 - \gamma^5)$ factor which appears in our case.

The three different types of solutions which can occur when a neutrino is incident from the left on the boundary with the vacuum, namely, regular transmission of a neutrino ($p > p_{\text{trap}}$), "regular" trapping ($p_{\text{Klein}} < p < p_{\text{trap}}$) and "Klein's paradox" trapping ($\alpha < p < p_{\text{Klein}}$) are illustrated in Fig. 4.4. Fig. 4.4(a) shows the dispersion relations in the medium (solid curve) and in the vacuum (dashed curve) as well as the three "critical" values of the momentum, $p = \alpha, p_{\text{Klein}}$ and p_{trap} . Fig. 4.4(b) shows a plot of the reflection coefficient R as a function of the incident momentum, p , starting at $p = \alpha$. Note that R is greater than unity for $\alpha < p < p_{\text{Klein}}$.

Klein's paradox has been studied extensively since it was first raised in 1929 as a critique of Dirac's equation for spin-1/2 particles. Soon afterwards, a smoothed-out version of the original step function potential was proposed and solved exactly by Sauter [71]. Sauter found that, although the reflection coefficient was always greater than unity in the "paradoxical" region of the parameter space, the amount by which it exceeded unity depended on the slope of the potential as it decreased to zero. It was found that for most "realistic" potentials, the paradoxical effects were almost negligible in magnitude. As it turns out, there is no problem with Dirac's equation itself, but only with the interpretation of it as a single-particle wave equation. A full quantum field theoretic treatment of the problem shows that the reflection of the fermions from the boundary of the potential interferes destructively with pair production processes and leads to a new reflection coefficient which is *exactly* unity [72, 73].

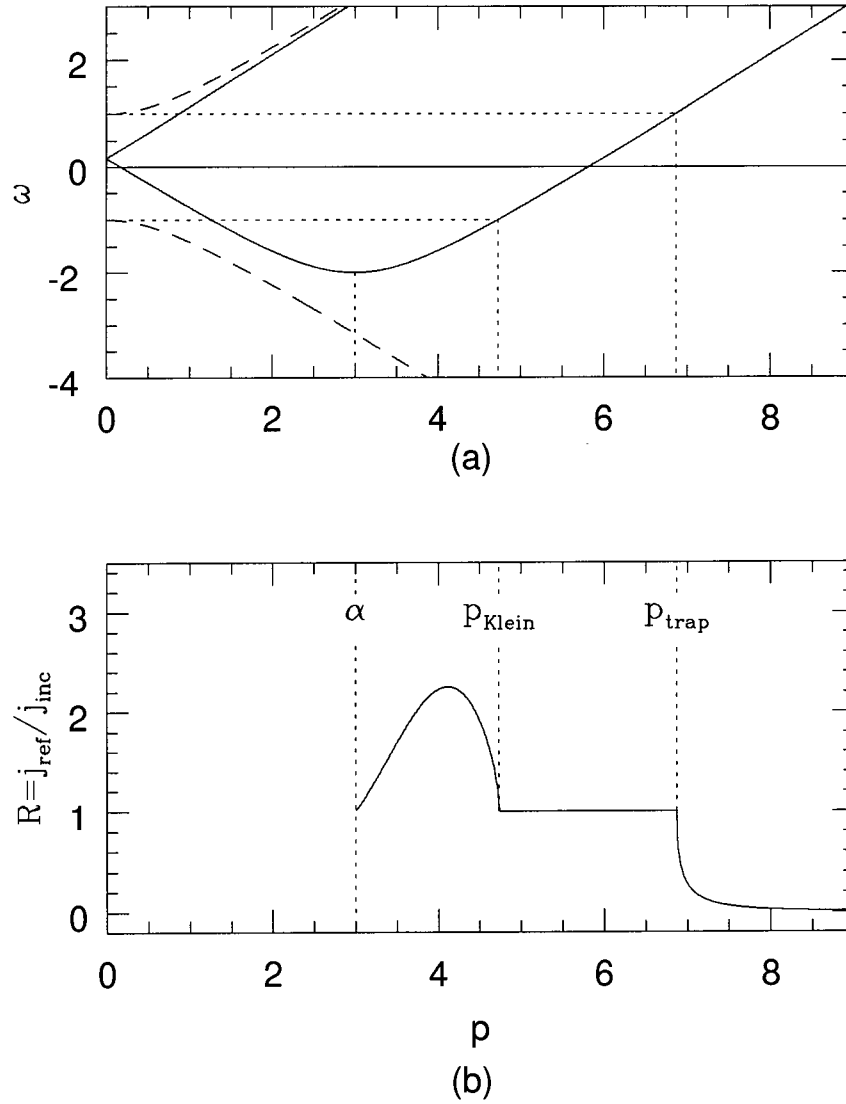


Figure 4.4: (a) Dispersion relations and (b) reflection coefficient, R , which show the analogue of "Klein's paradox" which occurs in our model. In these plots we have set $\alpha=3$ and $m=1$, in arbitrary units. The solid and dashed curves in (a) correspond to the dispersion relations in matter and in vacuum, respectively.

One would expect the same considerations to apply in the case which we are studying. Clearly the fact that the reflection coefficient R can be greater than unity signals the breakdown of the interpretation of our Dirac equation as a single particle wave equation. One might also expect, in analogy with Sauter's result, that the effect would be negligible if the step function density profile was replaced by one in which the density went gradually to zero. Regardless of what the "classical" calculation yields, however, the fact remains that if a neutrino is produced inside the medium with energy less than m , it will be totally reflected from the boundary.

We have so far taken our medium to be semi-infinite in extent, that is, $\alpha(z) = \alpha\theta(-z)$. In any realistic situation which we may wish to consider, however, the density of the medium goes to zero in all directions of space. It is easy to demonstrate that, having been totally reflected from the first boundary, the neutrino is subsequently also reflected back from the opposite boundary. Recall that when we considered the reflection from the boundary on the right, the incident and reflected momenta were determined by choosing the two momenta associated with the same energy on the dispersion curve corresponding to spin in the $-z$ direction. Since spin is conserved in the interaction, the interaction at the left boundary is solved simply by interchanging the two momenta, and so we again have perfect reflection⁴.

We have so far restricted our attention to the case of normal incidence at the boundary; i.e., we have set $\vec{p}_\perp = 0$. The inclusion of transverse momentum components may be accomplished in a straightforward, though interesting, way. In order to solve the Dirac equation, Eq. (4.25), in this more general case, it is convenient to seek solutions inside the medium which are eigenstates of helicity. Thus we define

$$\tilde{\chi}_L(h, z) = f_L(h, |\vec{p}|) \beta^{(h)}(\vec{p}) e^{ip_z z}, \quad (4.38)$$

⁴In order to properly study such "bound states," we should of course put in both boundaries right from the start. This would lead to a discretization of the momenta of the bound particles.

$$\tilde{\chi}_R(h, z) = f_R(h, |\vec{p}|) \beta^{(h)}(\vec{p}) e^{ip_z z}, \quad (4.39)$$

in which $f_{L,R}$ are functions and $\beta^{(h)}(\vec{p})$ are two-component helicity eigenstates satisfying

$$\vec{\sigma} \cdot \vec{p} \beta^{(h)}(\vec{p}) = h |\vec{p}| \beta^{(h)}(\vec{p}), \quad h = \pm 1. \quad (4.40)$$

Solving for the dispersion relations yields four solutions for a given value of $|\vec{p}|$,

$$\omega^\pm = -\alpha \pm \sqrt{(|\vec{p}| + h\alpha)^2 + m^2}, \quad (4.41)$$

in obvious analogy with what was obtained in the $\vec{p}_\perp=0$ case (c.f. Eq. (4.18).) Once again the upper and lower signs in the “ \pm ” are interpreted as corresponding to the neutrino and anti-neutrino solutions, respectively. The four spinors corresponding to a given momentum \vec{p} are then given by

$$\tilde{\psi}^\pm(h, z) = \begin{pmatrix} \frac{1}{m} [\omega^\pm(h, |\vec{p}|) - h|\vec{p}|] \beta^{(h)}(\vec{p}) \\ \beta^{(h)}(\vec{p}) \end{pmatrix} e^{ip_z z}. \quad (4.42)$$

The general procedure for constructing classical solutions corresponding to an incident wave being reflected from the boundary is then the same as for the normal-incidence case studied in detail above. The only added complication is that in this more general case the reflected wave can in general have components with two different momenta. Suppose for example that the incident wave corresponds to a neutrino with momentum p_z and negative helicity. The momentum of the reflected wave is found by looking for other values of p_z (\vec{p}_\perp is conserved) which give the same energy, ω . In general there may be two solutions, given by

$$p_z^- = -p_z, \quad (4.43)$$

$$p_z^- = \pm [p_z^2 + 4\alpha^2 - 2\alpha|\vec{p}|]^{1/2}, \quad (4.44)$$

in which the “ \pm ” sign in the second solution must be chosen judiciously in order to correspond to a reflected wave. The first of these solutions always exists if $\vec{p}_\perp \neq 0$ and

corresponds to a reflected wave with negative helicity *relative to* $(\vec{p}_\perp, -p_z)$. This solution was absent in the normal-incidence case since in that case it would have corresponded to a reflected wave with its spin flipped. The second solution may or may not correspond to an oscillating solution, depending on the magnitude of the transverse momentum. Thus, of the two reflected solutions, one always corresponds to an oscillating wave and the other may oscillate or be damped out, depending on the angle of incidence.

4.2.3 The Majorana Case

In the case of Majorana neutrinos, there is only a single (left-handed) field, χ_L . The effective Lagrangian is given by

$$\mathcal{L}_{\text{eff}} = \bar{\psi}_M \left[\frac{1}{2}(i\not{\partial} - m) + \alpha\gamma^0(1 - \gamma^5) \right] \psi_M, \quad (4.45)$$

where

$$\psi_M = \begin{pmatrix} \chi_L \\ -i\sigma^2\chi_L^* \end{pmatrix} \quad (4.46)$$

in the chiral representation. In general one needs to be somewhat careful when dealing with Majorana fermions. For example, even at the classical level, the fields need to be taken as Grassman-valued, or else the mass term disappears. The dispersion relations in this case can be obtained by solving the equations of motion, as was first done by Mannheim [65]. The details of this calculation are included in Appendix A. The resulting expression for the negative helicity case is given by

$$\omega = \pm \sqrt{(|\vec{p}| - 2\alpha)^2 + m^2}. \quad (4.47)$$

Thus in this case the energy has a minimum value, $\omega=m$, which occurs at $|\vec{p}|=2\alpha$. In fact, the dispersion relation in matter is identical to that in vacuum except for a lateral shift to the right. This implies in particular that, in contradistinction to the Dirac case,

there is *no trapping* of Majorana neutrinos in the medium. It is also interesting to note that the dispersion relation for Majorana neutrinos in the medium may be obtained from that for Dirac neutrinos by first shifting the curve vertically by α and then horizontally, also by α .

4.3 Dispersion Relations for Two Neutrino Flavours

We turn now to consider a more realistic scenario in which there are two neutrino flavours and in which there is both neutral current and charged current coupling to the medium. We first derive the quartic equation governing the dispersion relations in the Dirac case and examine the solutions in some representative cases. It is clear again that in this case there is neutrino trapping. We then examine the Majorana case, in which the dispersion relations are quadratic and are thus readily analyzed. After this we briefly consider an alternative model which has been studied in the literature which has *no* chiral coupling and yet still yields a minimum in the dispersion relation at non-zero momentum. Finally, we comment on neutrino oscillations in these models.

4.3.1 Dirac Case

We begin with the Dirac Equation in the mass basis for a pair of massive Dirac neutrinos with both neutral and charged current coupling to a medium:

$$\{\not{p} - M + (\beta - \alpha Q) \gamma^0 (1 - \gamma_5)\} \psi = 0 \quad (4.48)$$

where M is the **diagonal** 2×2 mass matrix, $\beta \propto \rho G_F$ is the contribution of the neutral current which couples only to the left handed neutrinos and $\alpha \propto \rho_e G_F$ represents the charged current contribution which couples only to ν_e . This coupling is assured by the

mixing matrix

$$Q = \begin{pmatrix} \cos^2(\theta) & \sin(\theta)\cos(\theta) \\ \sin(\theta)\cos(\theta) & \sin^2(\theta) \end{pmatrix}. \quad (4.49)$$

α and β may be calculated by computing the one loop contributions to the neutrino self-energy in the background medium. The Feynman diagrams corresponding to these processes are shown in Fig. 4.5 and yield [66, 67, 75]

$$\alpha = \frac{G_F}{\sqrt{2}} \rho_e \quad (4.50)$$

and

$$\beta = -\frac{G_F}{\sqrt{2}} \sum_f (T_3^{(f)} - 2Q^{(f)} \sin^2 \theta_W) \rho_f \quad (4.51)$$

in which the sum in (4.51) runs over all fermions in the medium, $T_3^{(f)}$ is the third component of the fermion's weak isospin and $Q^{(f)}$ is its charge. If there are appreciable densities of anti-particles in the medium, then ρ_f needs to be replaced by $\rho_f - \rho_{\bar{f}}$ in these expressions.

In the Chiral representation we write

$$\psi = \begin{pmatrix} \chi_L \\ \chi_R \end{pmatrix} \quad (4.52)$$

and the Dirac Equation becomes

$$(\omega - \vec{\sigma} \cdot \vec{p}) \chi_R = M \chi_L, \quad \{(\omega + \vec{\sigma} \cdot \vec{p}) + 2(\beta - \alpha Q)\} \chi_L = M \chi_R. \quad (4.53)$$

For simplicity we may assume the momentum to be in the \hat{z} direction in which case the solutions to the Dirac Equation will be eigenstates of σ_3 :

$$\chi_L = \begin{pmatrix} L_+ \\ 0 \end{pmatrix}, \quad \chi_R = \begin{pmatrix} R_+ \\ 0 \end{pmatrix}; \quad \text{or} \quad \chi_L = \begin{pmatrix} 0 \\ L_- \end{pmatrix}, \quad \chi_R = \begin{pmatrix} 0 \\ R_- \end{pmatrix} \quad (4.54)$$

leading to the equations:

$$\{\omega^2 - p^2 + 2(\omega \mp p)(\beta - \alpha Q) - M^2\} L_{\pm} = 0, \quad (4.55)$$

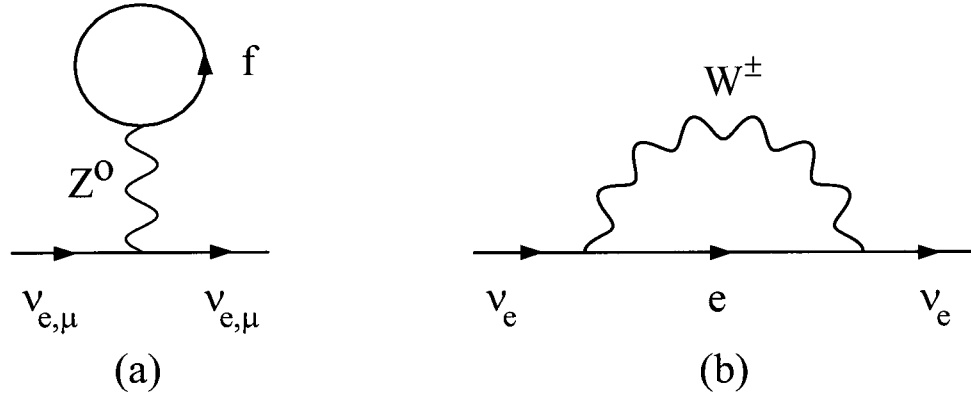


Figure 4.5: Density-dependent one-loop diagrams contributing to the neutrino self-energy in a realistic model with both neutral-current and charged-current couplings. In (a) the “f” stands for the contributions due to all fermions in the medium which have neutral current couplings. In (b) we have assumed that the medium contains electrons and positrons, but no other charged leptons.

$$R_\pm = \frac{1}{(\omega \mp p)} M L_\pm. \quad (4.56)$$

To find the energy eigenvalues we rewrite Eq. (4.55) as:

$$\{\omega^2 - p^2 - \mu^2 + 2(\omega \mp p)\beta - 2\alpha(\omega \mp p)N_\mp\} L_\pm = 0 \quad (4.57)$$

where $\mu^2 = \langle m^2 \rangle = (m_1^2 + m_2^2)/2$ is the mean squared mass and

$$N_\mp = \begin{pmatrix} \cos^2(\theta) - \xi_\mp & \sin(\theta) \cos(\theta) \\ \sin(\theta) \cos(\theta) & \sin^2(\theta) + \xi_\mp \end{pmatrix} \quad (4.58)$$

with

$$\xi_\mp = \frac{\Delta^2}{4\alpha(\omega \mp p)} \quad (4.59)$$

and $\Delta^2 = m_2^2 - m_1^2$. It thus remains only to find the eigenvalues of N_\mp .

The eigenvalues of N_\mp are:

$$\lambda_1^\mp = \frac{1}{2} \left(1 + \sqrt{1 - 4\xi_\mp (\cos(2\theta) - \xi_\mp)} \right) \quad (4.60)$$

$$\lambda_2^\mp = \frac{1}{2} \left(1 - \sqrt{1 - 4\xi_\mp (\cos(2\theta) - \xi_\mp)} \right). \quad (4.61)$$

Plugging these back into the Dirac Equation leads to the following quartic equation for the energy eigenvalues:

$$\left[\omega^2 - p^2 - \mu^2 + (2\beta - \alpha)(\omega - sp) \right]^2 = \alpha^2(\omega - sp)^2 - \alpha\Delta^2 \cos(2\theta)(\omega - sp) + \frac{1}{4}\Delta^2, \quad (4.62)$$

in which $s=\pm 1$ is the eigenvalue of σ_3 , the spin projection in the $+z$ direction. In special cases this expression reduces to those found in the papers of Mannheim (in which the neutral current contribution has been left out) and Pantaleone (in which one of the masses has been set to zero.)

It may not at first be obvious that all eight of the solutions ω of (4.62) corresponding to a fixed value of the momentum are real. This is, however, the case, which may be seen as follows. (The proof is equally straightforward for any number of flavours, so we will do it immediately in the general case.) In the general case the Dirac Equation in the mass basis becomes

$$\left\{ \not{p} - M + \left(\beta - \alpha \mathcal{U}^\dagger N_e \mathcal{U} \right) \gamma^0 (1 - \gamma_5) \right\} \psi = 0 \quad (4.63)$$

in which \mathcal{U} is the mixing matrix in flavour space and $N_e = \text{diag}(1, 0, \dots, 0)$ is also a matrix in flavour space. Pre-multiplying this expression by γ^0 leads to the eigenvalue equation

$$\mathcal{N} \psi = \omega \psi, \quad (4.64)$$

where

$$\mathcal{N} = \gamma^0 \vec{\gamma} \cdot \vec{p} + \gamma^0 M - \left(\beta - \alpha \mathcal{U}^\dagger N_e \mathcal{U} \right) (1 - \gamma^5). \quad (4.65)$$

Since \mathcal{N} is hermitian for real \vec{p} , the eigenvalues of Eq. (4.64) are guaranteed to be real. This completes the proof.

It is best to analyze the expression governing the dispersion relations, Eq. (4.62), by first considering some special cases. The very simplest case is when $m_1=m_2=0$, which

yields

$$\omega = p + (\beta - \alpha)(s - 1) \quad (4.66)$$

$$\omega = -p - (\beta - \alpha)(s + 1) \quad (4.67)$$

for the electron neutrinos and

$$\omega = p + \beta(s - 1) \quad (4.68)$$

$$\omega = -p - \beta(s + 1) \quad (4.69)$$

for the muon neutrinos. These expressions are easy to understand. Four of the dispersion relations are unchanged from their values in the vacuum, since positive helicity neutrinos are also right-handed (chiral) and are thus unaffected by the left-handed Standard Model interactions. The remaining four dispersion relations are displaced vertically from their vacuum values by amounts proportional to their couplings to the medium. Note that only the dispersion relation corresponding to ν_e is affected by the charged current contribution, α .

Another simple case occurs when the coupling θ is set to zero. In this case the dispersion relations for ν_e and ν_μ decouple, as one would expect, and we find

$$\omega = -(\beta - \alpha) \pm \sqrt{(p + s(\beta - \alpha))^2 + m_1^2} \quad (4.70)$$

and

$$\omega = -\beta \pm \sqrt{(p + s\beta)^2 + m_2^2} \quad (4.71)$$

for the electron and muon neutrinos, respectively. These expressions are in exact agreement with what we found in the single-neutrino case in Sec. 4.2.1. Once again the dispersion relations corresponding to the massless case undergo “level repulsion” when a finite mass is added.

Since the equations governing the on-shell behaviour in the two-flavour Dirac case are quartic, it is difficult to obtain explicit expressions of the dispersion relations in cases which are not straightforward extensions of the single-flavour case. Of course quartic equations *are* analytically solvable and, furthermore, we know that in our case all the solutions will be real. In general, however, practically no insight can be gained by examining the expressions of such solutions. One approach which is somewhat helpful if the coupling θ is not too large is to use a graphical approach. In this case one expects the solutions of the coupled system to look similar to those of the uncoupled case except that there will be level repulsion due to the coupling. This behaviour is demonstrated explicitly in Fig. 4.6(a), in which the dotted and solid curves correspond to $\theta=0$ and 0.2, respectively. One interesting feature in the two-neutrino case is that the heavier neutrino, which would have been trapped for certain cases with no coupling, can now “leak out” due to its coupling to the lighter mass eigenstate. That is, only states with energy less than the mass of the lightest mass eigenstate are strictly “trapped” now.

It is also possible to derive approximate solutions of the quartic equations if the neutrinos are relativistic. In that case approximate solutions are given by

$$\omega \simeq p - (2\beta - \alpha) + \frac{\mu^2}{2p} \pm \frac{1}{4p} \left[(4\alpha p - \Delta^2 \cos(2\theta))^2 + \Delta^2 \sin^2(2\theta) \right]^{1/2}, \quad (4.72)$$

$$\omega \simeq -p - (2\beta - \alpha) - \frac{\mu^2}{2p} \mp \frac{1}{4p} \left[(4\alpha p + \Delta^2 \cos(2\theta))^2 + \Delta^2 \sin^2(2\theta) \right]^{1/2}, \quad (4.73)$$

$$\omega \simeq \pm \left(p + \frac{m_{1,2}^2}{2p} \right), \quad (4.74)$$

where the corrections to the above expressions go like $\alpha\mu^2/p^2$, $\beta\mu^2/p^2$ and μ^4/p^3 . Of these expressions, (4.72) gives the energy of the negative-helicity particle eigenstates and (4.73) gives the energy of the positive-helicity *anti*-particle eigenstates. These are in agreement with the usual result and show that the neutral current contribution “factorizes” in the relativistic limit; that is, the difference between the two negative-helicity particle energies

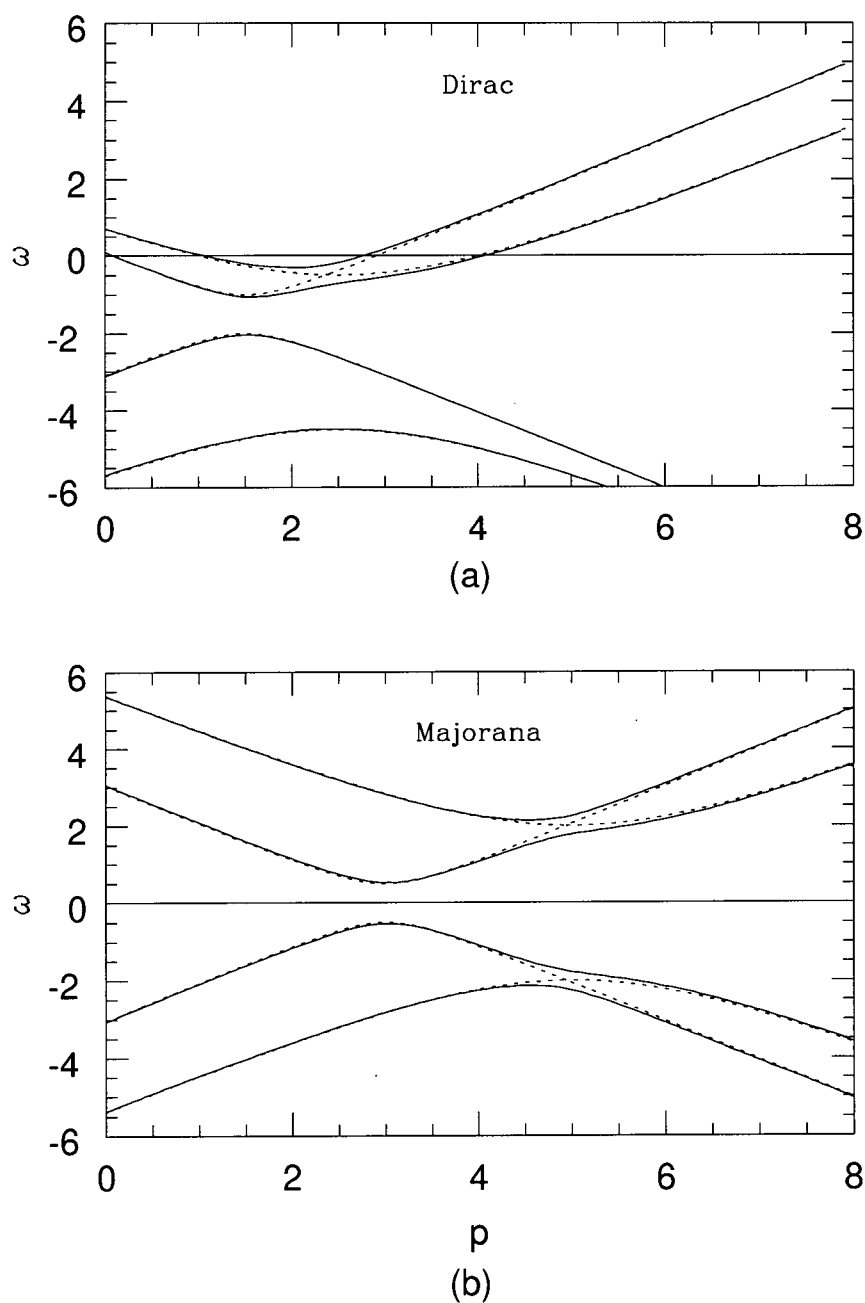


Figure 4.6: Dispersion relations for two neutrinos in (a) the Dirac case (negative helicity) and (b) the Majorana case. In both cases we have set $\alpha=1.0$, $\beta=2.5$, $m_1=0.5$ and $m_2=2.0$, in arbitrary units. The dotted and solid curves correspond to $\theta=0$ and 0.2 , respectively.

is independent of β . Furthermore, it is clear that, if $\alpha > 0$ (which occurs if the background contains more electrons than positrons) then a resonance can occur when $4\alpha p = \Delta^2 \cos(2\theta)$. This is the well-known MSW resonance. The remaining dispersion relations, given in Eq. (4.74), are unchanged from their vacuum values (since the potential is left-handed) and correspond to the positive-helicity neutrinos and negative-helicity anti-neutrinos.

4.3.2 Majorana Case

The case of Majorana neutrinos is interesting for two reasons. First of all, it is the favoured realistic scenario in models which have massive neutrinos, for example in models which employ the “see-saw” mechanism. Secondly, it turns out that the equations governing the dispersion relations are *quadratic* rather than *quartic*, which means that in principle they should be easier to analyze.

The calculation proceeds in a manner similar to that followed in Sec. 4.2.3, the only complication being the additional mixing in flavour space. We omit the details and simply present the result. The negative-helicity dispersion relations in this case are determined by the equation

$$(\omega^2 - p^2 - \Delta_+^2(p)) (\omega^2 - p^2 - \Delta_-^2(p)) = 0, \quad (4.75)$$

where

$$\begin{aligned} \Delta_{\pm}^2(p) = & \frac{1}{2} (m_1^2 + m_2^2 + 4p(\alpha - 2\beta) + 2\alpha(\alpha - 2\beta) + 8\beta^2) \\ & \pm \frac{1}{2} \left\{ [(m_2^2 - m_1^2) \cos(2\theta) - 4\alpha p - 4\alpha(\alpha - 2\beta)]^2 \right. \\ & \left. + (m_2 - m_1)^2 [(m_1 + m_2)^2 + 4\alpha^2] \sin^2(2\theta) \right\}^{1/2}. \end{aligned} \quad (4.76)$$

Thus the four solutions are

$$\omega = \pm \sqrt{p^2 + \Delta_+^2(p)}, \quad (4.77)$$

$$\omega = \pm \sqrt{p^2 + \Delta_-^2(p)}. \quad (4.78)$$

These again reduce to Mannheim's result if we set $\beta=0$ [65]. It is interesting to note that these solutions are not functions only of $m_1^2 + m_2^2$ and $m_2^2 - m_1^2$, as is the case in the relativistic regime.

Fig. 4.6(b) shows a plot of the dispersion relations for Majorana neutrinos in a medium. The dotted and solid curves correspond to the cases with no coupling and with $\theta=0.2$, respectively. Again the curves with non-zero coupling are similar to those with no coupling, except for the "level repulsion" which occurs in the former case. The parameters in this plot are identical to those in the analogous plot for Dirac neutrinos shown in Fig. 4.6(a). Clearly the dispersion relations are quite different in the two cases. This is easily understood by recalling the discussion of Majorana neutrinos in the single-neutrino case in Sec. 4.2.3. There we noted that the Majorana curve could be obtained from the Dirac one by shifting the Dirac curve up and to the right by " α ." In the two-neutrino case, the Majorana curves for $\theta=0$ may be obtained in a similar way from the corresponding Dirac curves (except that the shifts are different for the two curves since ν_μ has only neutral current contributions and ν_e has both neutral current and charged current contributions.)

In all cases examined the minimum of the dispersion relations is always greater than or equal to the minimum mass and so again there appears to be no trapping in the Majorana case.

For relativistic neutrinos the exact expressions for the energies may be simplified somewhat to give

$$\omega \simeq p - (2\beta - \alpha) + \frac{\mu^2}{2p} \pm \frac{1}{4p} \left[(4\alpha p - \Delta^2 \cos(2\theta))^2 + \Delta^2 \sin^2(2\theta) \right]^{1/2}, \quad (4.79)$$

$$\omega \simeq -p + (2\beta - \alpha) - \frac{\mu^2}{2p} \mp \frac{1}{4p} \left[(4\alpha p - \Delta^2 \cos(2\theta))^2 + \Delta^2 \sin^2(2\theta) \right]^{1/2}, \quad (4.80)$$

the first of which is in agreement with the analogous expression, Eq. (4.72), given above for the Dirac case. Since a Majorana neutrino is its own anti-particle, there is no analogue

here of the expression for the anti-particle energy given in Eq. (4.73) for the Dirac case.

4.3.3 The Vector Model

In the models considered so far, the fact that the dispersion relations have minima at non-zero values of the momentum is due to the chiral nature of the potential in the effective Dirac equation. That is, since the potential depends on the spin, the curves are displaced to the right or left depending on whether the neutrino's spin is parallel or anti-parallel to its momentum. As we have seen, this phenomenon occurs for a single neutrino flavour and persists when another flavour is added. It is amusing to note that it is possible to obtain a minimum at non-zero momentum even with a purely vector interaction, although this effect requires the presence of at least two neutrino fields. Such a model was studied several years ago by Chang and Zia [76]. The effective Lagrangian is in this case given by

$$\{\not{p} - M - \alpha Q \gamma^0\} \psi = 0, \quad (4.81)$$

where the matrix Q is as defined in Eq. (4.49). The above equation is similar to Eq. (4.48) except for the absence of the $(1 - \gamma^5)$ factor which was present in that case. We have also set $\beta=0$ for simplicity. The equations governing the dispersion relations may be derived in a manner similar to the Dirac case above to yield

$$\begin{aligned} & \left[(\omega - \alpha \cos^2 \theta)^2 - p^2 - m_1^2 \right] \left[(\omega - \alpha \sin^2 \theta)^2 - p^2 - m_2^2 \right] \\ & = 2\alpha^2 \sin^2 \theta \cos^2 \theta (\omega^2 + p^2 - \alpha\omega + m_1 m_2) + \alpha^4 \sin^4 \theta \cos^4 \theta \end{aligned} \quad (4.82)$$

which is independent of the spin and is symmetric under $p \rightarrow -p$. Apriori it might then seem impossible to generate a minimum at non-zero p . Indeed, for a single neutrino flavour this is the case. For two flavours, however, something very interesting can happen. Suppose we first set θ to zero and imagine increasing α by so much that the negative energy ν_e solution overlaps with the positive energy ν_μ solution. When a non-zero

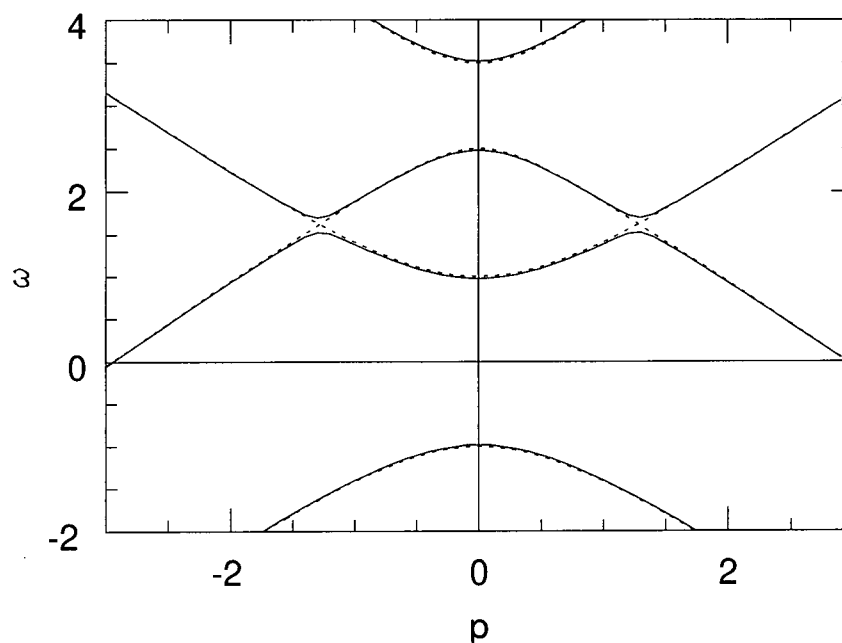


Figure 4.7: Dispersion relations in the two-neutrino vector model, with $\alpha=3.0$, $m_1=0.5$ and $m_2=1.0$, in arbitrary units. The dotted and solid curves correspond to $\theta=0$ and 0.2 , respectively.

coupling is included, these levels repel each other and minima develop near the former crossing points, symmetrically placed about the origin. This feature is illustrated in Fig. 4.7. Thus in this case as well it is possible to have minima in the dispersion relations at non-zero values of the momentum. Note that this case is still somewhat different from the chiral cases which we have studied above, since the first and second derivatives at the origin are zero and negative, respectively, corresponding to a negative effective mass at the origin. This is not the case in chiral theories.

4.3.4 Neutrino Oscillations

We have so far mostly restricted our attention to an investigation of the forms of the dispersion relations themselves and have not considered in detail the effects that these

would have on the oscillations of neutrinos. We first note that in the relativistic regime, the standard MSW results are recovered; that is, (i) the neutral current contribution factorizes and (ii) the negative-helicity states obtain the appropriate dispersion relations in matter while the positive-helicity states revert to their vacuum dispersion relations.

For non-relativistic neutrinos, however, the situation is in some sense far more interesting. One novel effect which arises in the Dirac case purely as a result of the chiral nature of the potential is that in principle one could observe neutrino oscillations *with only a single neutrino flavour*. This could happen since, for non-relativistic neutrinos, the left-handed interactions responsible for producing neutrinos would produce both negative- and positive-helicity neutrinos. Since these propagate with different phase velocities in the medium, they would in general get out of phase with each other, producing oscillations in the probability to detect left-handed neutrinos. For relativistic neutrinos this effect disappears since the amplitude to produce and detect a positive-helicity neutrino becomes negligible. Note, however, that the difference in phase velocities remains and would lead to oscillations if only positive-helicity neutrinos could be produced and detected.

The generalization of this effect to the two-neutrino case gives the result that in general there could be oscillations between four different states. This would lead to an oscillation probability which is a superposition of four different oscillation curves.

4.4 Discussion and Conclusions

In this chapter we have examined the coherent interactions of a neutrino with a background medium by examining the solutions of the effective Dirac equation for the neutrino. A close analysis revealed that the dispersion relations corresponding to such a Dirac equation have a non-trivial form, even in the simple case in which there is only a single

neutrino flavour. In particular, we have examined the interesting effects which arise due to the minimum of the dispersion relation which occurs for non-zero momentum. We have shown that, quite generally for Dirac neutrinos, the minimum value of the energy is less than the neutrino's mass, which implies that for any such background there will be trapping of very low energy neutrinos. In order to support our idea that neutrinos could be trapped by a medium, we then presented a study of the solutions of the Dirac equation and showed that, at least at the classical level, there were solutions corresponding to "trapped" neutrinos. In cases in which the strength of the potential exceeded twice the rest mass of the neutrino in vacuum, we have had to face the version of Klein's paradox which arises in our model. We have argued that, in perfect analogy with the usual formulation of Klein's paradox, our problem may also be resolved by a careful field theoretic treatment (although we have not here considered this treatment.) Since the neutrino in the medium does not have enough energy to exist in the vacuum, it simply must be trapped. We point out that there is nothing "special" about our model which leads to Klein's paradox; rather, any approach which models the propagation of low-mass neutrinos in very dense media would be faced with the same problem. An analysis of the case of a single Majorana neutrino flavour in this medium revealed that in that case there is no trapping by the medium.

We have also presented a study of the dispersion relations for Dirac and Majorana neutrinos in the case in which there are two flavours. In these cases we found that the trapping phenomenon in the Dirac case persisted and the absence of one in the Majorana case also appeared to persist. Furthermore, the neutral current contribution to the oscillation probabilities was found to "factorize" in the relativistic regime, but not in the non-relativistic case. In the latter case it was shown that in principle there could actually exist neutrino oscillations with only a *single* flavour of neutrino, due to the different phase velocities of the helicity eigenstates.

Chapter 5

Conclusions

In this thesis we have considered the propagation and interactions of neutrinos, both in vacuum and in matter. In Chap. 1 we gave a brief introduction to the physics of neutrinos, noting that if neutrinos are indeed massive, then it is quite natural to assume that they are also “mixed.” We then showed that the mixing of neutrinos leads quite generally to “neutrino oscillations”: if a neutrino of a given flavour is produced, there will in general be a non-zero probability to detect it some time later as having a different flavour. This probability oscillates with the distance between the source and detector. In Sec. 1.2.2 we showed that the oscillation probability could be enhanced in matter due to a coherent interaction with the background particles. It was noted that the resonant enhancement of neutrino oscillations as neutrinos exit the sun (the MSW effect) could account for the “missing” neutrinos in the solar neutrino problem.

In Sec. 1.3 we began to focus on some of the issues which make the subject of “neutrino oscillations” so fascinating from the point of view of fundamental quantum mechanics. We first noted that any discussion of neutrino oscillations in general assumes that the neutrinos are localized in space and time; i.e., they are not “plane waves.” If the neutrino’s energy or momentum are known “too well” then it becomes possible to identify the mass of the neutrino exchanged between the source and detector and the oscillations are necessarily destroyed. This point was argued by making an appeal to the uncertainty principle. In Sec. 1.3.2 we discussed an apparent paradox in the $B - \bar{B}$ system which occurs when one attempts to convert an oscillation probability in *time* into one in distance.

The error which led to the ambiguity was clear, but the situation did signal the need to have a reliable method to calculate oscillation probabilities directly in space. This problem was studied in detail in Chap. 3.

In Chap. 2 we considered coherent and incoherent broadening effects on the oscillations of relativistic neutrinos. We began by examining the specific case of the very long-wavelength oscillations of the mono-energetic neutrinos produced by beryllium decay in the sun. It was noted that in order to observe oscillations with wavelengths on the order of the earth-sun distance, it was necessary that the initial beam of neutrinos have a very narrow width in energy. Some sources of broadening were discussed and then we began to consider whether the two types of broadening – coherent and incoherent – could be distinguished at the detector. It was found that while such effects are due to distinct physical processes which could in principle be controlled at the source, they are in general indistinguishable at the detector.

In Chap. 3 we returned to discuss some of the issues brought up in Chap. 1. Namely, is there a reliable and correct way to calculate neutrino oscillations as a function of the distance between the source and detector? We began by examining two approaches which do not explicitly incorporate a “source” and “detector,” but found them both to be unreliable, particularly when non-relativistic neutrinos were involved. We then constructed a simple model for bosonic neutrinos which *did* explicitly involve a source and detector and found that such an approach had many advantages. The main advantage was found to be that the quantities which one might wish to calculate had real “physical” interpretations. This was not the case in the former approaches in which the formal quantities such as the probability amplitude or the current density did not have any real physical meaning which could be distinguished.

Our simple model using a source and detector allowed for a systematic approach to the problem. We first considered the case with only a single neutrino, which enabled us

to understand the efficiency with which the system produced and detected neutrinos of different masses. We found that in general this efficiency *did* have a mass-dependence, but this dependence was well-understood to be a quirk of our model and could furthermore be eliminated by suitably tuning the parameters of the model. Once we had coupled more neutrino fields to the source and detector, we were able to define the neutrino oscillation probability in a very “physical” way and to study its dependence on both the masses of the exchanged neutrinos and on the time resolution of the detector. We verified our assertion in Chap. 2 that a long coherent measurement in time could “revive” the oscillations of neutrino wave packets that had separated spatially. It was found from the point of view of our system that this “reviving” of the oscillations occurs because, according to the detector, the wave packets had not separated yet. This point is simple and yet quite interesting: the “width” of the wave packet as seen by the detector is dependent on the detector’s own time resolution. We noted that from the point of view of our source/detector system, the concept of the neutrino’s “wave packet” is actually somewhat artificial. The “width” of the neutrino is determined symmetrically by the production and detection events, so there seems no clear reason to interpret the neutrino’s “wave packet” as being something which is determined by the source.

We also considered the extension of our formalism to a more realistic model in which the neutrinos were modelled correctly as fermions. We discussed some of the extra complications due to the neutrino’s spin and noted that in general the efficiency of this system at producing and detecting neutrinos would be expected to depend on the neutrinos’ masses.

In Chap. 4 we shifted to a discussion of neutrino propagation in very dense media. We were particularly interested in examining the effects due to the strange dispersion relations which occur in that case. These dispersion relations are odd because they have minima at non-zero values of the momentum and, in the case of Dirac (but not Majorana)

neutrinos, because their minima generically have values less than the neutrino's mass. This latter feature implies that Dirac neutrinos with low enough energy will be trapped by the medium. We examined the trapping of neutrinos in some detail by looking at the classical solutions of the Dirac equation. It was found that in certain cases we had to face "Klein's paradox." Noting that Klein's paradox is not really a paradox at all, but rather a signal that the single-particle interpretation of Dirac's equation is breaking down, we emphasized that the neutrinos *were* indeed trapped, even in this case.

We also noted that, since the interaction with the medium splits the degeneracy in the helicity eigenstates, it is generally possible to have neutrino oscillations (for non-relativistic neutrinos) with only a *single* neutrino flavour. This can occur because the left-handed interactions through which neutrinos are produced and detected can produce linear combinations of negative *and* positive helicity eigenstates, which subsequently propagate with a different phase velocity.

Bibliography

- [1] Pauli's open letter, addressed to the "Radioactive Ladies and Gentleman" attending a physics conference in Tübingen, has been published in: W. Pauli, "On the Earlier and More Recent History of the Neutrino," in *Neutrino Physics*, edited by K. Winter (Cambridge University Press, Cambridge, 1991), pp. 4-5.
- [2] J. Chadwick, *Verh. d. deutschen Phys. Ges.* **16** (1914) 383.
- [3] C.L. Cowan, Jr., F. Reines, F.B. Harrison, H.W. Kruse and A.D. McGuire, *Science* **124** (1956) 103.
- [4] J.N. Bahcall, "Neutrino Astrophysics" (Cambridge University Press, Cambridge, 1990), pp. 423-433.
- [5] K.S. Hirata, *et al.*, *Phys. Rev. Lett.* **58** (1987) 1490; R.M. Bionta, *et al.*, *Phys. Rev. Lett.* **58** (1987) 1494.
- [6] J.N. Bahcall, talk given at TRIUMF, Fall, 1995 (unpublished).
- [7] Two of the most recent models may be found in: J.N. Bahcall and M.H. Pinsonneault, *Rev. Mod. Phys.* **67** (1995) 781; J. Christensen-Dalsgaard, *et al.*, GONG Collaboration, *Science* **272** (1995) 1286.
- [8] J.N. Bahcall, "How Well do Standard Solar Models Describe the Results of Solar Neutrino Experiments," invited talk at the symposium on *The Inconstant Sun*, Naples, March 18 (1996), astro-ph/9606161. To be published in *Memorie della Società*, eds. G. Cauzzi and C. Marmolino.
- [9] The four experiments are: Homestake [10], Kamiokande [11], GALLEX [12] and SAGE [13].
- [10] R. Davis, Jr., *Prog. Part. Nucl. Phys.* **32** (1994) 13.
- [11] Y. Suzuki, KAMIOKANDE Collaboration, *Nucl. Phys. B (Proc. Suppl.)* **38** (1995) 54.
- [12] P. Anselmann, *et al.*, GALLEX Collaboration, *Phys. Lett. B* **342** (1995) 440.
- [13] J.N. Abdurashitov, *et al.*, SAGE Collaboration, *Phys. Lett. B* **328** (1994) 234.

- [14] P. Langacker, "Solar Neutrinos," invited talk at the *32nd International School of Subnuclear Physics*, Erice, July (1994), hep-ph/9411339.
- [15] L. Wolfenstein, Phys. Rev. D **17** (1978) 2369; Phys. Rev. D **20** (1979) 2634.
- [16] S.P. Mikheyev and A. Yu. Smirnov, Yad. Fiz. **42** (1985) 1441 [Sov. J. Nucl. Phys. **42** (1985) 913]; Il Nuovo Cimento C **9** (1986) 17.
- [17] A. B. McDonald, *Proceedings of the 9th Lake Louise Winter Institute*, A. Astbury, *et al.* eds., World Scientific (1994) 1.
- [18] See, for example, C. Quigg, "Gauge Theories of the Strong, Weak, and Electromagnetic Interactions," Frontier in Physics Lecture Note Series, Vol. 56, edited by D. Pines (Addison-Wesley Publishing Company, New York, 1983) and references therein.
- [19] B. Pontecorvo, Sov. Phys. JETP **26** (1968) 984.
- [20] See S.M. Bilenky, C. Giunti and C.W. Kim, "Atmospheric Neutrino Oscillations Among Three Neutrino Flavours and Long-baseline Experiments," hep-ph/9505301.
- [21] G.L. Fogli, E. Lisi and D. Montanino, Phys. Rev. D **49** (1994) 3626.
- [22] C. W. Kim and A. Pevsner, "Neutrinos in Physics and Astrophysics," Contemporary Concepts in Physics, Vol. 8, edited by H. Feshbach (Harwood Acad. Publishers, Chur, 1993).
- [23] For a recent review of tests of the Standard Model, the reader is referred to the latest version of the *Review of Particle Physics*: P. Langacker and J. Erler, Phys. Rev. D **54** (1996) 85.
- [24] Many of the reasons for expecting physics beyond the Standard Model are discussed in: H.E. Haber and G.L Kane, Phys. Rep. **117** (1985) 75. See also: P. Renton, "Electroweak Interactions: an Introduction to the Physics of Quarks and Leptons" (Cambridge University Press, Cambridge, 1990), pp. 542-564.
- [25] P. Langacker, "Massive Neutrinos in Gauge Theories," in *Neutrinos*, edited by H.V. Klapdor (Springer-Verlag, Berlin, 1988), pp. 71-115.
- [26] R.M. Barnett *et al.* (Particle Data Group), Phys. Rev. D **54** (1996) 1.
- [27] M. Aguilar-Benitez *et al.* (Particle Data Group), Phys. Rev. D **50** (1994) 1173.
- [28] C. Athanassopoulos, *et al.*, LSND Collaboration, "Evidence for $\bar{\nu}_\mu \rightarrow \bar{\nu}_e$ Oscillations from the LSND Experiment at LAMPF," nucl-ex/9605003.

- [29] F. von Feilitzsch, "Neutrino Properties," in *Neutrinos*, edited by H.V. Klapdor (Springer-Verlag, Berlin, 1988), pp. 1-33.
- [30] C. Giunti, C.W. Kim and U.W. Lee, Phys. Rev. D **45** (1992) 2414.
- [31] The reader is referred to P. Renton, "Electroweak Interactions: an Introduction to the Physics of Quarks and Leptons" (Cambridge University Press, Cambridge, 1990), pp. 451-463, and references therein.
- [32] J.D. Jackson, "Classical Electrodynamics," Second Edition (John Wiley and Sons, New York, 1975), pp. 453-459.
- [33] T.K. Kuo and J. Panatialeone, Rev. Mod. Phys. **61** (1989) 937.
- [34] A. Messiah, "Quantum Mechanics," volume II (John Wiley and Sons, Inc., New York, 1958), pp. 744-755.
- [35] L. Landau, Phys. Z. Sowjetunion, **2** (1932) 46; C. Zener, Proc. R. Soc. London, Ser. A **137** (1932) 696.
- [36] S.J. Parke, Phys. Rev. Lett. **57** (1986) 1275.
- [37] K.S. Babu, J.C. Pati and F. Wilczek, Phys. Lett. B **359** (1995) 351.
- [38] B. Kayser, Phys. Rev. D **24** (1981) 110.
- [39] H. Lipkin, Phys. Lett. B **348** (1995) 604.
- [40] Y.N. Srivastava, A. Widom and E. Sassaroli, Phys. Lett. B **344** (1995) 436; see also Ref. [41] for more details and for factors of 2 in other processes.
- [41] Y.N. Srivastava, A. Widom and E. Sassaroli, Zeit. f. Phys. C **66** (1995) 601; "Real and Virtual Strange Processes," hep-ph/9507330; "Comment on "EPR without 'collapse of the wave function' ",," hep-ph/9511294.
- [42] J. Lowe, B. Bassalleck, H. Burkhardt, A. Rusek, G.J. Stephenson Jr. and T. Goldman, "No Λ Oscillations," hep-ph/9605234. (This paper was written in response to the calculation in Ref. [40].)
- [43] Y. Grossman and H. Lipkin, "A Simple General Treatment of Flavor Oscillations," hep-ph/9606315.
- [44] K. Kiers, S. Nussinov and N. Weiss, Phys. Rev. D **53** (1996) 537-547.
- [45] V. Gribov and B. Pontecorvo, Phys. Lett. B **28** (1969) 493.

- [46] L. Krauss and F. Wilczek, Phys. Rev. Lett. **55** (1985) 122.
- [47] S. Nussinov, Phys. Lett. B **63** (1976) 201.
- [48] A. Loeb, Phys. Rev. **D39** (1989) 1009.
- [49] C.W. Giunti, C.W. Kim and U.W. Lee, Phys. Lett. B **274** (1992) 87.
- [50] F. Low, Private Communication (to S. Nussinov.)
- [51] See Refs. [15, 16]. For an excellent review see also Ref. [33].
- [52] This version of the Klein-Gordon equation is similar to that encountered in the context of Optical Potential models in Nuclear Physics. See, for example, E. H. Auerbach, D. M. Fleming, and M. M. Sternheim, Phys. Rev. **162** (1967) 1683; **171** (1968) 1781.
- [53] Y. Aharonov and L. Vaidman, Phys. Lett. A **178** (1993) 38; Y. Aharonov, J. Anandan, and L. Vaidman, Phys. Rev. A **47** (1993) 4616. See also W. G. Unruh, Phys. Rev. A **50** (1994) 882; W. G. Unruh, Ann. N.Y. Acad. Sci. **755** (1995) 560.
- [54] C. Giunti, C.W. Kim and U.W. Lee, Phys. Rev. D **44** (1991) 3635; see also Ref. [59].
- [55] C. Giunti, C.W. Kim, J.A. Lee and U.W. Lee, Phys. Rev. D **48** (1993) 4310.
- [56] J. Rich, Phys. Rev. D **48** (1993) 4318.
- [57] W. Grimus and P. Stockinger, "Real Oscillations of Virtual Neutrinos," hep-ph/9603430.
- [58] B. Ancochea, A. Bramon, R. Muñoz-Tapia and M. Nowakowski, "Space-dependent Probabilities for $K^0 - \bar{K}^0$ Oscillations," hep-ph/9605454.
- [59] C.W. Kim, C. Giunti and U.W. Lee, Nucl. Phys. B (Proc. Suppl.) **28A** (1992) 172.
- [60] W. G. Unruh and R. M. Wald, Phys. Rev. D **29** (1984) 1047.
- [61] C. Itzykson and J.-B. Zuber, "Quantum Field Theory," (McGraw-Hill Inc., New York, 1980).
- [62] M. Blasone and G. Vitiello, Ann. Phys. **244** (1995) 283.
- [63] E. Alfinito, M. Blasone, A. Iorio and G. Vitiello, Phys. Lett. B **362** (1995) 91.
- [64] This connection has also been noted recently in Ref. [57].
- [65] P.D. Mannheim, Phys. Rev. **D37**, 1935 (1988).

- [66] J.F. Nieves, Phys. Rev. D **40**, 866 (1989).
- [67] D. Nötzold and G. Raffelt, Nucl. Phys. **B307**, 924 (1988).
- [68] J. Pantaleone, Phys. Lett. B **268**, 227 (1991); Phys. Rev. D **46**, 510 (1992).
- [69] A. Loeb, Phys. Rev. Lett. **64**, 115 (1990).
- [70] O. Klein, Z. Physik **53**, 157 (1929).
- [71] F. Sauter, Z. Physik **69**, 742 (1931); Z. Physik **73**, 547 (1932).
- [72] A. Hansen and F. Ravndal, Phys. Scripta **23**, 1036 (1981). For a competing point of view, which claims that there is in fact a problem, see Ref. [74].
- [73] For a discussion of the Klein paradox in the context of black hole physics, see T. Damour, "Klein Paradox and Vacuum Polarization," in *Proceedings of the First Marcel Grossman Meeting on General Relativity*, Trieste, 1975, edited by R. Ruffini (North Holland Publishing Co., Oxford, 1977), p. 459; also, N. Deruelle and R. Ruffini, Phys. Lett. **57B**, 248 (1975).
- [74] P.J.M. Bongaarts and S.N.M. Ruijsenaars, Ann. Phys. **101**, 289 (1976).
- [75] P.B. Pal and T.N. Pham, Phys. Rev. D **40**, 259 (1989).
- [76] L.N. Chang and R.K.P. Zia, Phys. Rev. D **38**, 1669 (1988).
- [77] B. Kayser and A. Goldhaber, Phys. Rev. D **28** (1983) 2341.
- [78] B. Kayser, Phys. Rev. D **30** (1984) 1023.
- [79] P.D. Mannheim, Int. J. Theor. Phys. **23** (1984) 643.
- [80] H.E. Haber and G.L Kane, Phys. Rep. **117** (1985) 75.
- [81] V.B. Berestetskii, E.M. Lifshitz and L.P. Pitaevskii, "Relativistic Quantum Theory," translated by J.B. Sykes and J.S. Bell (Pergamon Press, Oxford, 1971).

Appendix A

Majorana Neutrinos

In this appendix we review some of the properties of Majorana neutrinos. We follow closely the treatment given in Ref. [22, pp. 17-30]. (The reader is also referred to the discussions in Refs. [77, 78, 79].) In Sec. A.2 we explicitly derive the dispersion relations for a Majorana neutrino propagating in a medium in the case in which there is only a single flavour, following fairly closely the treatment of Mannheim [65].

A.1 The Majorana Condition

One way to see some of the differences between Majorana and Dirac fermions is to look at the mode expansion of the field operators. For a Dirac fermion the field operator may be expressed in terms of creation and annihilation operators as

$$\psi(\vec{x}, t) = \int \frac{d^3p}{(2\pi)^{3/2}} \sum_s \left[u(\vec{p}, s) a(\vec{p}, s) e^{-ip \cdot x} + v(\vec{p}, s) b^\dagger(\vec{p}, s) e^{ip \cdot x} \right], \quad (\text{A.1})$$

where a and b^\dagger annihilate a particle and create an anti-particle, respectively. Since the “Majorana condition” involves the behaviour of the field under charge conjugation, let us review some of the properties of the charge conjugation operator \mathbf{C} . \mathbf{C} is a unitary operator defined in terms of its operation on single-particle states as follows

$$\mathbf{C}|\psi(\vec{p}, s)\rangle = \eta_c |\bar{\psi}(\vec{p}, s)\rangle, \quad (\text{A.2})$$

where η_c is a phase and where

$$|\psi(\vec{p}, s)\rangle \equiv a^\dagger(\vec{p}, s)|0\rangle, \quad (\text{A.3})$$

$$|\bar{\psi}(\vec{p}, s)\rangle \equiv b^\dagger(\vec{p}, s)|0\rangle. \quad (\text{A.4})$$

From Eqs. (A.3,A.4) it follows that

$$\mathbf{C}a^\dagger(\vec{p}, s)\mathbf{C}^{-1} = \eta_c b^\dagger(\vec{p}, s), \quad (\text{A.5})$$

$$\mathbf{C}b^\dagger(\vec{p}, s)\mathbf{C}^{-1} = \eta_c^* a^\dagger(\vec{p}, s), \quad (\text{A.6})$$

so that the charge conjugate of the field ψ may be defined as

$$\psi^c \equiv \mathbf{C}\psi\mathbf{C}^{-1} = \int \frac{d^3p}{(2\pi)^{3/2}} \sum_s \left[u(\vec{p}, s)\eta_c^* b(\vec{p}, s)e^{-ip\cdot x} + v(\vec{p}, s)\eta_c^* a^\dagger(\vec{p}, s)e^{ip\cdot x} \right]. \quad (\text{A.7})$$

The operator \mathbf{C} acts only on the creation and annihilation operators. It is also possible to define the conjugate field ψ^c in terms of a charge conjugation *matrix*, C , which acts only on the spinor indices. The charge conjugation matrix is defined such that

$$C^\dagger = C^{-1}, \quad C^T = -C. \quad (\text{A.8})$$

Using the fact that the u and v spinors are related by

$$u(\vec{p}, s) = C\bar{v}^T(\vec{p}, s), \quad u(\vec{p}, s) = C\bar{v}^T(\vec{p}, s), \quad (\text{A.9})$$

one may easily show that

$$\psi^c = \mathbf{C}\psi\mathbf{C}^{-1} = \eta_c^* C\bar{\psi}^T. \quad (\text{A.10})$$

The “Majorana condition” on Majorana fermions may be stated as

$$\psi_M = \psi_M^c, \quad (\text{A.11})$$

which, from (A.7), implies that

$$a(\vec{p}, s) = \eta_c^* b(\vec{p}, s). \quad (\text{A.12})$$

Thus, for a Majorana fermion the mode expansion is given by

$$\psi_M(x) = \int \frac{d^3p}{(2\pi)^{3/2}} \sum_s \left[u(\vec{p}, s)a(\vec{p}, s)e^{-ip\cdot x} + v(\vec{p}, s)\eta_c^* a^\dagger(\vec{p}, s)e^{ip\cdot x} \right], \quad (\text{A.13})$$

so that there is no longer any distinction between the “particle” and the “anti-particle.” There are now only two degrees of freedom compared to the four degrees of freedom present in the Dirac case.

Since Majorana particles have only two degrees of freedom, it is sometimes convenient to express their fields directly in terms of two-component spinors instead of in terms of four-component spinors¹. Let us work within the “chiral” representation, setting

$$\gamma^0 = \begin{pmatrix} 0 & 1 \\ 1 & 0 \end{pmatrix}, \quad \vec{\gamma} = \begin{pmatrix} 0 & \vec{\sigma} \\ -\vec{\sigma} & 0 \end{pmatrix}, \quad (\text{A.14})$$

$$\gamma^5 = \begin{pmatrix} -1 & 0 \\ 0 & 1 \end{pmatrix}, \quad C = i\gamma^2\gamma^0 = \begin{pmatrix} i\sigma^2 & 0 \\ 0 & -i\sigma^2 \end{pmatrix}. \quad (\text{A.15})$$

In this representation a left-handed four-component spinor ψ_L may be expressed in terms of a two component spinor χ_L as follows

$$\psi_L = \begin{pmatrix} \chi_L \\ 0 \end{pmatrix}. \quad (\text{A.16})$$

The charge conjugate of ψ_L is given by

$$\psi_L^c = C\bar{\psi}_L^T = \begin{pmatrix} 0 \\ -i\sigma^2\chi_L^* \end{pmatrix}, \quad (\text{A.17})$$

so that a Majorana fermion may be expressed in terms of the single two-component spinor χ_L as

$$\psi_M = \psi_L + \psi_L^c = \begin{pmatrix} \chi_L \\ -i\sigma^2\chi_L^* \end{pmatrix}. \quad (\text{A.18})$$

¹In many cases, however, it is more convenient to stay within the four-component formalism. In many supersymmetric field theories, for example, many of the superpartners are Majorana particles. In such cases it is convenient, when evaluating Feynman diagrams, to express the fields in terms of four-component spinors. The Majorana nature of the particles exhibits itself in special counting rules which must be applied when evaluating the diagrams. For an extensive discussion of this topic, see Ref. [80].

The Lagrangian for a free Majorana fermion may then be written as

$$\mathcal{L} = \frac{1}{2} \bar{\psi}_M (i \not{\partial} - m) \psi_M \quad (\text{A.19})$$

$$= \chi_L^\dagger (i \partial_0 - i \vec{\sigma} \cdot \vec{\nabla}) \chi_L + \frac{im}{2} (\chi_L^\dagger \sigma^2 \chi_L^* - \chi_L^T \sigma^2 \chi_L). \quad (\text{A.20})$$

It is interesting to note that at the classical level the two mass terms each vanish identically if χ_L is not taken to be Grassmann-valued.

A.2 A Majorana Neutrino in Matter

The effective Lagrangian for a Majorana neutrino propagating in a constant-density medium may generically be written as

$$\mathcal{L}_{\text{eff}} = \bar{\psi}_M \left[\frac{1}{2} (i \not{\partial} - m) + \alpha \gamma^0 (1 - \gamma^5) \right] \psi_M \quad (\text{A.21})$$

$$= \chi_L^\dagger (i \partial_0 - i \vec{\sigma} \cdot \vec{\nabla} + 2\alpha) \chi_L + \frac{im}{2} (\chi_L^\dagger \sigma^2 \chi_L^* - \chi_L^T \sigma^2 \chi_L). \quad (\text{A.22})$$

Variation of this effective Lagrangian yields the following equation of motion

$$(i \partial_0 - i \vec{\sigma} \cdot \vec{\nabla} + 2\alpha) \chi_L = -im \sigma^2 \chi_L^*. \quad (\text{A.23})$$

In order to solve this expression, let us write the field χ_L in terms of creation and annihilation operators as follows [65]

$$\chi_L(x) = \int \frac{d^3 p}{(2\pi)^{3/2}} e^{i \vec{p} \cdot \vec{x}} \sum_{h=\pm 1} [P_h(\vec{p}, E) \beta_{(h)}(\vec{p}) e^{-i E_h t} + N_h(\vec{p}, E) \beta_{(h)}(\vec{p}) e^{i E_h t}], \quad (\text{A.24})$$

where the creation and annihilation operators are included in P_h and N_h . The two-component column vectors $\beta_{(h)}(\vec{p})$ are eigenvectors of helicity

$$\vec{\sigma} \cdot \vec{p} \beta_{(\pm)}(\vec{p}) = \pm |\vec{p}| \beta_{(\pm)}(\vec{p}), \quad (\text{A.25})$$

It is useful to write out the expressions for $\beta_{(\pm)}$ explicitly [81, p. 72]

$$\beta_{(+)} = \begin{pmatrix} \cos(\theta/2) e^{-i\phi/2} \\ \sin(\theta/2) e^{i\phi/2} \end{pmatrix}, \quad \beta_{(-)} = \begin{pmatrix} -\sin(\theta/2) e^{-i\phi/2} \\ \cos(\theta/2) e^{i\phi/2} \end{pmatrix}, \quad (\text{A.26})$$

where θ and ϕ are the polar angles of the vector \vec{p} with respect to some axis. We may use the expressions in (A.26) to derive the following useful relations

$$\sigma^2 \beta_{(+)}^*(-\vec{p}) = \pm \beta_{(+)}(\vec{p}), \quad \sigma^2 \beta_{(-)}^*(-\vec{p}) = \pm \beta_{(-)}(\vec{p}), \quad (\text{A.27})$$

in which the two possible signs arise because we may take $\phi \rightarrow \phi \pm \pi$ when we take $\vec{p} \rightarrow -\vec{p}$. In the following it is important to consistently follow one prescription or the other.

Applying the equation of motion to the field in Eq. (A.24) gives the following four equations

$$(E_h + h|\vec{p}| + 2\alpha) P_h(\vec{p}, E_h) = m (iN_h^*(-\vec{p}, E_h)), \quad (\text{A.28})$$

$$(E_h - h|\vec{p}| - 2\alpha) (iN_h^*(-\vec{p}, E_h)) = m (P_h(\vec{p}, E_h)), \quad (\text{A.29})$$

from which we may easily derive the dispersion relations

$$E_h = \pm \sqrt{(|\vec{p}| + 2\alpha h)^2 + m^2}. \quad (\text{A.30})$$

Appendix B

Derivation of a Position-dependent Probability Using a Current

In this appendix we shall derive an expression for a position-dependent probability by integrating the spatial component of a conserved two-current over time. This derivation complements the discussion in Sec. 3.2.

In this approach we shall neglect the neutrinos' helicity degrees of freedom and model them by complex scalar fields, which may be written in the usual way in terms of creation and annihilation operators as

$$\phi_\alpha(x, t) = \sum_i \mathcal{U}_{\alpha i} \int d\tilde{p}_i \left[e^{-ip_i \cdot x} a_p^i + e^{ip_i \cdot x} b_p^{i\dagger} \right], \quad (\text{B.1})$$

where

$$d\tilde{p}_i \equiv \frac{dp}{4\pi E_i(p)} \quad (\text{B.2})$$

and where a_p^i and $b_p^{i\dagger}$ are the operators which annihilate a neutrino and create an anti-neutrino, respectively, with momentum p . The creation and annihilation operators are taken to satisfy the following commutation relations¹

$$\left[a_p^i, a_{p'}^{j\dagger} \right] = \left[b_p^i, b_{p'}^{j\dagger} \right] = 4\pi E_i \delta_{ij} \delta(p - p'). \quad (\text{B.3})$$

We then define the “flavour” current operator in terms of the fields as follows

$$j_\beta^\mu(x, t) \equiv i \phi_\beta^\dagger(x, t) \overset{\leftrightarrow}{\partial}^\mu \phi_\beta(x, t) :, \quad (\text{B.4})$$

where

$$a \overset{\leftrightarrow}{\partial}^\mu b \equiv a \partial^\mu b - (\partial^\mu a) b \quad (\text{B.5})$$

¹Using commutation instead of anti-commutation relations has no undesirable effects on our calculation.

and where the colons denote normal ordering of the operators. The sum of this operator over β satisfies current conservation as a result of the Klein-Gordon equation; that is

$$\sum_{\beta} \partial_{\mu} j_{\beta}^{\mu}(x, t) = 0, \quad (\text{B.6})$$

as may easily be verified.

We may now construct an α neutrino single-particle state by letting the creation operators $a_q^{k\dagger}$ act on the vacuum²

$$|\tilde{\phi}_{\alpha}(t)\rangle \equiv \sum_k \mathcal{U}_{\alpha k}^* \int d\tilde{q}_k e^{-iE_k(q)t} f_k(q) a_q^{k\dagger} |0\rangle. \quad (\text{B.7})$$

Finally, we define our idealized two-vector current density to be the expectation value of the current operator in the single-particle state (B.7)

$$J_{\alpha \rightarrow \beta}^{\mu}(x, t) \equiv \langle \tilde{\phi}_{\alpha}(t) | j_{\beta}^{\mu}(x, 0) | \tilde{\phi}_{\alpha}(t) \rangle, \quad (\text{B.8})$$

where we have chosen to work in the Schrödinger representation. We interpret the zero-th component of the above expression as being the relativistic generalization of the probability density and the first component as being the current density.

Our expression for the two-vector current density, Eq. (B.8), has several attractive features. In the first place, it is easily seen to satisfy current conservation when summed over β

$$\sum_{\beta} \partial_{\mu} J_{\alpha \rightarrow \beta}^{\mu}(x, t) = 0. \quad (\text{B.9})$$

Integrating this relation over some one-dimensional “volume” yields

$$\sum_{\beta} \frac{\partial}{\partial t} \int_{x_1}^{x_2} dx J_{\alpha \rightarrow \beta}^0(x, t) = \sum_{\beta} \left(J_{\alpha \rightarrow \beta}^1(x_1, t) - J_{\alpha \rightarrow \beta}^1(x_2, t) \right). \quad (\text{B.10})$$

Thus, the rate of change of the probability to find a neutrino in the segment (x_1, x_2) is equal to the difference of the incoming and outgoing currents, summed over flavours.

²In practice, the functions $f_k(q)$ will also depend on α , but that dependence does not in any way affect our present calculation.

The close tie between the probability and current densities leads to another attractive feature of this formalism: once the probability density is normalized over position, the current density is *automatically* normalized over time.

Let us then examine the normalization condition. Eq. (B.8) may be expanded in terms of creation and annihilation operators to give

$$J_{\alpha \rightarrow \beta}^{\mu}(x, t) = \sum_{i,j,k,l} \mathcal{U}_{\alpha k}^* \mathcal{U}_{\alpha l} \mathcal{U}_{\beta i} \mathcal{U}_{\beta j}^* \int d\tilde{q}_k d\tilde{q}_l' d\tilde{p}_i d\tilde{p}_j' f_l^*(q') f_k(q) (p_i + p_j')^{\mu} \times e^{i(p-p')x - i(E_k(q) - E_l(q'))t} \langle 0 | a_{q'}^l a_{p'}^{j\dagger} a_p^i a_q^{k\dagger} | 0 \rangle. \quad (\text{B.11})$$

Employing the commutation relations (B.3), we find that

$$\langle 0 | a_{q'}^l a_{p'}^{j\dagger} a_p^i a_q^{k\dagger} | 0 \rangle = (4\pi)^2 E_i(p) E_j(p') \delta_{ik} \delta_{jl} \delta(p - q) \delta(p' - q'), \quad (\text{B.12})$$

so that

$$J_{\alpha \rightarrow \beta}^{\mu}(x, t) = \sum_{i,j} \mathcal{U}_{\alpha i}^* \mathcal{U}_{\alpha j} \mathcal{U}_{\beta i} \mathcal{U}_{\beta j}^* \int d\tilde{p}_i d\tilde{p}_j' f_j^*(p') f_i(p) (p_i + p_j')^{\mu} e^{i(p-p')x - i(E_i(p) - E_j(p'))t}. \quad (\text{B.13})$$

The normalization condition is gotten by requiring that the zero-th component of Eq. (B.13) is correctly normalized over position; that is, we require

$$\int dx \sum_{\beta} J_{\alpha \rightarrow \beta}^0(x, t) = 1. \quad (\text{B.14})$$

Inserting (B.13) into this expression yields the normalization condition

$$\sum_i |\mathcal{U}_{\alpha i}|^2 \int d\tilde{p}_i |f_i(p)|^2 = 1. \quad (\text{B.15})$$

If it is desired that the mass eigenstates be individually normalized, then we could furthermore require

$$\int d\tilde{p}_i |f_i(p)|^2 = 1, \quad \forall i. \quad (\text{B.16})$$

We may similarly integrate the first component of (B.13) over time to obtain

$$\int dt \sum_{\beta} J_{\alpha \rightarrow \beta}^1(x, t) = \sum_i |\mathcal{U}_{\alpha i}|^2 \int d\tilde{p}_i d\tilde{p}'_i f_i(p) f_i^*(p') (2\pi) e^{i(p-p')x} (p+p') \delta(E_i - E'_i). \quad (\text{B.17})$$

In order for this expression to reduce to Eq. (B.15) we need to require that

$$f_i(p) = f_i(p) \theta(p), \quad (\text{B.18})$$

that is, we need to require that the wavepacket contains only right-moving components. The reason for this requirement is easy to understand. $J_{\alpha \rightarrow \beta}^1(x, t)$ is a current and as such it gets positive contributions from right-moving particles and negative contributions from left-moving particles. If our detector is located at some position x to the right of the source, then the current can get left-moving contributions from negative times. In order to avoid such problems, we shall always require that Eq. (B.18) hold at least approximately. Making this assumption, we may use the relation (3.8) to simplify the expression for the time integral

$$\begin{aligned} \int dt \sum_{\beta} J_{\alpha \rightarrow \beta}^1(x, t) &= \sum_i |\mathcal{U}_{\alpha i}|^2 \int d\tilde{p}_i d\tilde{p}'_i f_i(p) f_i^*(p') (2\pi) (p+p') \frac{E_i}{p} \delta(p-p') \\ &= \sum_i |\mathcal{U}_{\alpha i}|^2 \int d\tilde{p}_i |f_i(p)|^2 \\ &= 1, \end{aligned} \quad (\text{B.19})$$

as advertised. It is worth noting that the factor of $1/p$ which comes up when converting the energy delta function to a momentum delta function gets exactly cancelled in this approach so that there are no problems near the origin in momentum space. This was not the case in the approach studied in Sec. 3.1, where doing the time integral exactly led to a divergence near the origin (c.f. the discussion following Eq. (3.9).)

It is now straightforward to define an oscillation probability as a function of distance

$$P_{\alpha \rightarrow \beta}(x) \equiv \int dt J_{\alpha \rightarrow \beta}^1(x, t). \quad (\text{B.20})$$

Finally, we may write this expression out explicitly by employing Eq. (3.8) to obtain

$$\begin{aligned}
 P_{\alpha \rightarrow \beta}(x) &= \sum_{i,j} \mathcal{U}_{\alpha i}^* \mathcal{U}_{\alpha j} \mathcal{U}_{\beta i} \mathcal{U}_{\beta j}^* \theta(m_i^2 - m_j^2) \\
 &\times \int \frac{dp}{8\pi E_i} \frac{(p + p'_{ij})}{p'_{ij}} f_i(p) f_j^*(p'_{ij}) e^{i(p - p'_{ij})x} + \text{c.c.}, \quad (\text{B.21})
 \end{aligned}$$

where

$$p'_{ij} \equiv \sqrt{p^2 + \Delta_{ij}}. \quad (\text{B.22})$$

Appendix C

Derivation of the $t_2 \rightarrow \infty$ Limit of $\mathcal{A}_{\text{step}}$

In this appendix we shall derive an approximation for the $t_2 \rightarrow \infty$ limit of the integral given in Eq. (3.62) and investigate under what circumstances the approximation is valid.

The form for the integral given in Eq. (3.62) is convenient for numerical work, but is not particularly convenient for the limit which we wish to consider. Let us instead go back to the definition of this expression, gotten by inserting Eq. (3.60) into Eq. (3.57). We may now formally take the limit as $t_2 \rightarrow \infty$ by giving Ω_2 a small imaginary piece. This yields

$$\begin{aligned} \mathcal{A}_{\text{step}}(x_D, t_1, \infty) = & -i\tilde{N} \int_m^\infty \frac{dE}{E - \Omega_2 - i\epsilon} \exp \left[-\frac{1}{2}(E - \Omega_1)^2 \sigma_{t_1}^2 \right. \\ & \left. - \frac{1}{2}k^2(\sigma_{x_1}^2 + \sigma_{x_2}^2) - i(E - \Omega_2)t_1 \right] \sin(kx_D), \end{aligned} \quad (\text{C.1})$$

where the limit $\epsilon \rightarrow 0^+$ is understood. This integral may be simplified by employing the relation

$$\frac{1}{E - \Omega_2 - i\epsilon} = i\pi\delta(E - \Omega_2) + PP \frac{1}{E - \Omega_2} \quad (\text{C.2})$$

to obtain

$$\begin{aligned} \mathcal{A}_{\text{step}}(x_D, t_1, \infty) = & \tilde{N}\pi \exp \left[-\frac{1}{2}(\Omega_2 - \Omega_1)^2 \sigma_{t_1}^2 - \frac{1}{2}(\Omega_2^2 - m^2)(\sigma_{x_1}^2 + \sigma_{x_2}^2) \right] \sin(\bar{k}x_D) \\ & -i\tilde{N}PP \int_m^\infty \frac{dE}{E - \Omega_2} \exp \left[-\frac{1}{2}(E - \Omega_1)^2 \sigma_{t_1}^2 \right. \\ & \left. - \frac{1}{2}k^2(\sigma_{x_1}^2 + \sigma_{x_2}^2) - i(E - \Omega_2)t_1 \right] \sin(kx_D), \end{aligned} \quad (\text{C.3})$$

where we have defined

$$\bar{k} \equiv \sqrt{\Omega_2^2 - m^2}. \quad (\text{C.4})$$

In order to approximate Eq. (C.3) it is useful to make a change of variables. On the interval $(0, \Omega_2)$ we define $\tilde{E} = \Omega_2 - E$ and on (Ω_2, ∞) we define $\tilde{E} = E - \Omega_2$. Then the integral in (C.3) may be approximated by

$$\begin{aligned}
i\tilde{N} \int_0^{\Omega_2-m} \frac{d\tilde{E}}{\tilde{E}} \left\{ \exp \left[i\tilde{E}t_1 - \frac{1}{2}(\tilde{E} - \Delta\Omega)^2 \sigma_{t_1}^2 \right. \right. \\
\left. \left. - \frac{1}{2}((\tilde{E} - \Omega_2)^2 - m^2)(\sigma_{x_1}^2 + \sigma_{x_2}^2) \right] \sin \left(\sqrt{(\tilde{E} - \Omega_2)^2 - m^2} x_D \right) \right. \\
\left. - \exp \left[-i\tilde{E}t_1 - \frac{1}{2}(\tilde{E} + \Delta\Omega)^2 \sigma_{t_1}^2 \right. \right. \\
\left. \left. - \frac{1}{2}((\tilde{E} + \Omega_2)^2 - m^2)(\sigma_{x_1}^2 + \sigma_{x_2}^2) \right] \sin \left(\sqrt{(\tilde{E} + \Omega_2)^2 - m^2} x_D \right) \right\}, \quad (\text{C.5})
\end{aligned}$$

where $\Delta\Omega \equiv \Omega_2 - \Omega_1$ and where the only approximation so far is that the interval (Ω_2, ∞) has been truncated to $(\Omega_2, 2\Omega_2 - m)$. This approximation is valid if the major contribution to the integral comes from energies close to Ω_2 . In order to further approximate the integral, let us make the *ansatz* that the integral in (C.5) is dominated by values so close to $\tilde{E}=0$ that is valid to set $\tilde{E}=0$ in the gaussian pieces. At the end of the calculation we will be able to see in which cases this is a reasonable approximation. When dealing with the oscillating terms we must be a bit more careful. Writing the sine's in terms of exponentials and Taylor-expanding the arguments to first order in \tilde{E} (which essentially amounts to ignoring the spreading of the wavepackets) leads to the following approximation for (C.5)

$$\begin{aligned}
& \frac{1}{2}\tilde{N} \exp \left[-\frac{1}{2}(\Omega_2 - \Omega_1)^2 \sigma_{t_1}^2 - \frac{1}{2}(\Omega_2^2 - m^2)(\sigma_{x_1}^2 + \sigma_{x_2}^2) \right] \\
& \times \int_0^{\Omega_2-m} \frac{d\tilde{E}}{\tilde{E}} \left[e^{i\tilde{E}t_1} \left(e^{i(\bar{k}-\tilde{E}/\bar{v})x_D} - e^{-i(\bar{k}-\tilde{E}/\bar{v})x_D} \right) \right. \\
& \left. - e^{-i\tilde{E}t_1} \left(e^{i(\bar{k}+\tilde{E}/\bar{v})x_D} - e^{-i(\bar{k}+\tilde{E}/\bar{v})x_D} \right) \right] \\
& = -i\tilde{N} \exp [\dots] \int_0^{\Omega_2-m} \frac{d\tilde{E}}{\tilde{E}} \left[e^{i\bar{k}x_D} \sin \left(\tilde{E} \left(\frac{x_D}{\bar{v}} - t_1 \right) \right) \right. \\
& \left. + e^{-i\bar{k}x_D} \sin \left(\tilde{E} \left(\frac{x_D}{\bar{v}} + t_1 \right) \right) \right], \quad (\text{C.6})
\end{aligned}$$

where

$$\bar{v} \equiv \frac{\sqrt{\Omega_2^2 - m^2}}{\Omega_2}. \quad (\text{C.7})$$

The final step in the approximation is to note that, if

$$\frac{x_D}{\bar{v}} \pm t_1 \gg \sigma_{t_1} \quad (\text{C.8})$$

and if $|\Delta\Omega\sigma_{t_1}|$ is of order unity, then we may approximate the sine terms by delta functions, since

$$\lim_{L \rightarrow \infty} \frac{\sin(xL)}{x} = \pi\delta(x). \quad (\text{C.9})$$

This brings us to the desired result

$$\begin{aligned} \mathcal{A}_{\text{step}}(x_D, t_1, \infty) \simeq & -i\tilde{N}\pi \exp \left[i\bar{k}x_D - \frac{1}{2}(\Omega_2 - \Omega_1)^2\sigma_{t_1}^2 \right. \\ & \left. - \frac{1}{2}(\Omega_2^2 - m^2)(\sigma_{x_1}^2 + \sigma_{x_2}^2) \right]. \end{aligned} \quad (\text{C.10})$$

Note that the condition in Eq. (C.8) simply requires that the detector be turned on before any appreciable amount of flux reaches it.